

RECEIVED: November 12, 2014

REVISED: April 30, 2015

ACCEPTED: July 21, 2015

PUBLISHED: August 27, 2015

Search for new phenomena in events with three or more charged leptons in pp collisions at $\sqrt{s} = 8 \text{ TeV}$ with the ATLAS detector



The ATLAS collaboration

E-mail: atlas.publications@cern.ch

ABSTRACT: A generic search for anomalous production of events with at least three charged leptons is presented. The data sample consists of pp collisions at $\sqrt{s} = 8 \text{ TeV}$ collected in 2012 by the ATLAS experiment at the CERN Large Hadron Collider, and corresponds to an integrated luminosity of 20.3 fb^{-1} . Events are required to have at least three selected lepton candidates, at least two of which must be electrons or muons, while the third may be a hadronically decaying tau. Selected events are categorized based on their lepton flavour content and signal regions are constructed using several kinematic variables of interest. No significant deviations from Standard Model predictions are observed. Model-independent upper limits on contributions from beyond the Standard Model phenomena are provided for each signal region, along with prescription to re-interpret the limits for any model. Constraints are also placed on models predicting doubly charged Higgs bosons and excited leptons. For doubly charged Higgs bosons decaying to $e\tau$ or $\mu\tau$, lower limits on the mass are set at 400 GeV at 95% confidence level. For excited leptons, constraints are provided as functions of both the mass of the excited state and the compositeness scale Λ , with the strongest mass constraints arising in regions where the mass equals Λ . In such scenarios, lower mass limits are set at 3.0 TeV for excited electrons and muons, 2.5 TeV for excited taus, and 1.6 TeV for every excited-neutrino flavour.

KEYWORDS: Hadron-Hadron Scattering

ARXIV EPRINT: [1411.2921](https://arxiv.org/abs/1411.2921)

Contents

1	Introduction	1
2	The ATLAS detector	2
3	Event selection	3
4	Signal regions	6
5	Simulation	7
6	Background estimation	9
7	Systematic uncertainties	12
8	Results	13
9	Model testing	14
10	Interpretation	20
11	Conclusion	26
A	Yields and cross-section limits	27
	The ATLAS collaboration	44

1 Introduction

With the delivery and exploitation of over 20 fb^{-1} of integrated luminosity at a centre-of-mass energy of 8 TeV in proton-proton collisions at the CERN Large Hadron Collider, many models of new physics now face significant constraints on their allowed parameter space. Final states including three or more charged, prompt, and isolated leptons have received significant attention, both in measurements of Standard Model (SM) diboson [1–3] and Higgs boson production [4, 5], and in searches for new phenomena. Anomalous production of multi-lepton final states arises in many beyond the Standard Model (BSM) scenarios, including excited-lepton models [6, 7], the Zee-Babu neutrino mass model [8–10], supersymmetry [11–19], models with pair production of vector-like quarks [20], and models with doubly charged Higgs bosons [21, 22] including Higgs triplet models [23, 24]. An absence of significant deviations from SM predictions in previous measurements and dedicated searches motivates an inclusive search strategy, sensitive to a variety of production modes and kinematic features.

In this paper, the results of a search for the anomalous production of events with at least three charged leptons are presented. The dataset used was collected in 2012 by the ATLAS detector at the Large Hadron Collider, and corresponds to an integrated luminosity of 20.3 fb^{-1} of pp collisions at $\sqrt{s} = 8\text{ TeV}$. Events with at least three leptons are categorized using their flavour content, and signal regions are constructed using several kinematic variables, to cover a wide range of different BSM scenarios. Inspection of the signal regions reveals no significant deviations from the expected background, and model-independent upper limits on contributions from BSM sources are evaluated. A prescription for confronting other models with these results is also provided, along with per-lepton efficiencies parameterized by lepton flavour and kinematics.

The model-independent limits are also used to provide constraints on two benchmark models. The first model predicts the Drell-Yan production of doubly charged Higgs bosons [21, 22], which then decay into lepton pairs. The decays can include flavour-violating terms that can lead to final states such as $\ell^\pm\tau^\pm\ell^\mp\tau^\mp$, where ℓ denotes an electron or muon, and the tau lepton is allowed to decay hadronically or leptonically. Lepton-flavor-conserving decays are not considered in this paper. The second benchmark scenario is a composite fermion model predicting the existence of excited leptons [25]. The excited leptons, which may be neutral (ν^*) or charged (ℓ^*), are produced in a pair or in association with a SM lepton either through contact interactions or gauge-mediated processes. Their decay proceeds via the same mechanisms, with rates that depend on the lepton mass and a compositeness scale, Λ . The final states of such events often contain three or more charged leptons with large momentum.

Related searches for new phenomena in events with multi-lepton final states have not shown any significant deviation from SM expectations. The CMS Collaboration has conducted a search similar to the one presented here using 5 fb^{-1} of 7 TeV data [26] and also with 19.5 fb^{-1} of 8 TeV data [27]. The ATLAS Collaboration has performed searches for supersymmetry in multi-lepton final states [28–30], as have experiments at the Tevatron [31, 32]. The search presented here complements the previous searches by providing model-independent limits and by exploring new kinematic variables. Compared to a similar analysis presented in ref. [33] using 7 TeV data, this search tightens the lepton requirements on the momentum transverse to the beamline (p_T) from $10(15)\text{ GeV}$ to $15(20)\text{ GeV}$ for electrons and muons (hadronically decaying taus), includes new signal regions to target models producing heavy-flavour signatures and events without Z bosons, and tightens the requirements for previously defined signal regions to exploit the higher centre-of-mass energy and integrated luminosity of the 2012 data sample.

2 The ATLAS detector

The ATLAS detector [34] at the LHC covers nearly the entire solid angle around the collision point.¹ It consists of an inner tracking detector surrounded by a thin superconducting

¹ATLAS uses a right-handed coordinate system with its origin at the nominal interaction point (IP) in the centre of the detector and the z -axis along the beam pipe. The x -axis points from the IP to the centre of the LHC ring, and the y -axis points upward. Cylindrical coordinates (r, ϕ) are used in the transverse

solenoid, electromagnetic and hadronic calorimeters, and a muon spectrometer incorporating three large superconducting toroid magnets with eight coils each.

The inner-detector system is immersed in a 2 T axial magnetic field and provides charged-particle tracking in the range $|\eta| < 2.5$. A high-granularity silicon pixel detector covers the vertex region and typically provides three measurements per track, with one hit being usually registered in the innermost layer. It is followed by a silicon microstrip tracker, which usually provides four two-dimensional measurement points per track. These silicon detectors are complemented by a transition radiation tracker, which enables radially extended track reconstruction up to $|\eta| = 2.0$. The transition radiation tracker also provides electron identification information based on the fraction of hits (typically 30 in total) above a higher energy threshold corresponding to transition radiation.

The calorimeter system covers the pseudorapidity range $|\eta| < 4.9$. Within the region $|\eta| < 3.2$, electromagnetic calorimetry is provided by barrel and endcap high-granularity lead/liquid-argon (LAr) electromagnetic calorimeters, with an additional thin LAr presampler covering $|\eta| < 1.8$, to correct for energy loss in material upstream of the calorimeters. Hadronic calorimetry is provided by a steel/scintillator-tile calorimeter, segmented into three barrel structures within $|\eta| < 1.7$, and two copper/LAr hadronic endcap calorimeters. The solid angle coverage is completed with forward copper/LAr and tungsten/LAr calorimeter modules optimized for electromagnetic and hadronic measurements respectively.

The muon spectrometer comprises separate trigger and high-precision tracking chambers measuring the deflection of muons in a magnetic field generated by superconducting air-core toroids. The precision chamber system covers the region $|\eta| < 2.7$ with three layers of monitored drift tubes, complemented by cathode strip chambers in the forward region, where the background is highest. The muon trigger system covers the range $|\eta| < 2.4$ with resistive plate chambers in the barrel, and thin gap chambers in the endcap regions.

A three-level trigger system is used to select interesting events [35]. The Level-1 trigger is implemented in hardware and uses a subset of detector information to reduce the event rate to a design value of at most 75 kHz. This is followed by two software-based trigger levels which together reduce the event rate to about 400 Hz.

3 Event selection

Events are required to have fired either a single-electron or single-muon trigger. The electron and muon triggers impose a p_T threshold of 24 GeV along with isolation requirements on the lepton. To recover efficiency for higher p_T leptons, the isolated lepton triggers are complemented by triggers without isolation requirements but with a higher p_T threshold of 60 (36) GeV for electrons (muons). In order to ensure that the trigger has constant efficiency as a function of lepton p_T , the offline event selection requires at least one lepton (electron or muon) with $p_T > 26$ GeV consistent with having fired the relevant single-lepton trigger. A muon associated with the trigger must lie within $|\eta| < 2.4$, while a triggered

plane, ϕ being the azimuthal angle around the beam pipe. The pseudorapidity is defined in terms of the polar angle θ as $\eta = -\ln \tan(\theta/2)$.

electron must lie within $|\eta| < 2.47$, excluding the calorimeter barrel/endcap transition region ($1.37 \leq |\eta| < 1.52$). Additional muons in the event must lie within $|\eta| < 2.5$ and have $p_T > 15$ GeV. Additional electrons must satisfy the same η requirements as triggered electrons and have $p_T > 15$ GeV. The third lepton in the event may be an additional electron or muon satisfying the same requirements as the second lepton, or a hadronically decaying tau (τ_{had}) with $p_T^{\text{vis}} > 20$ GeV and $|\eta^{\text{vis}}| < 2.5$, where p_T^{vis} and η^{vis} denote the p_T and η of the visible products of the tau decay, with no corrections for the momentum carried by neutrinos. Throughout this paper, the four-momenta of tau candidates are defined only by the visible decay products.

Events must have a reconstructed primary vertex with at least three associated tracks with $p_T > 0.4$ GeV. In events with multiple primary vertex candidates, the primary vertex is chosen to be the one with the highest Σp_T^2 , where the sum is over all reconstructed tracks associated with the vertex. Events with pairs of leptons that are of the same flavour but opposite sign and have an invariant mass below 15 GeV are excluded to avoid backgrounds from low-mass resonances.

The lepton selection includes requirements to reduce the contributions from non-prompt or fake leptons. These requirements exploit the transverse and longitudinal impact parameters of the tracks with respect to the primary vertex, the isolation of the lepton candidates from nearby hadronic activity, and in the case of electron and τ_{had} candidates, the lateral and longitudinal profiles of the shower in the electromagnetic calorimeter. These requirements are described in more detail below. There are also requirements for electrons on the quality of the reconstructed track and its match to the cluster in the calorimeter.

Electron candidates are required to satisfy the “tight” identification criteria described in ref. [36], updated for the increased number of multiple interactions per bunch crossing (pileup) in the 2012 dataset. The tight criteria include requirements on the track properties and shower development of the electron candidate. Muons must have tracks with hits in both the inner tracking detector and muon spectrometer, and must satisfy criteria on track quality described in ref. [37].

The transverse impact parameter significance is defined as $|d_0/\sigma(d_0)|$, where d_0 is the transverse impact parameter of the reconstructed track with respect to the primary vertex and $\sigma(d_0)$ is the estimated uncertainty on d_0 . This quantity must be less than 3.0 for both the electron and muon candidates. The longitudinal impact parameter z_0 must satisfy $|z_0 \sin(\theta)| < 0.5$ mm for both the electrons and muons.

Electrons and muons are required to be isolated through the use of two variables sensitive to the amount of nearby hadronic activity. The first, $p_{T,\text{track}}^{\text{iso}}$, is the scalar sum of the transverse momenta of all tracks with $p_T > 1$ GeV in a cone of $\Delta R = \sqrt{(\Delta\eta)^2 + (\Delta\phi)^2} = 0.3$ around the lepton axis. The sum excludes the track associated with the lepton candidate, and also excludes tracks inconsistent with originating from the primary vertex. The second, $E_{T,\text{cal}}^{\text{iso}}$, is the sum of the transverse energy of cells in the electromagnetic and hadronic calorimeters in a cone of size $\Delta R = 0.3$ around the lepton axis. For electron candidates, this sum excludes a rectangular region around the candidate axis of 0.125×0.172 in $\eta \times \phi$ (corresponding to 5×7 cells in the main sampling layer of the electromagnetic

calorimeter) and is corrected for the incomplete containment of the electron transverse energy within the excluded region. For muons, the sum only includes cells above a certain threshold in order to suppress noise, and does not include cells with energy deposits from the muon candidate. For both the electrons and muons, the value of $E_{\text{T},\text{cal}}^{\text{iso}}$ is corrected for the expected effects of pileup interactions. Electron and muon candidates are required to have $p_{\text{T},\text{track}}^{\text{iso}}/p_{\text{T}} < 0.1$ and $E_{\text{T},\text{cal}}^{\text{iso}}/p_{\text{T}} < 0.1$. The isolation requirements are tightened for leptons with $p_{\text{T}} > 100 \text{ GeV}$, which must satisfy $p_{\text{T},\text{track}}^{\text{iso}} < (10 \text{ GeV} + 0.01 \times p_{\text{T}} [\text{GeV}])$ and $E_{\text{T},\text{cal}}^{\text{iso}} < (10 \text{ GeV} + 0.01 \times p_{\text{T}} [\text{GeV}])$. The tighter cut for high- p_{T} leptons reduces non-prompt backgrounds to negligible levels.

Jets are used as a measure of the hadronic activity within the event as well as seeds for reconstructing τ_{had} candidates. Jets are reconstructed using the anti- k_t algorithm [38], with radius parameter $R = 0.4$. The jet four-momenta are corrected for the non-compensating nature of the calorimeter, for inactive material in front of the calorimeters, and for pileup [39, 40]. Jets used in this analysis are required to have $p_{\text{T}} > 30 \text{ GeV}$ and lie within $|\eta| < 4.9$. Jets within the acceptance of the inner tracking detector must fulfil a requirement, based on tracking information, that they originate from the primary vertex. Jets containing b -hadrons are identified using a multivariate technique [41] based on quantities such as the impact parameters of the tracks associated with the jet. The working point of the identification algorithm used in this analysis has an efficiency for tagging b -jets of 80%, with corresponding rejection factors of approximately 30 for light-jets and 3 for charm-jets, as determined for jets with $p_{\text{T}} > 20 \text{ GeV}$ within the inner tracker's acceptance in simulated $t\bar{t}$ events.

Tau leptons decaying to an electron (muon) and neutrinos are selected with the electron (muon) identification criteria described above, and are classified as electrons (muons). Hadronically decaying tau candidates are seeded by reconstructed jets and are selected using an identification algorithm based on a boosted decision tree (BDT) trained to distinguish hadronically decaying tau leptons from quark- and gluon-initiated jets [42]. The BDT uses track and calorimeter quantities associated with the tau candidate, including the properties of nearby tracks and the shower development in the calorimeter. It is trained separately for tau candidates with one and three charged decay products, referred to as “one-prong” and “three-prong” taus, respectively. In this analysis, only one-prong τ_{had} candidates satisfying the criteria for the “tight” working point [42] are considered. This working point is roughly 40% efficient for one-prong τ_{had} candidates originating from W or Z boson decays, and has a jet rejection factor of roughly 300 in multi-jet topologies. Additional requirements to remove τ_{had} candidates initiated by prompt electrons or muons are also imposed.

To further ensure the prompt nature of our lepton candidates, and to resolve ambiguities in cases where tracks and clusters of energy deposited in the calorimeter are reconstructed as multiple physics objects, the following logic is applied. Muon candidates with a jet within $\Delta R < 0.4$ are neglected. If a reconstructed jet lies within $\Delta R < 0.2$ of an electron or τ_{had} candidate, this object is considered to be a lepton and the jet is neglected. If the separation of the jet axis from an electron candidate satisfies $0.2 < \Delta R < 0.4$, the electron is considered non-isolated due to the nearby hadronic activity and is neglected.

Jets within $0.2 < \Delta R < 0.4$ of τ_{had} candidates are considered as separate objects within the τ_{had} reconstruction algorithm, and are not explicitly treated here. Electrons within $\Delta R < 0.1$ of a muon candidate are also neglected, as are τ_{had} candidates within $\Delta R < 0.2$ of electron or muon candidates. Finally, if two electrons are separated by $\Delta R < 0.1$, the candidate with lower p_T is neglected.

The missing transverse momentum is defined as the negative vector sum of the transverse momenta of reconstructed jets and leptons, using the energy calibration appropriate for each object [43]. Any remaining calorimeter energy deposits unassociated with reconstructed objects are also included in the sum. The magnitude of the missing transverse momentum is denoted E_T^{miss} .

4 Signal regions

Events satisfying all selection criteria are classified into one of two channels. Events in which at least three of the lepton candidates are electrons or muons are selected first, followed by events with two electrons or muons (or one of each) and at least one τ_{had} candidate. These two channels are referred to as $\geq 3e/\mu$ and $2e/\mu + \geq 1\tau_{\text{had}}$ respectively.

Next, events are further divided into three categories. The first category includes events that contain at least one opposite-sign, same-flavour (OSSF) pair of leptons with an invariant mass within 20 GeV of the Z boson mass. This category also includes events in which an OSSF pair can combine with a third lepton to satisfy the same invariant mass requirement, allowing this category to capture events in which a Z boson decays to four leptons (e.g. via $Z \rightarrow \ell\ell \rightarrow \ell\ell\gamma^* \rightarrow \ell\ell\ell'\ell'$) or has some significant final-state radiation that is reconstructed as a prompt electron. This category is referred to as “on- Z ”. The second category is composed of events that contain an OSSF pair of leptons that do not satisfy the on- Z requirements; this category is labelled “off- Z , OSSF”. The final category is composed of all remaining events, and is labelled “no-OSSF”. The wide dilepton mass window used to define the on- Z category is chosen to reduce the leakage of events with real Z bosons into the off- Z categories, which would otherwise see larger backgrounds from SM production of ZZ , WZ , and $Z+\text{jets}$ events. In $\geq 3e/\mu$ events, the categorization is performed using only the three leading leptons (ordered by lepton p_T). In $2e/\mu + \geq 1\tau_{\text{had}}$ events, the categorization is performed using the two light-flavour leptons and the τ_{had} candidate with the highest p_T . The categorization always ignores any additional leptons.

Several kinematic variables are used to characterize events that satisfy all selection criteria. The variable H_T^{leptons} is defined as the scalar sum of the p_T , or p_T^{vis} for τ_{had} candidates, of the three leptons used to categorize the event. The variable $p_T^{\ell,\text{min}}$ is defined as the minimum p_T of the three leptons used to categorize the event. The variable H_T^{jets} is defined as the scalar sum of the p_T of all selected jets in the event. The “effective mass”, m_{eff} , is the scalar sum of E_T^{miss} , H_T^{jets} , and the p_T of all identified leptons in the event. For events classified as on- Z , the transverse mass (m_T^W) is constructed using the E_T^{miss} and the highest- p_T lepton not associated with a Z boson candidate. It is defined as $m_T^W = \sqrt{2p_T^\ell E_T^{\text{miss}}(1 - \cos(\Delta\phi))}$ where $\Delta\phi$ is the azimuthal angle between the lepton and the missing transverse momentum. In on- Z events where a triplet of leptons forms the

Variable	Lower Bounds [GeV]			Additional Requirements	
H_T^{leptons}	200	500	800		
$p_T^{\ell,\min}$	50	100	150		
E_T^{miss}	0	100	200	300	$H_T^{\text{jets}} < 150 \text{ GeV}$
E_T^{miss}	0	100	200	300	$H_T^{\text{jets}} \geq 150 \text{ GeV}$
m_{eff}	600	1000	1500		
m_{eff}	0	600	1200		$E_T^{\text{miss}} \geq 100 \text{ GeV}$
m_{eff}	0	600	1200		$m_T^W \geq 100 \text{ GeV, on-}Z$
Variable	Multiplicity				
b -tags	≥ 1	≥ 2			

Table 1. Kinematic requirements for the signal regions defined in the analysis. The signal regions are constructed by combining these criteria with the six exclusive event categories. The regions with combined requirements on m_{eff} and m_T^W are an exception as they are only defined for the on- Z category.

Z -boson candidate, another Z boson is defined using the OSSF pair of leptons with the largest invariant mass, and m_T^W is constructed using the third lepton. In events in which two Z boson candidates can be formed from the three leading leptons, the candidate with mass closer to the pole mass is defined as the Z boson.

Signal regions are defined in each channel and category by requiring one or more variables to exceed minimum values. Signal regions based on H_T^{leptons} are made without requirements on other variables, as are regions based on $p_T^{\ell,\min}$ and the number of b -tagged jets. Signal regions based on E_T^{miss} are defined separately for events with H_T^{jets} below and above 150 GeV, which serves to distinguish weak production (e.g. $pp \rightarrow W^* \rightarrow \ell^* \nu^*$) from strong production (e.g. $pp \rightarrow Q\bar{Q}' \rightarrow W\bar{q}Zq'$, where Q is some new heavy quark). Signal regions based on m_{eff} are constructed with and without additional requirements of $E_T^{\text{miss}} \geq 100 \text{ GeV}$ and $m_T^W \geq 100 \text{ GeV}$. The definitions of all 138 signal regions are given in table 1.

Several of the categories and signal regions described above are new with respect to the analysis performed using the 7 TeV dataset [33]. The distinction between the off- Z , OSSF and the off- Z , no-OSSF categories is introduced, as are the signal regions defined using the variables $p_T^{\ell,\min}$, m_T^W , and the number of b -tagged jets. As mentioned earlier, thresholds that define signal regions in the 7 TeV analysis are also raised to exploit the higher centre-of-mass energy and larger dataset at 8 TeV.

5 Simulation

Simulated samples are used to estimate backgrounds from events with three or more prompt leptons, where prompt leptons are those originating in the hard scattering process or from the decays of gauge bosons. The response of the ATLAS detector is modelled [44] using the GEANT4 [45] toolkit, and simulated events are reconstructed using the same software

as used for collision data. Small post-reconstruction corrections are applied to account for differences in reconstruction and trigger efficiency, energy resolution, and energy scale between data and simulation [37, 46, 47]. Additional pp interactions (pileup) in the same or nearby bunch crossings are modelled with PYTHIA 6.425 [48]. Simulated events are reweighted to reproduce the distribution of the average number of pp interactions per crossing observed in data over the course of the 2012 run.

The largest SM backgrounds with at least three prompt leptons are WZ and ZZ production where the bosons decay leptonically. These processes are modelled with SHERPA [49] using version 1.4.3 (1.4.5) for WZ (ZZ). These samples include the continuum Drell-Yan processes (γ^*), where the boson has an invariant mass above twice the muon (tau) mass for decays to muons (taus), and above 100 MeV for decays to electrons. Diagrams where a γ^* is produced as radiation from a final-state lepton and decays to additional leptons, i.e. $W \rightarrow \ell^* \nu \rightarrow \ell \gamma^* \nu \rightarrow \ell \ell' \ell' \nu$ and $Z \rightarrow \ell \ell^* \rightarrow \ell \ell \gamma^* \rightarrow \ell \ell' \ell' \ell'$, where ℓ and ℓ' need not have the same flavour, are also included. Simulated samples of SM $Z\gamma^* \rightarrow \ell^+ \ell^- e^+ e^-$ events generated with MADGRAPH 5.1.3.28 [50] are used to verify that this analysis has negligible acceptance for $Z\gamma^*$ events when the mass of the γ^* is less than 100 MeV. The simulation and reconstruction efficiency of such events was probed in an analysis of Dalitz decays [51], where good agreement of simulation and data was observed. The leading-order predictions from SHERPA are cross-checked with next-to-leading-order (NLO) calculations from VBFNLO-2.6.2 [52]. Diagrams including a SM Higgs boson give negligible contributions compared to other diboson backgrounds in all signal regions under study.

The production of $t\bar{t} + W/Z$ processes (also denoted $t\bar{t} + V$) is simulated with ALPGEN 2.13 [53] for the hard scattering, HERWIG 6.520 [54] for the parton shower and hadronization, and JIMMY 4.31 [55] for the underlying event. Single-top production in association with a Z boson (tZ) is simulated with MADGRAPH 5.1.3.28 [50]. Both the $t\bar{t} + V$ and tZ samples use PYTHIA 6.425 for the parton shower and hadronization. These samples also include production of $t\bar{t}\gamma^*$ and $t\gamma^*$, with the mass of the generated γ^* required to be above 5 GeV. As for $Z\gamma^*$, cross checks with dedicated MADGRAPH samples in which the mass of the γ^* is allowed to drop to twice the electron mass show that the contributions from such events are negligible in this search. Corrections to the normalization from higher-order effects for these samples are 30% [56, 57]. Leptons from Drell-Yan processes produced in association with a photon that converts in the detector (denoted $Z + \gamma$ in the following) are modelled with SHERPA 1.4.1. Additional samples are used to model dilepton backgrounds for control regions with fewer than three leptons. Events from $t\bar{t}$ production are generated using POWHEG-BOX [58] with PYTHIA 6.425 used for the parton shower and hadronization. Production of $Z + \text{jets}$ is performed with ALPGEN 2.13 [53] for the hard scattering and PYTHIA6.425 for the parton shower.

Samples of doubly charged Higgs bosons, generated with PYTHIA 8.170 [59], are normalized to NLO cross sections. The samples include events with pair-produced doubly charged Higgs bosons mediated by a Z/γ^* , and do not include single-production or associated production with a singly charged state. Samples of excited charged leptons and excited neutrinos are generated with PYTHIA 8.175 using the effective Lagrangian described in ref. [25].

The CT10 [60] parton distribution functions (PDFs) are used for the SHERPA and POWHEG-BOX samples. MRST2007 LO** [61] PDFs are used for the PYTHIA and HERWIG samples. For POWHEG-BOX, MADGRAPH and ALPGEN, the CTEQ6L1 [62] PDFs are used. The underlying event tune for POWHEG-BOX and PYTHIA 8.175 is the ATLAS Underlying Event Tune 2 (AUET2) [63], while for the PYTHIA 6.425 and MADGRAPH samples the tune is AUET2B [64]. The ALPGEN $t\bar{t}V$ samples use AUET2B, while the ALPGEN $Z+jets$ samples use P2011C [65].

6 Background estimation

Standard Model processes that produce events with three or more lepton candidates fall into three classes. The first consists of events in which prompt leptons are produced in the hard interaction or in the decays of gauge bosons. A second class of events includes Drell-Yan production in association with an energetic γ , which then converts in the detector to produce a single reconstructed electron. A third class of events includes events with at least one non-prompt, non-isolated, or fake lepton candidate satisfying the identification criteria described above.

The first class of backgrounds is dominated by $WZ \rightarrow \ell\nu\ell'\ell'$ and $ZZ \rightarrow \ell\ell'\ell'\ell'$ events. Smaller contributions come from $t\bar{t} + W$, $t\bar{t} + Z$, and $t + Z$ events, where the vector bosons, including those from top quark decays, decay leptonically. Contributions from triboson events, such as WWW , and events containing a Higgs boson, are negligible. All processes in this class of backgrounds are modelled with the dedicated simulated samples described above. Reconstructed leptons in the simulated samples are required to be consistent with the decay of a vector boson or tau lepton using generator-level information.

The second class of backgrounds, from Drell-Yan production in association with a hard photon, is also modelled with simulation. Prompt electrons reconstructed with incorrect charge (charge-flips) are modelled in simulation, with correction factors derived using $Z \rightarrow ee$ events in data. Similar corrections are applied to photons reconstructed as prompt electrons.

The class of events that includes non-prompt or fake leptons, referred to here as the reducible background, is estimated using *in situ* techniques that rely minimally on simulation. Such backgrounds for muons arise from semileptonic b - or c -hadron decays, from in-flight decays of pions or kaons, and from energetic particles that reach the muon spectrometer. Non-prompt or fake electrons can also arise from misidentified hadrons or jets. Hadronically decaying taus have large backgrounds from narrow, low-track-multiplicity jets that mimic τ_{had} signatures.

The reducible background is estimated by reweighting events with one or more leptons that do not satisfy the nominal identification criteria, but satisfy a set of relaxed criteria, defined separately for each lepton flavour. To define the relaxed criteria for electrons, the identification working point is changed from tight to loose [36]. For muons, the $|d_0/\sigma(d_0)|$ and isolation cuts are loosened. For taus, the BDT working point is changed from tight to loose. The reweighting factors are defined as the ratio of fake or non-prompt leptons that satisfy the nominal criteria to those which only fulfil the relaxed criteria. These factors

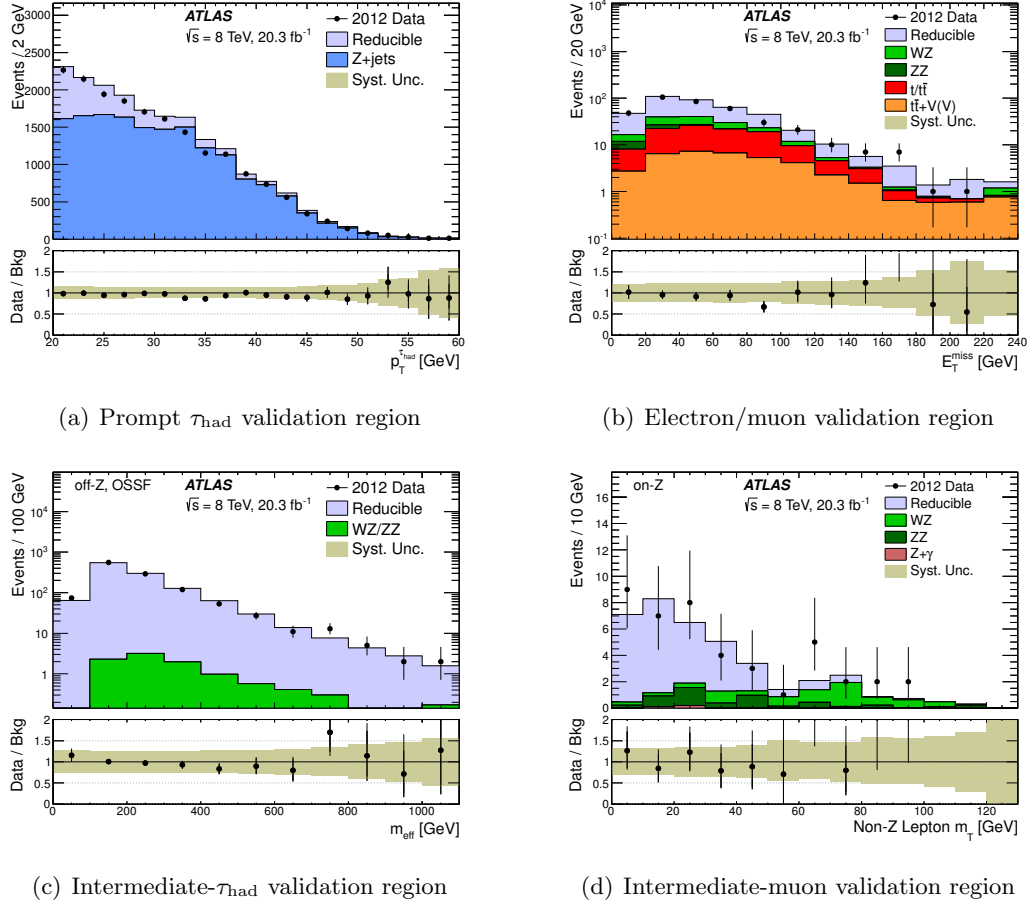


Figure 1. (a) Tau p_T distribution for τ_{had} candidates in the enriched τ_{had} validation region. (b) Missing transverse momentum distribution in the $t\bar{t}$ validation region for electrons and muons. (c) Effective mass distribution in the intermediate τ_{had} validation region, in the off- Z , OSSF category. (d) Distribution of the transverse mass of the missing transverse momentum and the muon not associated with the Z -boson candidate in the intermediate-muon validation region. Signal contamination from doubly charged Higgs bosons and excited leptons in all validation regions is negligible. The lower panel shows the ratio of data to the expected SM backgrounds in each bin. The last bin in all figures includes overflows.

are measured as a function of the candidate p_T and η in samples of data that are enriched in non-prompt and fake leptons. Corrections for the contributions from prompt leptons in the background-enriched samples are taken from simulation.

The background estimates and lepton modelling are tested in several validation regions. The τ_{had} modelling and background estimation are tested in a region enriched in $Z \rightarrow \tau\tau \rightarrow \mu\tau_{\text{had}}$ events. This region is constructed by placing requirements on the invariant mass of the muon and τ_{had} pair, on the angles between the muon, τ_{had} and missing transverse momentum, and on the muon and E_T^{miss} transverse mass. These requirements were optimized to suppress the contribution from $W \rightarrow \mu\nu + \text{jets}$ events. The τ_{had} p_T distribution in this validation region is shown in figure 1(a).

Region	Prompt	Fake	Total Expected	Observed
$Z \rightarrow \tau_{\text{lep}}\tau_{\text{had}}$	16400 ± 800	2900 ± 700	19300 ± 1100	18323
$t\bar{t}: \ell\ell$	130 ± 40	230 ± 60	360 ± 70	375
$t\bar{t}: \ell\tau_{\text{had}}$	37 ± 3	1700 ± 400	1700 ± 400	1469
Intermediate electron	130 ± 70	53 ± 17	180 ± 80	207
Intermediate muon	13 ± 2	26 ± 8	39 ± 8	43
Intermediate tau, on- Z	74 ± 7	19000 ± 5000	19000 ± 5000	17361
Intermediate tau, off- Z , OSSF	11 ± 2	1160 ± 290	1170 ± 290	1155
Intermediate tau, off- Z , no-OSSF	21 ± 3	320 ± 80	340 ± 80	340

Table 2. Expected and observed event yields for all validation regions. The expected contributions from signal processes such as excited leptons or doubly charged Higgs bosons are negligible in all validation regions.

A validation region rich in $t\bar{t}$ events is defined to test the estimates of the reducible background. Events in this region have exactly two identified lepton candidates with the same charge (but any flavour combination), at least one b -tag, and $H_T^{\text{jets}} \leq 500$ GeV. This sample is estimated to be primarily composed of lepton+jets $t\bar{t}$ events. The same-sign requirement suppresses events where both W bosons decay leptonically, and enhances the contributions from events where one lepton candidate originates from semileptonic b -decay. The upper limit on H_T^{jets} of 500 GeV reduces potential contamination from hypothesized signals. An example of the E_T^{miss} distribution in the $t\bar{t}$ region enriched in reducible backgrounds from the same-sign electrons and/or muons is shown in figure 1(b).

Additional validation regions that test the estimation of reducible backgrounds lepton identification criteria tighter than those used in the background-enriched samples but looser than and orthogonal to those used in the signal regions. This set of identification criteria is referred to as the “intermediate” selection, and leptons satisfying the intermediate selection are referred to as intermediately identified leptons, or simply intermediate leptons. The reweighting factors are remeasured for the intermediate selection and used in the validation region. Events are selected as in the analysis, with the intermediate selection used for a single lepton flavour. For intermediate electrons and muons, only events in the on- Z channel are considered, and intermediate leptons are required to have a flavour different from that of the OSSF pair forming the Z boson candidate. For intermediate taus, all channels are considered. An example of the m_{eff} distribution for the intermediate tau selection is shown in figure 1(c). For the intermediate muon validation region, the transverse mass distribution for intermediate muons combined with E_T^{miss} is shown in figure 1(d).

Good agreement between the expected and observed event yields is seen in all validation regions. A summary of expected and observed event yields for all validation regions is shown in table 2.

Source	Uncertainty [%]
Luminosity	2.8
Trigger efficiency	1
Lepton momentum scale/resolution	1
Lepton identification	2
Jet energy resolution	2
Jet energy scale	5
b -tagging efficiency	5
E_T^{miss} scale/resolution	4
$t\bar{t} + V$ cross section	30
WZ/ZZ cross section	7
WZ/ZZ shape	20–50
Charge misidentification	8
Non-prompt and fake τ_{had}	25
Non-prompt and fake e/μ	40

Table 3. Typical systematic uncertainties from various sources, in signal regions where the uncertainty is relevant. The uncertainties on the backgrounds are presented as the percent uncertainty on the total background estimate.

7 Systematic uncertainties

The backgrounds modelled with simulated samples have systematic uncertainties related to the trigger, selection efficiency, momentum scale and resolution, E_T^{miss} , and luminosity. These uncertainties, when evaluated as fractions of the total background estimate, are usually small, and are summarized in table 3. Predictions from simulations are normalized to the integrated luminosity collected in 2012. The uncertainty on the luminosity is 2.8% and is obtained following the same methodology as that detailed in ref. [66].

Uncertainties on the cross sections of SM processes modelled by simulation are also considered. The normalization of the $t\bar{t}+W$ and $t\bar{t}+Z$ backgrounds have an uncertainty of 30% based on PDF and scale variations [56, 57]. The SHERPA predictions [49] of the WZ and ZZ processes are cross-checked with next-to-leading-order predictions from VBFNLO. Scale uncertainties are evaluated by varying the factorization and renormalization scales up and down by a factor of two, and range from 3.5% for the inclusive prediction to 6.6% for events with at least one additional parton. PDF uncertainties are evaluated by taking the envelope of predictions from all PDF error sets for CT10-NLO, MSTW2008-NLO, and NNPDF-2.3-NLO, and are between 3% and 4%.

An additional uncertainty on the SHERPA predictions is applied to cover possible mis-modelling of events with significant jet activity. This shape uncertainty is evaluated using LOOPSIM+VBFNLO [67], which makes “beyond-NLO” predictions (denoted \bar{n} NLO) for high- p_T observables, and is based on the study presented in ref. [68]. Predictions of H_T^{jets} and m_{eff} at \bar{n} NLO are compared with those from SHERPA in a phase space similar to that

used in this analysis. Good agreement between SHERPA and the \bar{n} NLO predictions is observed across the full range of H_T^{jets} and m_{eff} . The uncertainty on the \bar{n} NLO prediction is evaluated by changing the renormalization and factorization scales used in the \bar{n} NLO calculation by factors of two. These uncertainties increase linearly with event activity with a slope of $(50\%) \times (H_T^{\text{jets}} [\text{TeV}])$ and are applied to the SHERPA predictions. A study of $Z + \text{jets}$ events at $\sqrt{s} = 7$ TeV [69] shows good agreement of SHERPA predictions with data in events with significant transverse activity, showing deviations of data from predictions within the uncertainties used here.

The estimates of the reducible background carry large uncertainties from several sources. These uncertainties are determined in dedicated studies using a combination of simulation and data. They account for potential biases in the methods used to extract the reweighting factors, and for the dependency of the reweighting factors on the event topology. The electron reweighting factors have uncertainties that range from 24% to 30% as a function of the electron p_T , while for muons the uncertainties range from 25% to 50%. For the estimates of fake τ_{had} candidates, the p_T -dependent uncertainty on the reweighting factors is approximately 25%. In signal regions where the relaxed samples are poorly populated, statistical uncertainties on the estimates of the reducible background become significant, especially in regions with high E_T^{miss} or H_T^{jets} requirements.

The relative uncertainty on the correction factors for electron charge-flip modelling in simulation is estimated to be 40%, resulting in a maximum uncertainty on the total background yield in any signal region of 11%. Studies of simulated data show that the majority of charge-flip electrons are due to bremmstrahlung photons that interact with detector material and convert to an electron-positron pair, yielding an energetic secondary lepton with the opposite sign of the prompt lepton. As this is the same process by which prompt photons mimic prompt leptons, the same 40% uncertainty is assigned to the modelling of prompt photons reconstructed as electrons.

In all signal regions, the dominant systematic uncertainty is either the uncertainty on the reducible background or the shape uncertainty on the diboson samples. In $2e/\mu+ \geq 1\tau_{\text{had}}$ channels, the uncertainty on the reducible background always dominates. In $\geq 3e/\mu$ channels, the WZ theory uncertainties dominate in most regions except in the no-OSSF categories, where the uncertainties on the reducible background are dominant. The uncertainties on $t\bar{t} + V$ are large in regions requiring two b -tagged jets. The uncertainties on the trigger, selection efficiency, momentum scale and resolution, and E_T^{miss} are always subdominant.

8 Results

Expected and observed event yields for the most inclusive signal regions are summarized in table 4. Results of the search in all signal regions are summarized in figure 2, which shows the deviation of the observed event yields from the expected yields, divided by the total uncertainty on the expected yield, for all signal regions. The total uncertainty on the expected yield includes statistical uncertainties on the background estimate as well as the systematic uncertainties discussed in the previous section. There are no signal regions

Channel	Prompt	Fake	Total Expected	Observed
off- Z , no-OSSF				
$\geq 3e/\mu$	13 ± 2	18 ± 5	30 ± 5	36
$2e/\mu + \geq 1\tau$	26 ± 3	180 ± 40	200 ± 40	208
off- Z , OSSF				
$\geq 3e/\mu$	206 ± 23	33 ± 9	239 ± 25	221
$2e/\mu + \geq 1\tau$	15 ± 2	630 ± 170	640 ± 170	622
on- Z				
$\geq 3e/\mu$	2900 ± 340	180 ± 40	3080 ± 350	2985
$2e/\mu + \geq 1\tau$	141 ± 13	10300 ± 2800	10400 ± 2800	9703

Table 4. Expected and observed event yields for the most inclusive signal regions.

in which the observed event yield exceeds the expected yield by more than three times the uncertainty on the expectation, and only one region in which the observed event yield is lower than expected by more than three times the uncertainty, i.e. the $\geq 3e/\mu$, off- Z no-OSSF category, with $H_T^{\text{jets}} < 150$ GeV and $E_T^{\text{miss}} > 100$ GeV. The smallest p -value is 0.05, which corresponds to a 1.7σ deviation, and is observed in the $m_{\text{eff}} > 1000$ GeV region in the $2e/\mu + \geq 1\tau_{\text{had}}$, on- Z channel. Examples of kinematic distributions for all channels and categories are shown in figure 3.

Since the data are in good agreement with SM predictions, the observed event yields are used to constrain contributions from new phenomena. The 95% confidence level (CL) upper limits on the number of events from non-SM sources (N_{95}) are calculated using the modified Frequentist CL_s prescription [70]. All statistical and systematic uncertainties on estimated backgrounds are incorporated into the limit-setting procedure, with correlations taken into account where appropriate. The N_{95} limits are then converted into limits on the “visible cross section” (σ_{95}^{vis}) using the relationship $\sigma_{95}^{\text{vis}} = N_{95} / \int L dt$, where $\int L dt$ is the integrated luminosity of the data sample.

Figure 4 shows the resulting observed limits, along with the median expected limits with $\pm 1\sigma$ and $\pm 2\sigma$ uncertainties. Table 5 shows the expected and observed limits for the most inclusive signal regions.

9 Model testing

The model-independent exclusion limits presented in section 8 can be re-interpreted in the scope of any model of new phenomena predicting final states with three or more leptons. This section provides a prescription for such re-interpretations. In order to convert the σ_{95}^{vis} limits into upper limits on the cross section in a specific model, the fiducial acceptance (\mathcal{A}) must be known. The efficiency to select signal events within the fiducial volume (fiducial efficiency, or ϵ_{fid}) is also needed. The 95% CL upper limit on the cross section σ_{95} is then given by

$$\sigma_{95} = \frac{\sigma_{95}^{\text{vis}}}{\mathcal{A} \times \epsilon_{\text{fid}}}. \quad (9.1)$$

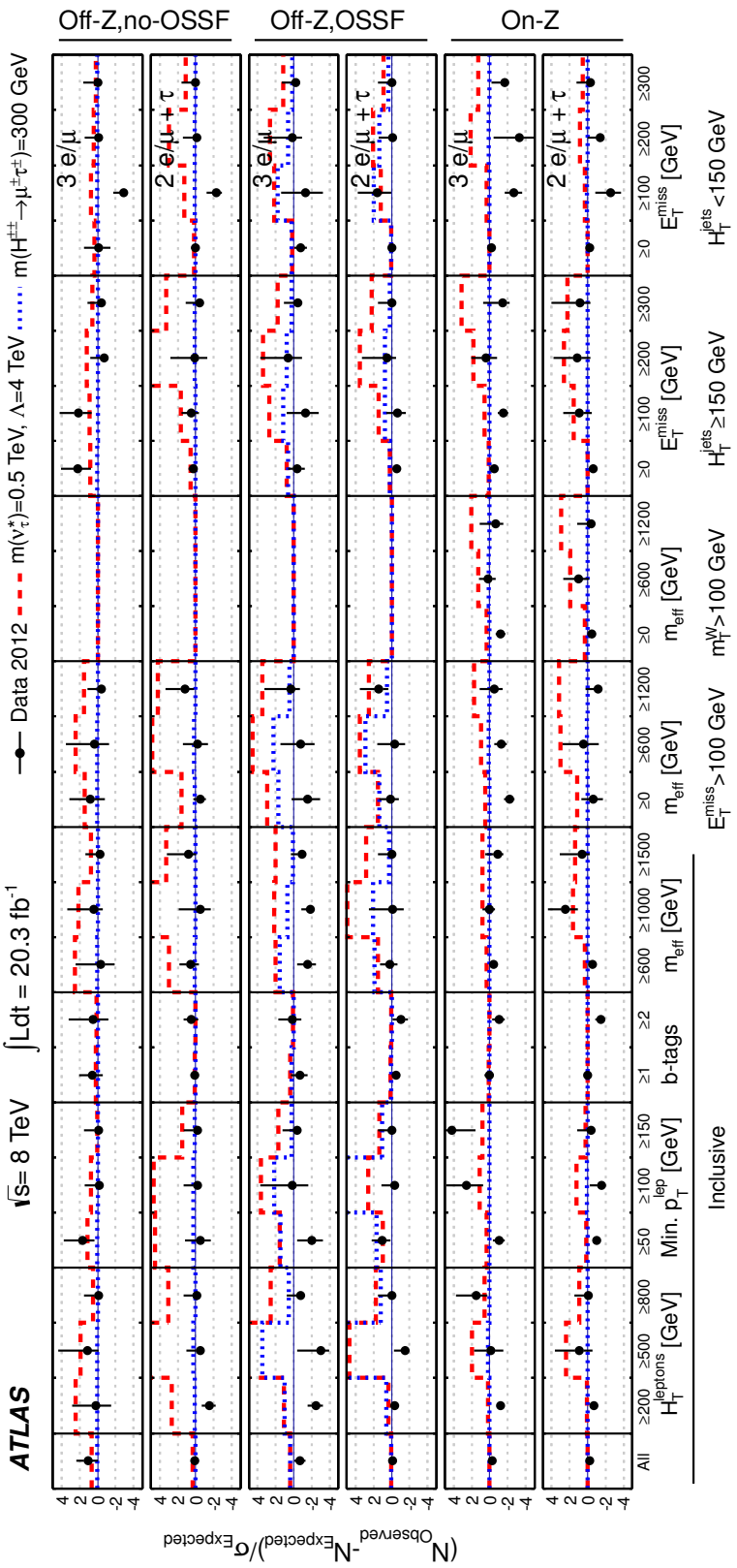


Figure 2. Deviations of observed event yields from expected yields, divided by the total uncertainty on the expected yield, for all signal regions under study. The total uncertainty on the expected yield includes statistical uncertainties on the background estimate as well as the systematic uncertainties discussed in the previous section. The error bars on the data points show Poisson uncertainties with 68% coverage. Expected yields for two benchmark BSM scenarios, a model with excited tau neutrinos with mass 500 GeV and compositeness scale 4 TeV, and a model with pair-produced doubly charged Higgs bosons with a mass 300 GeV decaying to $\mu\tau$, are shown by red and blue dashed lines, respectively.

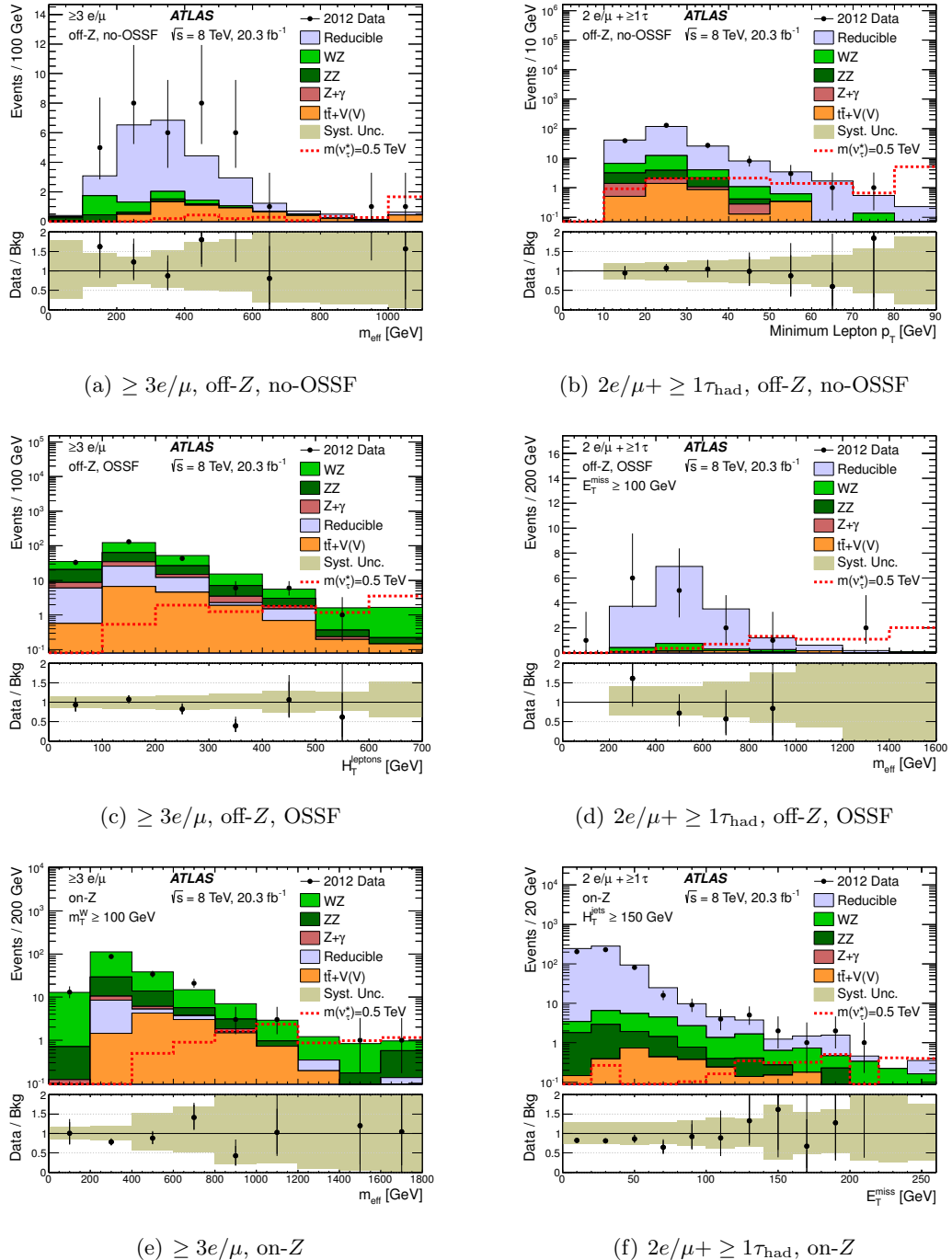


Figure 3. Sample results for all categories: (a) $\geq 3e/\mu$, off- Z , no-OSSF, (b) $2e/\mu+ \geq 1\tau_{\text{had}}$, off- Z , no-OSSF, (c) $\geq 3e/\mu$, off- Z , OSSF, (d) $2e/\mu+ \geq 1\tau_{\text{had}}$, off- Z , OSSF, (e) $\geq 3e/\mu$, on- Z and (f) $2e/\mu+ \geq 1\tau_{\text{had}}$, on- Z . A predicted signal of excited tau neutrinos is overlaid to illustrate the sensitivity of the different signal regions; the compositeness scale Λ of this signal scenario is 4 TeV. The lower panel shows the ratio of data to the expected SM backgrounds in each bin. The last bin in all figures includes overflows.

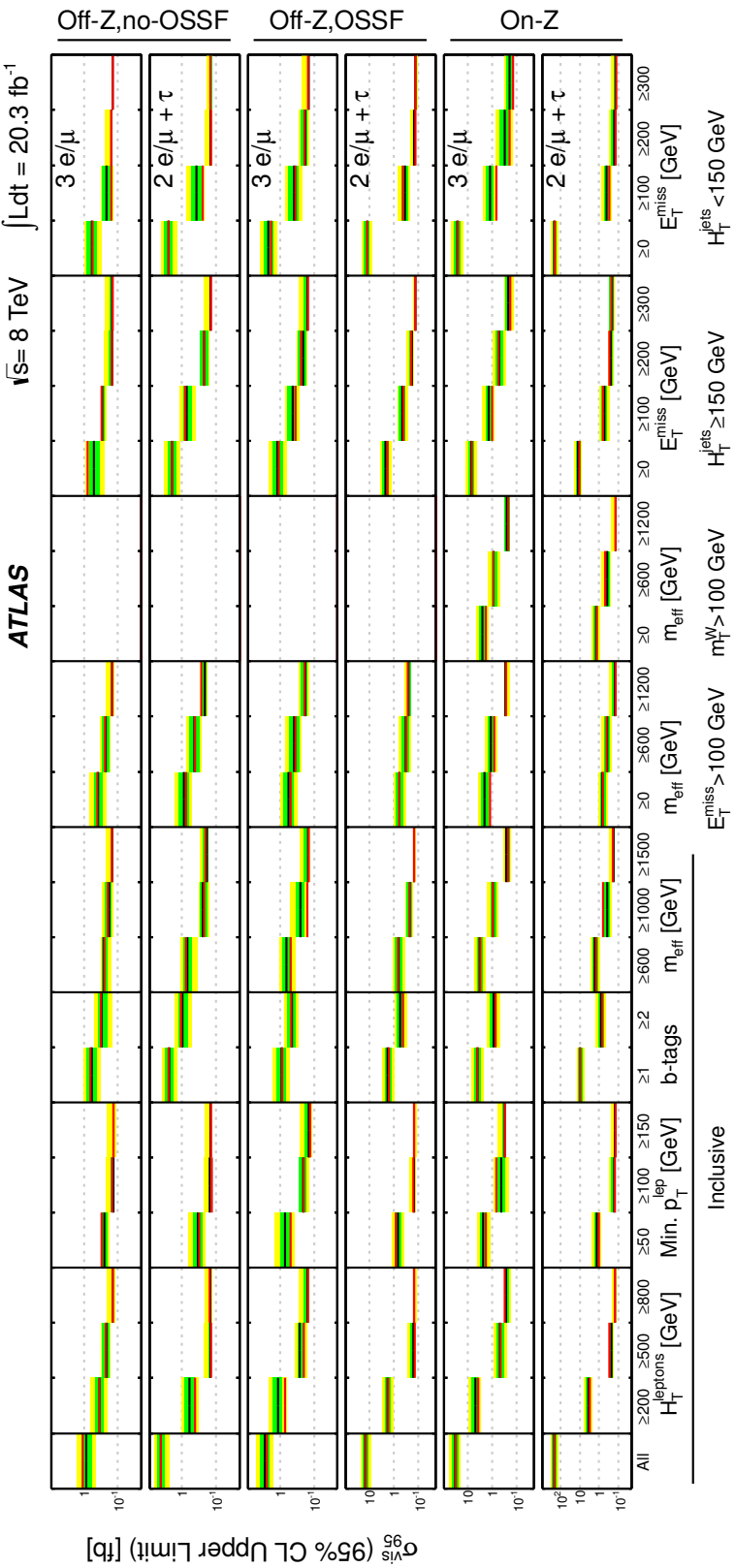


Figure 4. Expected (black) and observed (red) 95% CL upper limits on the visible cross section from BSM sources for all signal regions. Confidence intervals of one and two standard deviations on the expected limits are shown as green and yellow bands.

Channel	Expected [fb]	$\pm 1\sigma$ [fb]	$\pm 2\sigma$ [fb]	Observed [fb]
off- Z , no-OSSF				
$\geq 3e/\mu$	0.82	$+0.19$ -0.22	$+0.56$ -0.38	0.89
$2e/\mu + \geq 1\tau$	4.2	$+1.2$ -1.0	$+2.1$ -1.7	4.3
off- Z , OSSF				
$\geq 3e/\mu$	3.0	$+1.1$ -0.8	$+2.4$ -1.3	2.5
$2e/\mu + \geq 1\tau$	14.4	$+3.2$ -3.3	$+6.2$ -5.7	14.0
on- Z				
$\geq 3e/\mu$	33	$+11$ -9	$+24$ -15	31
$2e/\mu + \geq 1\tau$	220	$+50$ -50	$+90$ -90	207

Table 5. Expected and observed limits on σ_{95}^{vis} for inclusive signal regions, along with confidence intervals of one and two standard deviations on the expected limits.

Both \mathcal{A} and ϵ_{fid} are determined using simulated events at the particle level, i.e. using all particles after the parton shower and hadronization with mean lifetimes longer than 10^{-11} s. Event selection proceeds as described in section 3, with minor modifications detailed below. The acceptance is determined by selecting trilepton events, categorizing them, applying the signal region requirements, and dividing the resulting event yield by the signal yield before any selection. The fiducial efficiency is then determined using parameterized efficiencies provided below. Events should be generated without pileup — the effects of pileup are small, and are handled in the parameterized efficiencies.

Electron and muons are selected using the same $|\eta|$ requirements described in section 3, but with a lower p_T requirement of 10 GeV. Electrons or muons from tau decays must satisfy the same requirements as prompt leptons. The tau four-momentum at the particle level is defined using only the visible decay products, which include all particles except neutrinos. Hadronically decaying taus are required to have $p_T^{\text{vis}} \geq 15$ GeV and $|\eta^{\text{vis}}| < 2.5$.

Generated electrons and muons are required to be isolated. A track isolation energy at the particle level corresponding to $p_{T,\text{track}}^{\text{iso}}$, denoted $p_{T,\text{true}}^{\text{iso}}$, is defined as the scalar sum of transverse momenta of charged particles within a cone of $\Delta R = 0.3$ around the lepton axis. Particles used in the sum are included after hadronization and must have $p_T > 1$ GeV. A fiducial isolation energy corresponding to $E_{T,\text{cal}}^{\text{iso}}$, denoted $E_{T,\text{true}}^{\text{iso}}$, is defined as the sum of all particles inside the annulus $0.1 < \Delta R < 0.3$ around the lepton axis. Neutrinos and other stable, weakly interacting particles produced in models of new phenomena are excluded from both $p_{T,\text{true}}^{\text{iso}}$ and $E_{T,\text{true}}^{\text{iso}}$; muons are excluded from $E_{T,\text{true}}^{\text{iso}}$. Electrons and muons must satisfy $p_{T,\text{true}}^{\text{iso}}/p_T < 0.15$ and $E_{T,\text{true}}^{\text{iso}}/p_T < 0.15$.

A simulated sample of WZ events is used to extract the per-lepton efficiencies ϵ_ℓ . Generated leptons are matched to reconstructed lepton candidates that satisfy the selection criteria defined in section 3 by requiring their ΔR separation be less than 0.1 for prompt

p_T [GeV]	Prompt e		Prompt μ		$\tau \rightarrow e$		$\tau \rightarrow \mu$		τ_{had}
	$ \eta > 0.1$	$ \eta < 0.1$	$ \eta > 0.1$	$ \eta < 0.1$	$ \eta > 0.1$	$ \eta < 0.1$	$ \eta > 0.1$	$ \eta < 0.1$	
10–15	0.0256 ± 0.0003	0.0224 ± 0.0002	0.0071 ± 0.0003	0.0086 ± 0.0006					
15–20	0.522 ± 0.005	0.839 ± 0.008	0.402 ± 0.015	0.409 ± 0.029	0.62 ± 0.04	0.66 ± 0.19	0.0311 ± 0.0021		
20–25	0.607 ± 0.005	0.887 ± 0.007	0.478 ± 0.017	0.44 ± 0.04	0.66 ± 0.06	0.12 ± 0.04	0.148 ± 0.012		
25–30	0.654 ± 0.005	0.910 ± 0.007	0.490 ± 0.016	0.55 ± 0.04	0.68 ± 0.05	0.13 ± 0.03	0.229 ± 0.018		
30–40	0.708 ± 0.004	0.919 ± 0.005	0.492 ± 0.011	0.63 ± 0.04	0.71 ± 0.04	0.53 ± 0.13	0.217 ± 0.013		
40–50	0.737 ± 0.005	0.923 ± 0.005	0.499 ± 0.012	0.62 ± 0.05	0.74 ± 0.06	0.28 ± 0.11	0.292 ± 0.025		
50–60	0.761 ± 0.005	0.925 ± 0.006	0.527 ± 0.016	0.62 ± 0.06	0.71 ± 0.07	0.50 ± 0.20	0.245 ± 0.026		
60–80	0.784 ± 0.005	0.925 ± 0.006	0.512 ± 0.013	0.64 ± 0.07	0.78 ± 0.08	0.25 ± 0.13	0.307 ± 0.032		
80–100	0.815 ± 0.008	0.922 ± 0.008	0.530 ± 0.020	0.72 ± 0.13	0.65 ± 0.10	0.50 ± 0.25	0.227 ± 0.033		
100–200	0.835 ± 0.008	0.918 ± 0.008	0.528 ± 0.018	0.62 ± 0.11	0.75 ± 0.13	0.33 ± 0.19	0.28 ± 0.04		
200–400	0.851 ± 0.021	0.884 ± 0.022	0.465 ± 0.041						
400–600	0.84 ± 0.10	0.83 ± 0.10	0.17 ± 0.07						
≥ 600	0.90 ± 0.26								

Table 6. The fiducial efficiency for electrons, muons, and taus in different p_T ranges ($\epsilon_{\text{fid}}(p_T)$). For electrons and muons from tau decays, the p_T is that of the electron or muon, not the tau. The uncertainties shown reflect the statistical uncertainties of the simulated samples only.

electrons and muons, and less than 0.2 for taus. Reconstructed electrons and muons originating from true tau decays are also required to be within ΔR of 0.2 of the true lepton from the tau decay. The per-lepton fiducial efficiency, ϵ_ℓ , is defined as the ratio of the number of reconstructed leptons satisfying all selection criteria to the number of generated leptons within acceptance. Separate values of ϵ_ℓ are measured for each lepton flavour, and ϵ_ℓ is determined separately for leptons from tau decays. The effects of the trigger requirements are folded into the per-lepton efficiencies; for SM WZ events with both bosons on-shell, the trigger efficiency is over 95% when all offline selection criteria are applied.

The efficiencies as functions of p_T are shown in table 6, and efficiencies as functions of $|\eta|$ for electrons and taus are shown in table 7. For empty bins, the value from the preceding filled bin is the suggested central value. For electrons and taus, the final per-lepton efficiency is given as $\epsilon_\ell = \epsilon(p_T) \cdot \epsilon(\eta)/\langle \epsilon \rangle$, where $\langle \epsilon \rangle$ is the inclusive efficiency of the full sample, and is 0.66 for prompt electrons, 0.39 for electrons from tau decays, and 0.26 for hadronically decaying taus. The η dependence of the muon efficiencies is treated by separate p_T efficiency measurements for muons with $|\eta| < 0.1$ and those with $|\eta| \geq 0.1$.

Table 6 includes entries to cover cases where leptons with true p_T below the nominal p_T threshold of 15 (20) GeV for electrons and muons (taus) are reconstructed with p_T above threshold. These efficiencies are typically small, but are needed for proper modelling of events with low- p_T leptons.

The resulting per-lepton efficiencies are then combined to yield a selection efficiency for a given event satisfying the fiducial acceptance criteria. For events with exactly three leptons, the total efficiency for the event is the product of the individual lepton efficiencies. For events with more than three leptons, the additional leptons in order of descending p_T only contribute to the total efficiency when a lepton with higher p_T is not selected, leading to terms such as $\epsilon_1 \epsilon_2 \epsilon_4 (1 - \epsilon_3)$, where ϵ_i denotes the fiducial efficiency for the i^{th} p_T -ordered lepton. The method can be extended to cover the number of leptons expected in the model under consideration.

$ \eta $	Prompt e	$\tau \rightarrow e$	τ_{had}
0.0–0.1	0.650 ± 0.006	0.55 ± 0.06	0.166 ± 0.017
0.1–0.5	0.714 ± 0.004	0.500 ± 0.026	0.150 ± 0.009
0.5–1.0	0.722 ± 0.004	0.513 ± 0.026	0.188 ± 0.010
1.0–1.5	0.689 ± 0.004	0.421 ± 0.026	0.175 ± 0.010
1.5–2.0	0.635 ± 0.004	0.470 ± 0.030	0.142 ± 0.009
2.0–2.5	0.615 ± 0.004	0.433 ± 0.032	0.109 ± 0.008

Table 7. The fiducial efficiency for electrons and taus in different η ranges ($\epsilon_{\text{fid}}(\eta)$). For electrons from tau decays, the η is that of the electron, not the tau. The uncertainties shown reflect the statistical uncertainties of the simulated samples only.

Jets at the particle level are reconstructed from all stable particles, excluding muons and neutrinos, with the anti- k_t algorithm using a radius parameter $R = 0.4$. Overlaps between jets and leptons are removed as described in section 3. E_T^{miss} is defined as the magnitude of the vector sum of the transverse momenta of all neutrinos and any stable, non-interacting particles produced in models of new phenomena. The kinematic variables used to define signal regions are defined as in section 3.

Predictions of both the rates and kinematic properties of doubly charged Higgs and excited-lepton events, when made with the method described above, agree well with the same quantities after detector simulation. Uncertainties, based on the level of agreement seen across the studied models, are estimated at 10% for the $\geq 3e/\mu$ channels, and 20% for the $2e/\mu + \geq 1\tau_{\text{had}}$ channels. When calculating limits on specific models, these uncertainties must be applied to the estimated signal yields after selection to take into account the limited precision of the fiducial efficiency approach.

10 Interpretation

The results of the model-independent search are interpreted in the context of two specific models of new phenomena: a model with pair-produced doubly charged Higgs bosons, and a model with excited, non-elementary leptons.

Doubly charged Higgs bosons can be either pair-produced or produced in association with a singly charged state. In this paper, the $H^{\pm\pm}$ are assumed to be pair-produced, with decays to charged leptons. One feature of most models with $H^{\pm\pm}$ is the presence of lepton-flavour-violating terms, leading to decays such as $H^{\pm\pm} \rightarrow e^\pm \mu^\pm$ in addition to $H^{\pm\pm} \rightarrow e^\pm e^\pm$ or $H^{\pm\pm} \rightarrow \mu^\pm \mu^\pm$. Decays to electrons and/or muons have been probed at $\sqrt{s} = 8 \text{ TeV}$ in ref. [71], while decays to all flavours of leptons are probed at $\sqrt{s} = 7 \text{ TeV}$ in ref. [72]. In this paper, only the lepton-flavour-violating decays $H^{\pm\pm} \rightarrow e^\pm \tau^\pm$ and $H^{\pm\pm} \rightarrow \mu^\pm \tau^\pm$ are considered.

The visible cross-section limits presented above are used to constrain this model. The off- Z , OSSF category provides the largest acceptance for the lepton-flavour-violating decays; contributions from the remaining categories are small and have a negligible impact on the sensitivity. The signal regions based on H_T^{leptons} provide the best expected sen-

		Channel	$H^{\pm\pm}$ mass and decay mode					
			100 GeV		300 GeV		500 GeV	
σ [fb]	Combined	504		5.55		0.396		
\mathcal{A}	$\geq 3e/\mu$	0.14 ± 0.01	0.15 ± 0.01	0.35 ± 0.01	0.38 ± 0.02	0.39 ± 0.02	0.45 ± 0.02	
	$2e/\mu + \geq 1\tau_{\text{had}}$	0.33 ± 0.01	0.36 ± 0.01	0.48 ± 0.02	0.49 ± 0.02	0.49 ± 0.02	0.47 ± 0.02	
ϵ_{fid}	$\geq 3e/\mu$	0.24 ± 0.02	0.26 ± 0.02	0.36 ± 0.02	0.37 ± 0.01	0.40 ± 0.02	0.37 ± 0.01	
	$2e/\mu + \geq 1\tau_{\text{had}}$	0.21 ± 0.01	0.24 ± 0.01	0.29 ± 0.01	0.31 ± 0.01	0.32 ± 0.01	0.31 ± 0.01	
$\mathcal{A} \times \epsilon_{\text{fid}}$	$\geq 3e/\mu$	0.034 ± 0.002	0.039 ± 0.003	0.12 ± 0.01	0.14 ± 0.01	0.16 ± 0.01	0.17 ± 0.01	
	$2e/\mu + \geq 1\tau_{\text{had}}$	0.071 ± 0.003	0.087 ± 0.004	0.14 ± 0.01	0.15 ± 0.01	0.15 ± 0.01	0.14 ± 0.01	
Rec. $\mathcal{A} \times \epsilon$	$\geq 3e/\mu$	0.034 ± 0.004	0.046 ± 0.005	0.12 ± 0.01	0.12 ± 0.01	0.13 ± 0.01	0.14 ± 0.01	
	$2e/\mu + \geq 1\tau_{\text{had}}$	0.062 ± 0.006	0.083 ± 0.007	0.14 ± 0.01	0.16 ± 0.01	0.16 ± 0.01	0.18 ± 0.01	
Exp. Limit [fb]	$\geq 3e/\mu$	53^{+26}_{-17}	54^{+25}_{-17}	$5.0^{+2.6}_{-0.9}$	$6.7^{+3.0}_{-1.9}$	$2.7^{+1.4}_{-0.7}$	$2.3^{+1.0}_{-0.6}$	
	$2e/\mu + \geq 1\tau_{\text{had}}$	54^{+21}_{-14}	38^{+14}_{-10}	$2.6^{+0.4}_{-0.2}$	$2.4^{+0.4}_{-0.2}$	$1.3^{+0.5}_{-0.2}$	$1.1^{+0.5}_{-0.2}$	
	Combined	42^{+18}_{-12}	34^{+14}_{-9}	$2.6^{+0.4}_{-0.2}$	$2.6^{+1.0}_{-0.4}$	$1.2^{+0.5}_{-0.2}$	$1.1^{+0.4}_{-0.2}$	
Obs. Limit [fb]	$\geq 3e/\mu$	32	32	3.2	4.2	1.7	1.5	
	$2e/\mu + \geq 1\tau_{\text{had}}$	51	36	2.4	2.2	1.2	1.0	
	Combined	28	24	2.4	1.9	0.8	0.7	

Table 8. Theoretical cross section and the acceptances, efficiencies and 95% CL upper limits on the cross section for pair-produced $H^{\pm\pm}$ decaying to $e^\pm\tau^\pm$ and $\mu^\pm\tau^\pm$. Rec. $\mathcal{A} \times \epsilon$ represents the fraction of signal events passing all analysis cuts after detector-level simulation and event reconstruction.

sitivity, followed by limits based on $p_T^{\ell, \text{min}}$; here only limits based on H_T^{leptons} are used. For $H^{\pm\pm}$ masses up to 200 GeV, the signal region defined by $H_T^{\text{leptons}} > 200$ GeV is used; for higher masses the requirement is $H_T^{\text{leptons}} > 500$ GeV. Finally, both the $\geq 3e/\mu$ and $2e/\mu + \geq 1\tau_{\text{had}}$ channels are used to maximize the total acceptance.

Table 8 summarizes the expected acceptance, efficiency, and cross-section limit for several mass values, channels, and decay scenarios. The $\geq 3e/\mu$ and $2e/\mu + \geq 1\tau_{\text{had}}$ channels have comparable sensitivity for high masses, and are therefore combined when setting the final limits to improve the overall constraint on this model. The $H^{\pm\pm}$ can couple preferentially to left-handed ($H_L^{\pm\pm}$) or right-handed ($H_R^{\pm\pm}$) leptons, with the production cross section for the right-handed coupling scenario being roughly half that for the left-handed coupling scenario. The acceptance and efficiency are the same for both couplings. The final limits on $H^{\pm\pm} \rightarrow e^\pm\tau^\pm$ and $H^{\pm\pm} \rightarrow \mu^\pm\tau^\pm$ for both scenarios are shown in figure 5. In both cases, a branching ratio of 100% is assumed for the chosen decay. For $H^{\pm\pm} \rightarrow e^\pm\tau^\pm$, the expected mass limit for left-handed couplings is 350 ± 50 GeV, with an observed limit of 400 GeV. For $H^{\pm\pm} \rightarrow \mu^\pm\tau^\pm$, the expected mass limit for left-handed couplings is 370^{+20}_{-40} GeV, with an observed limit at 400 GeV. The expected (observed) limit on $H^{\pm\pm} \rightarrow \mu^\pm\tau^\pm$ from the 7 TeV ATLAS analysis [33] is 229 (237) GeV, which only uses the $\geq 3e/\mu$ channel. The corresponding observed limits from the 7 TeV CMS analysis [72] are 293 GeV for $H^{\pm\pm} \rightarrow e^\pm\tau^\pm$ and 300 GeV for $H^{\pm\pm} \rightarrow \mu^\pm\tau^\pm$.

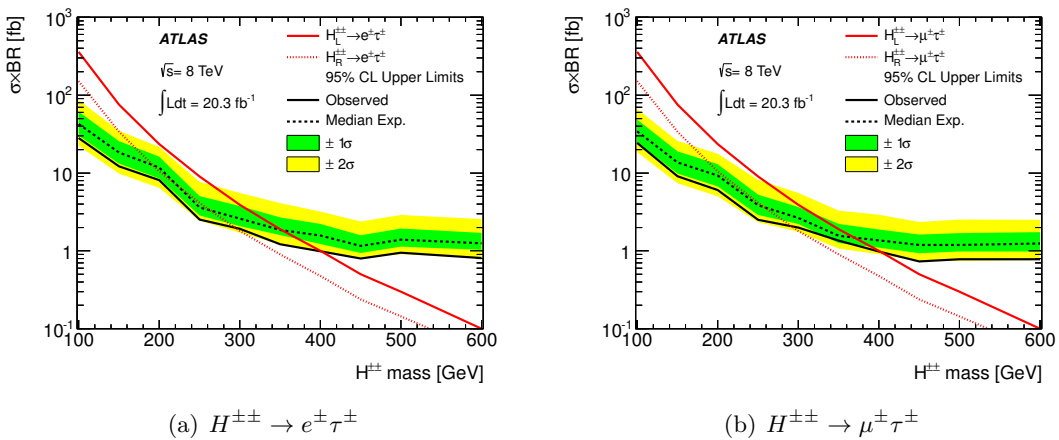


Figure 5. Observed and expected 95% upper limits on the cross section times branching ratio for $H^{\pm\pm}$ decaying to (a) $e^\pm \tau^\pm$ and (b) $\mu^\pm \tau^\pm$. Separate mass constraints are extracted for $H^{\pm\pm}$ coupling to left- and right-handed fermions from the intersections with the predicted cross sections shown by the dotted and solid red curves.

Composite fermion models often imply the existence of excited-lepton states [25]. Excited leptons are either pair-produced, produced in association with another excited lepton of a different flavour, or produced in association with a SM lepton [6, 7]. The production is mediated either by gauge bosons (gauge-mediated, GM) or by auxiliary, massive fields that can be approximated as a four-fermion contact interaction (CI) vertex. The scales of the CI and GM processes are assumed to be identical and called Λ , while the masses of the excited leptons are referred to as m_{ℓ^*} . The CI process dominates the production and decay of excited leptons for $m_{\ell^*}/\Lambda > 0.3$, while for lower values the GM process becomes important. Additionally, the parameters f_s , f and f' , corresponding to the SU(3), SU(2) and U(1) couplings of the model respectively, can be chosen arbitrarily and dictate the dynamics of the model. For this study, all coupling parameters are set to unity, as used in ref. [25]. This specific choice of $f = f'$ forbids the radiative decays of excited neutrinos.

Searches for excited electrons and muons have been performed using a similar benchmark model by CMS [73], at $\sqrt{s} = 7$ TeV, and by ATLAS [74], with 13 fb^{-1} at $\sqrt{s} = 8$ TeV. The most stringent lower limits on m_{ℓ^*} from these searches are at 2.2 TeV for $\Lambda = m_{\ell^*}$. Lower limits on the mass of excited leptons were set by the L3 experiment. These limits, which are independent of Λ , range from 91 GeV to 102 GeV, with limits on excited taus and excited tau neutrinos being somewhat weaker than those for other flavours [75].

The decay products for each excited neutrino are a neutrino (or charged lepton) of the same generation and a Z (W) boson, or a fermion pair. Similarly, excited charged leptons can decay into a charged lepton (or neutrino) of the same generation and a γ/Z (or W) boson, or into a fermion pair. For excited neutrinos, only the pair production of two excited neutrinos $\nu^* \bar{\nu}^*$ is taken into account; single production of excited neutrinos producing final states with three or more leptons is suppressed and its contribution is negligible. For the excited charged leptons, both single and pair production of excited states are taken into

account.

The upper limits on the visible cross section can be used to constrain m_{ℓ^*} and Λ . In all cases, the signal region with the best expected sensitivity is used to constrain each scenario. In the cases where the excited charged lepton or neutrino masses are large, the decay products typically carry a large amount of momentum. This leads to signal events with large H_T^{leptons} . Additionally, in this regime, the GM decay through Z bosons is disfavoured compared to the CI decay. Consequently, for such scenarios, the off- Z channel provides better sensitivity due to lower background rates.

The production of excited electrons, excited muons, and excited electron and muon neutrinos is constrained using the $\geq 3e/\mu$, off- Z , OSSF region requiring $H_T^{\text{leptons}} > 800 \text{ GeV}$ ($H_T^{\text{leptons}} > 500 \text{ GeV}$) for masses above (below) 600 GeV . Excited tau neutrinos with high values of m_{ℓ^*}/Λ are constrained using the $\geq 3e/\mu$, off- Z , OSSF region requiring $m_{\text{eff}} > 1.5 \text{ TeV}$. The only excited tau neutrino decays that preferentially produce final states with taus are the GM decays via a W boson, which become significant at lower values of m_{ℓ^*}/Λ . For such cases, the $2e/\mu + \geq 1\tau_{\text{had}}$, off- Z , no-OSSF region requiring $p_T^{\ell,\min} > 100 \text{ GeV}$ is used.

For excited taus, the $\geq 3e/\mu$, off- Z , OSSF region requiring $m_{\text{eff}} > 1.5 \text{ TeV}$ is used for masses above 1 TeV . For masses between 500 GeV and 1 TeV , the $\geq 3e/\mu$, off- Z , OSSF regions requiring $m_{\text{eff}} > 1 \text{ TeV}$ is used. For masses below 500 GeV , where the GM decay through Z bosons again becomes significant, the $2e/\mu + \geq 1\tau_{\text{had}}$, on- Z region requiring $p_T^{\ell,\min} > 100 \text{ GeV}$ is most sensitive.

Table 9 summarizes the expected acceptance and efficiency for several flavours, mass values and Λ values for the most sensitive signal region. Figure 6 shows the excluded regions of the mass parameter and the scale Λ for all lepton flavours extracted from the expected and observed upper limits on the visible cross section. Exclusion regions are also shown for the case where excited leptons are only produced via the CI process.

For low Λ -values, a broad range of masses up to 2 TeV can be excluded, while for higher Λ -values, only low masses are excluded. In the low-mass region, $\nu_\ell^* \rightarrow \ell + W$ is the main decay mode for excited neutrinos, while $\ell^* \rightarrow \ell + \gamma$ is the main decay mode for charged leptons. Therefore, pair-produced ν_e^* and ν_μ^* have the highest acceptance due to their final states with at least three leptons, and thus they have the most stringent limits.

The production cross section of pair-produced excited leptons via the GM process is independent of Λ , which leads to improved sensitivity at low excited-lepton masses. The low efficiency for reconstructing tau leptons leads to a relatively small gain in sensitivity for ν_τ^* from GM production.

For ν_e^* (ν_μ^*), the expected Λ -independent mass limit is $210 \pm 25 \text{ GeV}$ ($225 \pm 25 \text{ GeV}$), with an observed limit of 230 GeV (250 GeV). For masses higher than 300 GeV , the limits for these two particles follow approximately a line of: $\Lambda + 8.3 \times m_{\nu_\ell^*} = 14500 \text{ GeV}$. The most stringent upper limits on the mass of the excited leptons are found when $m_{\ell^*} = \Lambda$. In this case, the resulting limits are 3.0 TeV for excited electrons and muons, 2.5 TeV for excited taus, and 1.6 TeV for every excited-neutrino flavour.

	m_{ℓ^*} [GeV]	σ [fb]	\mathcal{A}	ϵ_{fid}	$\mathcal{A} \times \epsilon_{\text{fid}}$	Rec. $\mathcal{A} \times \epsilon$	Limit [fb]
$\Lambda = 4 \text{ TeV}$							
$\nu_e^* \bar{\nu}_e^*$	500	127	0.036 ± 0.001	0.63 ± 0.07	0.023 ± 0.003	0.023 ± 0.001	6.5
$\nu_e^* \bar{\nu}_e^*$	1500	0.562	0.041 ± 0.001	0.66 ± 0.07	0.027 ± 0.003	0.027 ± 0.001	5.6
$\nu_\mu^* \bar{\nu}_\mu^*$	500	127	0.036 ± 0.001	0.51 ± 0.06	0.018 ± 0.003	0.022 ± 0.001	6.8
$\nu_\mu^* \bar{\nu}_\mu^*$	1500	0.562	0.039 ± 0.001	0.52 ± 0.06	0.020 ± 0.004	0.025 ± 0.001	6.0
$\nu_\tau^* \bar{\nu}_\tau^*$	500	127	0.0022 ± 0.0003	0.43 ± 0.05	0.0009 ± 0.0003	0.0010 ± 0.0002	150
$\nu_\tau^* \bar{\nu}_\tau^*$	1500	0.562	0.014 ± 0.001	0.52 ± 0.06	0.007 ± 0.002	0.008 ± 0.001	19
$\tau^* \bar{\tau}^*$	500	127	0.0011 ± 0.0002	0.40 ± 0.04	0.0004 ± 0.0001	0.0002 ± 0.0001	750
$\tau^* \bar{\tau}^*$	1500	0.562	0.027 ± 0.001	0.29 ± 0.03	0.008 ± 0.002	0.006 ± 0.001	25
$\tau^* \bar{\tau}$	500	276	0.0012 ± 0.0002	0.47 ± 0.05	0.0006 ± 0.0002	0.0007 ± 0.0002	210
$\tau^* \bar{\tau}$	1500	1.41	0.032 ± 0.001	0.48 ± 0.05	0.015 ± 0.002	0.015 ± 0.001	10
$\Lambda = 10 \text{ TeV}$							
$\nu_e^* \bar{\nu}_e^*$	500	3.24	0.044 ± 0.001	0.61 ± 0.07	0.027 ± 0.004	0.030 ± 0.001	5.0
$\nu_e^* \bar{\nu}_e^*$	1500	0.015	0.088 ± 0.002	0.66 ± 0.07	0.058 ± 0.007	0.056 ± 0.002	2.7
$\nu_\mu^* \bar{\nu}_\mu^*$	500	3.24	0.041 ± 0.001	0.54 ± 0.06	0.022 ± 0.003	0.028 ± 0.001	5.4
$\nu_\mu^* \bar{\nu}_\mu^*$	1500	0.015	0.084 ± 0.002	0.50 ± 0.05	0.042 ± 0.006	0.052 ± 0.002	2.9
$\nu_\tau^* \bar{\nu}_\tau^*$	500	3.24	0.0020 ± 0.0006	0.19 ± 0.02	0.0004 ± 0.0002	0.0005 ± 0.0001	300
$\nu_\tau^* \bar{\nu}_\tau^*$	1500	0.015	0.012 ± 0.002	0.36 ± 0.04	0.0043 ± 0.0008	0.0045 ± 0.0004	33
$\tau^* \bar{\tau}^*$	500	3.24	0.0002 ± 0.0001	0.33 ± 0.04	0.0001 ± 0.0001	0.0001 ± 0.0001	1500
$\tau^* \bar{\tau}^*$	1500	0.015	0.0070 ± 0.0001	0.17 ± 0.02	0.0012 ± 0.0007	0.0022 ± 0.0003	68
$\tau^* \bar{\tau}$	500	3.81	0.0003 ± 0.0001	0.53 ± 0.06	0.0002 ± 0.0002	0.0002 ± 0.0002	750
$\tau^* \bar{\tau}$	1500	0.022	0.012 ± 0.001	0.48 ± 0.05	0.0056 ± 0.0015	0.0048 ± 0.0004	31

Table 9. Cross section, acceptances, efficiencies, and 95% CL upper limits on the cross section for various excited-lepton flavours and mass values using the $\geq 3e/\mu$, off- Z , OSSF region requiring $H_T^{\text{leptons}} > 800 \text{ GeV}$. The observed limit is equal to the expected limit in this signal region. Rec. $\mathcal{A} \times \epsilon$ represents the fraction of signal events passing all analysis cuts after detector-level simulation and event reconstruction.

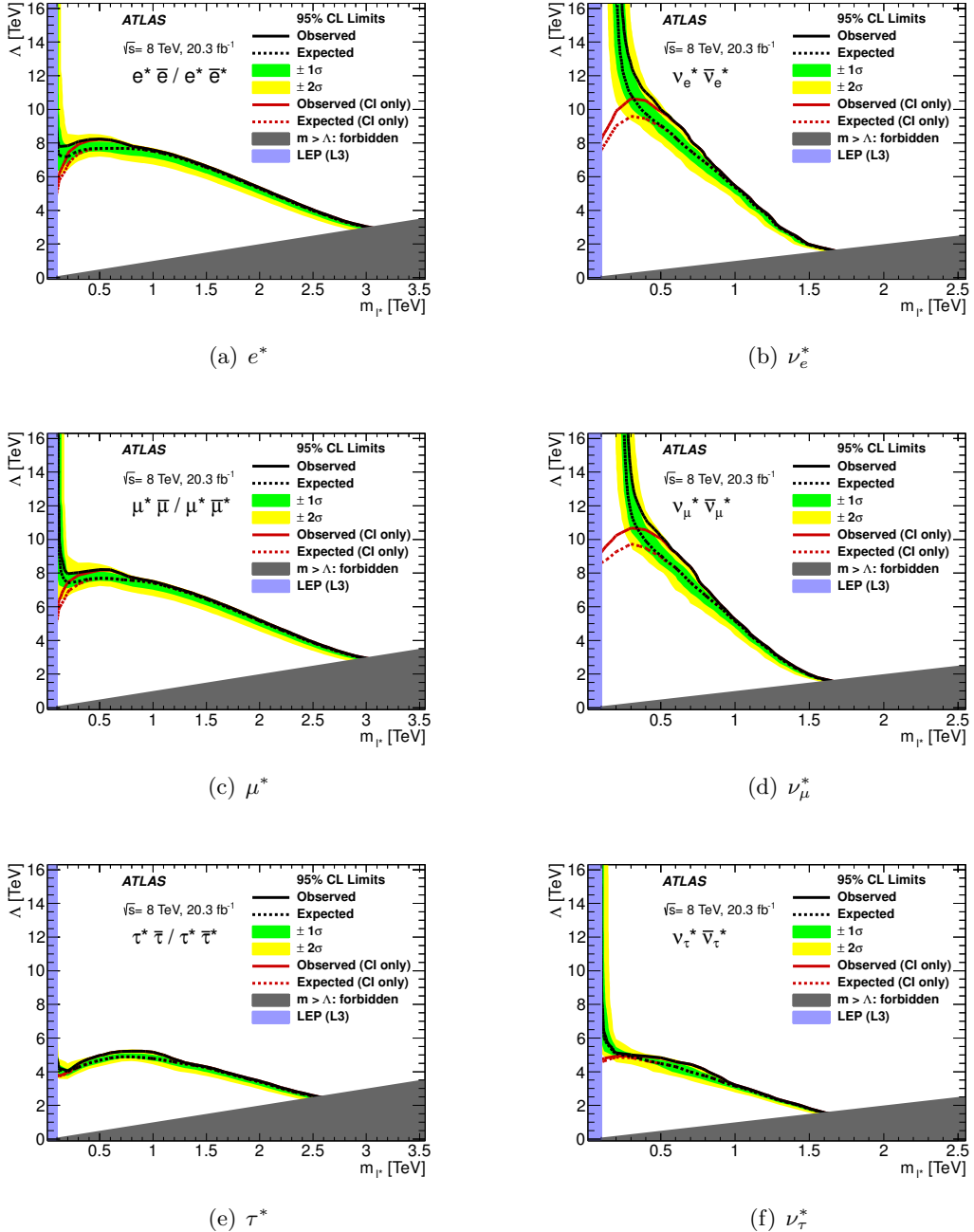


Figure 6. Observed and expected 95% CL limits on the mass parameter and the compositeness scale Λ for excited leptons. The region under the curve is excluded by this analysis, the blue region is excluded by LEP, and the gray region represents $m_{\ell^*} > \Lambda$ and is unphysical. The red line shows the limits taking only CI production into account.

11 Conclusion

A search for anomalous production of events with at least three charged leptons is presented, using 20.3 fb^{-1} of pp collisions at $\sqrt{s} = 8\text{ TeV}$ recorded by the ATLAS detector at the CERN Large Hadron Collider. Data distributions are compared to SM predictions in a variety of observables and final states, designed to probe a large range of BSM scenarios. Good agreement between the data and SM predictions is observed. Model-independent exclusion limits on visible cross sections are derived, and a prescription to re-interpret such limits for any model is presented. Additionally, limits are set on specific models predicting doubly charged Higgs bosons and excited leptons. Doubly charged Higgs bosons coupling to left-handed fermions and decaying exclusively to $e\tau$ or $\mu\tau$ pairs are constrained to have mass above 400 GeV at 95% confidence level. For excited leptons, the mass constraints depend on the compositeness scale, with the strongest mass constraints reached where the mass of the excited state and the compositeness scale are the same; the lower limits on the mass extend to 3.0 TeV for excited electrons and excited muons, 2.5 TeV for excited taus, and 1.6 TeV for every excited-neutrino flavour.

Acknowledgments

We thank CERN for the very successful operation of the LHC, as well as the support staff from our institutions without whom ATLAS could not be operated efficiently.

We acknowledge the support of ANPCyT, Argentina; YerPhI, Armenia; ARC, Australia; BMWFW and FWF, Austria; ANAS, Azerbaijan; SSTC, Belarus; CNPq and FAPESP, Brazil; NSERC, NRC and CFI, Canada; CERN; CONICYT, Chile; CAS, MOST and NSFC, China; COLCIENCIAS, Colombia; MSMT CR, MPO CR and VSC CR, Czech Republic; DNRF, DNSRC and Lundbeck Foundation, Denmark; EPLANET, ERC and NSRF, European Union; IN2P3-CNRS, CEA-DSM/IRFU, France; GNSF, Georgia; BMBF, DFG, HGF, MPG and AvH Foundation, Germany; GSRT and NSRF, Greece; RGC, Hong Kong SAR, China; ISF, MINERVA, GIF, I-CORE and Benoziyo Center, Israel; INFN, Italy; MEXT and JSPS, Japan; CNRST, Morocco; FOM and NWO, Netherlands; BRF and RCN, Norway; MNiSW and NCN, Poland; GRICES and FCT, Portugal; MNE/IFA, Romania; MES of Russia and NRC KI, Russian Federation; JINR; MSTD, Serbia; MSSR, Slovakia; ARRS and MIZŠ, Slovenia; DST/NRF, South Africa; MINECO, Spain; SRC and Wallenberg Foundation, Sweden; SER, SNSF and Cantons of Bern and Geneva, Switzerland; NSC, Taiwan; TAEK, Turkey; STFC, the Royal Society and Leverhulme Trust, United Kingdom; DOE and NSF, United States of America.

The crucial computing support from all WLCG partners is acknowledged gratefully, in particular from CERN and the ATLAS Tier-1 facilities at TRIUMF (Canada), NDGF (Denmark, Norway, Sweden), CC-IN2P3 (France), KIT/GridKA (Germany), INFN-CNAF (Italy), NL-T1 (Netherlands), PIC (Spain), ASGC (Taiwan), RAL (U.K.) and BNL (U.S.A.) and in the Tier-2 facilities worldwide.

A Yields and cross-section limits

Expected and observed event yields for all signal regions are provided in tables 10–17.

$H_T^{\text{leptons}} \geq$	$t\bar{t} + V(V)$	$VV(V)$	Reducible	Total	Observed
$\geq 3e/\mu, \text{off-}Z, \text{no-OSSF}$					
200 GeV	2.0 ± 0.6	1.6 ± 0.4	2.1 ± 1.1	5.7 ± 1.4	6
500 GeV	0.13 ± 0.06	0.09 ± 0.03	0 ± 0.7	0.22 ± 0.22	1
800 GeV	0.06 ± 0.04	0 ± 0.03	0 ± 0.7	0.06 ± 0.06	0
$2e/\mu+ \geq 1\tau, \text{off-}Z, \text{no-OSSF}$					
200 GeV	1.2 ± 0.4	2.3 ± 0.5	19 ± 6	22 ± 6	14
500 GeV	0.01 ± 0.01	0.03 ± 0.01	0.32 ± 0.32	0.36 ± 0.36	0
800 GeV	0 ± 0.003	0.01 ± 0.01	0.11 ± 0.11	0.12 ± 0.12	0
$\geq 3e/\mu, \text{off-}Z, \text{OSSF}$					
200 GeV	7.5 ± 2.3	63 ± 8	9 ± 4	78 ± 9	56
500 GeV	0.34 ± 0.12	3.3 ± 0.5	0 ± 0.7	3.7 ± 0.9	1
800 GeV	0.01 ± 0.01	0.54 ± 0.12	0 ± 0.7	0.5 ± 0.5	0
$2e/\mu+ \geq 1\tau, \text{OSSF}$					
200 GeV	0.64 ± 0.21	4.4 ± 0.6	68 ± 20	73 ± 20	67
500 GeV	0.06 ± 0.03	0.17 ± 0.04	1.1 ± 0.9	1.3 ± 0.9	0
800 GeV	0 ± 0.003	0 ± 0.03	0 ± 0.7	0 ± 0.7	0
$\geq 3e/\mu, \text{on-}Z$					
200 GeV	23 ± 7	410 ± 50	18 ± 8	450 ± 50	387
500 GeV	0.82 ± 0.25	10.9 ± 2.3	0.6 ± 0.8	12.3 ± 2.4	12
800 GeV	0.05 ± 0.03	0.92 ± 0.23	0.10 ± 0.10	1.1 ± 0.7	3
$2e/\mu+ \geq 1\tau, \text{on-}Z$					
200 GeV	1.1 ± 0.4	20.7 ± 2.7	160 ± 50	180 ± 50	148
500 GeV	0.02 ± 0.01	0.82 ± 0.23	1.2 ± 0.9	2.0 ± 1.0	3
800 GeV	0 ± 0.003	0.04 ± 0.02	0 ± 0.71	0.04 ± 0.04	0

Table 10. Expected and observed event yields for the H_T^{leptons} signal regions.

$p_T^{\ell, \text{min}} \geq$	$t\bar{t} + V(V)$	$VV(V)$	Reducible	Total	Observed
$\geq 3e/\mu, \text{off-}Z, \text{no-OSSF}$					
50 GeV	0.83 ± 0.27	0.45 ± 0.13	$0.28^{+0.70}_{-0.28}$	1.6 ± 0.8	4
100 GeV	0.09 ± 0.04	0.03 ± 0.01	$0^{+0.7}_{-0}$	$0.12^{+0.69}_{-0.12}$	0
150 GeV	0.06 ± 0.04	$0^{+0.03}_{-0}$	$0^{+0.7}_{-0}$	$0.06^{+0.70}_{-0.06}$	0
$2e/\mu + \geq 1\tau, \text{off-}Z, \text{no-OSSF}$					
50 GeV	0.43 ± 0.15	0.62 ± 0.13	5.0 ± 1.9	6.1 ± 1.9	5
100 GeV	0.01 ± 0.01	$0.03^{+0.05}_{-0.03}$	$0.11^{+0.71}_{-0.11}$	$0.15^{+0.72}_{-0.15}$	0
150 GeV	$0^{+0.005}_{-0}$	0.01 ± 0.00	$0.11^{+0.71}_{-0.11}$	$0.12^{+0.71}_{-0.12}$	0
$\geq 3e/\mu, \text{off-}Z, \text{OSSF}$					
50 GeV	3.7 ± 1.1	27.1 ± 3.4	1.8 ± 1.0	33 ± 4	25
100 GeV	0.17 ± 0.07	1.73 ± 0.25	$0^{+0.7}_{-0}$	1.9 ± 0.7	2
150 GeV	0.01 ± 0.01	0.24 ± 0.05	$0^{+0.7}_{-0}$	$0.25^{+0.69}_{-0.25}$	0
$2e/\mu + \geq 1\tau, \text{off-}Z, \text{OSSF}$					
50 GeV	0.33 ± 0.11	1.72 ± 0.25	15 ± 5	18 ± 5	23
100 GeV	$0^{+0.003}_{-0}$	0.14 ± 0.06	$0.12^{+0.72}_{-0.12}$	$0.26^{+0.72}_{-0.26}$	0
150 GeV	$0^{+0.003}_{-0}$	$0^{+0.03}_{-0}$	$0^{+0.7}_{-0}$	$0^{+0.7}_{-0}$	0
$\geq 3e/\mu, \text{on-}Z$					
50 GeV	8.7 ± 2.6	168 ± 19	6.3 ± 3.1	183 ± 19	163
100 GeV	0.54 ± 0.17	9.6 ± 1.6	$0.22^{+0.72}_{-0.22}$	10.4 ± 1.7	16
150 GeV	0.05 ± 0.02	0.88 ± 0.21	$0^{+0.7}_{-0}$	0.9 ± 0.7	4
$2e/\mu + \geq 1\tau, \text{on-}Z$					
50 GeV	0.31 ± 0.11	8.0 ± 1.2	54 ± 18	62 ± 18	45
100 GeV	0.01 ± 0.01	0.53 ± 0.22	$0.8^{+0.8}_{-0.8}$	1.3 ± 0.9	0
150 GeV	$0^{+0.003}_{-0}$	0.09 ± 0.07	$0.16^{+0.72}_{-0.16}$	$0.25^{+0.73}_{-0.25}$	0

Table 11. Expected and observed event yields for the minimum p_T^ℓ signal regions.

$b\text{-tags} \geq$	$t\bar{t} + V(V)$	$VV(V)$	Reducible	Total	Observed
$\geq 3e/\mu, \text{off-}Z, \text{no-OSSF}$					
1	5.3 ± 1.7	0.37 ± 0.12	11.1 ± 3.3	17 ± 4	19
2	2.2 ± 0.7	$0^{+0.03}_{-0}$	2.2 ± 1.0	4.4 ± 1.2	5
$2e/\mu + \geq 1\tau, \text{off-}Z, \text{no-OSSF}$					
1	3.1 ± 1.0	0.9 ± 0.4	91 ± 24	95 ± 24	98
2	1.3 ± 0.5	0.05 ± 0.03	29 ± 8	30 ± 8	34
$\geq 3e/\mu, \text{off-}Z, \text{OSSF}$					
1	13 ± 4	11.4 ± 2.0	15 ± 5	39 ± 7	34
2	5.5 ± 1.8	0.32 ± 0.17	2.7 ± 2.1	8.5 ± 2.8	9
$2e/\mu + \geq 1\tau, \text{off-}Z, \text{OSSF}$					
1	1.09 ± 0.35	0.88 ± 0.28	74 ± 21	76 ± 21	65
2	0.38 ± 0.19	$0.05^{+0.06}_{-0.05}$	17 ± 5	17 ± 5	12
$\geq 3e/\mu, \text{on-}Z$					
1	51 ± 16	144 ± 23	41 ± 11	235 ± 32	237
2	23 ± 8	8.0 ± 2.1	4.6 ± 1.5	36 ± 8	27
$2e/\mu + \geq 1\tau, \text{on-}Z$					
1	2.9 ± 0.9	8.8 ± 1.7	398 ± 11	410 ± 11	409
2	1.3 ± 0.4	0.26 ± 0.17	33 ± 9	34 ± 9	21

Table 12. Expected and observed event yields for the b -tag signal regions.

$m_{\text{eff}} \geq$	$t\bar{t} + V(V)$	$VV(V)$	Reducible	Total	Observed
$\geq 3e/\mu, \text{ off-}Z, \text{ no-OSSF}$					
600 GeV	1.7 ± 0.6	0.40 ± 0.13	1.2 ± 0.8	3.4 ± 1.0	3
1000 GeV	0.44 ± 0.16	$0.01^{+0.03}_{-0.01}$	$0.20^{+0.70}_{-0.20}$	0.7 ± 0.7	1
1500 GeV	$0.07^{+0.09}_{-0.07}$	$0^{+0.03}_{-0}$	$0.08^{+0.69}_{-0.08}$	$0.16^{+0.70}_{-0.16}$	0
$2e/\mu + \geq 1\tau, \text{ off-}Z, \text{ no-OSSF}$					
600 GeV	1.4 ± 0.5	1.23 ± 0.32	17 ± 5	19 ± 5	22
1000 GeV	0.26 ± 0.22	0.07 ± 0.05	2.2 ± 1.1	2.6 ± 1.1	2
1500 GeV	0.03 ± 0.02	0.01 ± 0.01	$0.17^{+0.73}_{-0.17}$	$0.20^{+0.73}_{-0.20}$	1
$\geq 3e/\mu, \text{ off-}Z, \text{ OSSF}$					
600 GeV	6.7 ± 2.1	13.4 ± 2.9	3.7 ± 2.5	24 ± 4	17
1000 GeV	1.1 ± 0.4	2.1 ± 0.8	$2.1^{+2.1}_{-2.1}$	5.3 ± 2.3	1
1500 GeV	0.08 ± 0.08	0.28 ± 0.15	$0.5^{+0.9}_{-0.5}$	$0.8^{+0.9}_{-0.8}$	0
$2e/\mu + \geq 1\tau, \text{ off-}Z, \text{ OSSF}$					
600 GeV	0.59 ± 0.19	0.87 ± 0.30	17 ± 5	18 ± 5	19
1000 GeV	0.17 ± 0.06	0.12 ± 0.10	1.8 ± 1.0	2.1 ± 1.0	2
1500 GeV	$0^{+0.003}_{-0}$	$0^{+0.05}_{-0}$	$0^{+0.7}_{-0}$	$0^{+0.7}_{-0}$	0
$\geq 3e/\mu, \text{ on-}Z$					
600 GeV	26 ± 8	126 ± 29	9.2 ± 3.5	161 ± 31	147
1000 GeV	4.6 ± 1.5	21 ± 8	1.1 ± 1.0	27 ± 8	27
1500 GeV	0.48 ± 0.17	3.2 ± 1.9	$0^{+0.6}_{-0}$	3.7 ± 2.0	2
$2e/\mu + \geq 1\tau, \text{ on-}Z$					
600 GeV	1.4 ± 0.5	8.7 ± 2.1	65 ± 19	75 ± 19	65
1000 GeV	0.26 ± 0.09	1.5 ± 0.6	3.6 ± 1.4	5.3 ± 1.6	11
1500 GeV	0.02 ± 0.02	0.31 ± 0.21	$0.08^{+0.71}_{-0.08}$	$0.4^{+0.7}_{-0.4}$	1

Table 13. Expected and observed event yields for the inclusive m_{eff} signal regions.

$m_{\text{eff}} \geq$	$t\bar{t} + V(V)$	$VV(V)$	Reducible	Total	Observed
$\geq 3e/\mu, \text{ off-}Z, \text{ no-OSSF}$					
Inclusive	1.7 ± 0.6	0.90 ± 0.24	4.0 ± 1.5	6.6 ± 1.6	8
600 GeV	0.71 ± 0.27	0.25 ± 0.06	0.8 ± 0.8	1.7 ± 0.8	2
1000 GeV	0.24 ± 0.15	0.01 ± 0.00	$0.15^{+0.70}_{-0.15}$	$0.4^{+0.7}_{-0.4}$	1
1200 GeV	0.14 ± 0.09	0.01 ± 0.00	$0.15^{+0.70}_{-0.15}$	$0.29^{+0.70}_{-0.29}$	0
$2e/\mu + \geq 1\tau, \text{ off-}Z, \text{ no-OSSF}$					
Inclusive	1.3 ± 0.4	2.0 ± 0.4	29 ± 8	32 ± 8	28
600 GeV	0.81 ± 0.29	0.66 ± 0.19	8.0 ± 2.5	9.5 ± 2.5	9
1000 GeV	$0.16^{+0.20}_{-0.16}$	0.06 ± 0.05	1.4 ± 0.9	1.6 ± 0.9	2
1200 GeV	0.10 ± 0.05	$0.01^{+0.05}_{-0.01}$	$0.4^{+0.8}_{-0.4}$	$0.5^{+0.8}_{-0.5}$	2
$\geq 3e/\mu, \text{ off-}Z, \text{ OSSF}$					
Inclusive	4.6 ± 1.4	12.2 ± 1.9	3.6 ± 1.4	20.4 ± 2.8	16
600 GeV	2.8 ± 0.9	4.7 ± 1.1	0.8 ± 0.8	8.2 ± 1.7	7
1000 GeV	0.47 ± 0.17	1.2 ± 0.4	$0.16^{+0.71}_{-0.16}$	1.8 ± 0.9	1
1200 GeV	0.18 ± 0.09	0.39 ± 0.19	$0.16^{+0.71}_{-0.16}$	0.7 ± 0.7	1
$2e/\mu + \geq 1\tau, \text{ off-}Z, \text{ OSSF}$					
Inclusive	0.54 ± 0.18	1.47 ± 0.31	14 ± 4	16 ± 4	17
600 GeV	0.34 ± 0.13	0.44 ± 0.17	4.8 ± 1.8	5.6 ± 1.8	5
1000 GeV	0.15 ± 0.07	$0.07^{+0.08}_{-0.07}$	$0.6^{+0.8}_{-0.6}$	0.8 ± 0.8	2
1200 GeV	$0^{+0.006}_{-0}$	$0.07^{+0.08}_{-0.07}$	$0.17^{+0.73}_{-0.17}$	$0.24^{+0.73}_{-0.24}$	2
$\geq 3e/\mu, \text{ on-}Z$					
Inclusive	14 ± 4	148 ± 19	5.7 ± 1.9	167 ± 20	123
600 GeV	8.7 ± 2.7	41 ± 9	1.3 ± 0.9	51 ± 10	39
1000 GeV	2.5 ± 0.8	9.1 ± 3.2	$0^{+0.69}_{-0}$	11.6 ± 3.5	12
1200 GeV	1.01 ± 0.33	4.0 ± 1.8	$0^{+0.69}_{-0}$	5.0 ± 2.0	4
$2e/\mu + \geq 1\tau, \text{ on-}Z$					
Inclusive	1.01 ± 0.32	12.1 ± 1.7	13.8 ± 4.1	26.9 ± 4.5	24
600 GeV	0.62 ± 0.21	4.1 ± 1.0	3.5 ± 1.4	8.2 ± 1.7	9
1000 GeV	0.16 ± 0.06	1.2 ± 0.4	$0.4^{+0.8}_{-0.4}$	1.7 ± 0.9	0
1200 GeV	0.07 ± 0.03	0.53 ± 0.27	$0.33^{+0.74}_{-0.33}$	0.9 ± 0.8	0

Table 14. Expected and observed event yields for the high- E_T^{miss} , m_{eff} signal regions.

$m_{\text{eff}} \geq$	$t\bar{t} + V(V)$	$VV(V)$	Reducible	Total	Observed
$\geq 3e/\mu, \text{ on-}Z$					
Inclusive	11.2 ± 3.5	174 ± 23	9.0 ± 2.7	194 ± 24	164
600 GeV	5.5 ± 1.7	22 ± 6	0.9 ± 0.9	28 ± 6	29
1200 GeV	0.33 ± 0.12	2.5 ± 1.3	$0.16^{+0.71}_{-0.16}$	3.0 ± 1.5	2
$2e/\mu + \geq 1\tau, \text{ on-}Z$					
Inclusive	0.38 ± 0.13	2.2 ± 0.9	51 ± 17	54 ± 17	46
600 GeV	0.10 ± 0.06	0.12 ± 0.08	5.4 ± 2.2	5.6 ± 2.2	8
1200 GeV	0.01 ± 0.01	0.04 ± 0.04	$0.22^{+0.73}_{-0.22}$	$0.27^{+0.73}_{-0.27}$	0

Table 15. Expected and observed event yields for the high- m_T^W , m_{eff} signal regions.

$E_T^{\text{miss}} \geq$	$t\bar{t} + V(V)$	$VV(V)$	Reducible	Total	Observed
$\geq 3e/\mu, \text{ off-}Z, \text{ no-OSSF}$					
Inclusive	3.7 ± 1.2	0.85 ± 0.26	7.1 ± 2.2	11.7 ± 2.5	18
100 GeV	1.2 ± 0.4	0.24 ± 0.06	2.6 ± 1.1	4.0 ± 1.2	8
200 GeV	0.18 ± 0.07	0.01 ± 0.01	$0.34^{+0.71}_{-0.34}$	$0.5^{+0.7}_{-0.5}$	0
300 GeV	0.12 ± 0.07	$0^{+0.03}_{-0}$	$0.15^{+0.70}_{-0.15}$	$0.28^{+0.70}_{-0.28}$	0
$2e/\mu + \geq 1\tau, \text{ off-}Z, \text{ no-OSSF}$					
Inclusive	2.7 ± 0.8	3.7 ± 0.7	71 ± 19	77 ± 19	83
100 GeV	1.1 ± 0.4	1.18 ± 0.29	19 ± 5	21 ± 5	24
200 GeV	0.04 ± 0.04	$0.16^{+0.18}_{-0.16}$	1.7 ± 0.9	1.9 ± 1.0	2
300 GeV	0.01 ± 0.01	0.05 ± 0.03	$0.25^{+0.73}_{-0.25}$	$0.31^{+0.73}_{-0.31}$	0
$\geq 3e/\mu, \text{ off-}Z, \text{ OSSF}$					
Inclusive	11.7 ± 3.5	32 ± 6	12 ± 4	56 ± 8	53
100 GeV	3.6 ± 1.1	5.0 ± 1.2	1.9 ± 1.0	10.5 ± 1.9	8
200 GeV	0.41 ± 0.17	0.86 ± 0.24	$0.21^{+0.71}_{-0.21}$	1.5 ± 0.8	2
300 GeV	$0.04^{+0.05}_{-0.04}$	0.28 ± 0.12	$0^{+0.7}_{-0}$	$0.33^{+0.70}_{-0.33}$	0
$2e/\mu + \geq 1\tau, \text{ off-}Z, \text{ OSSF}$					
Inclusive	1.07 ± 0.35	2.4 ± 0.6	95 ± 26	98 ± 26	83
100 GeV	0.39 ± 0.13	0.63 ± 0.21	10.1 ± 3.2	11.1 ± 3.2	9
200 GeV	0.03 ± 0.02	0.20 ± 0.11	$0.35^{+0.74}_{-0.35}$	$0.6^{+0.8}_{-0.6}$	1
300 GeV	$0^{+0.003}_{-0}$	$0.02^{+0.05}_{-0.02}$	$0^{+0.71}_{-0}$	$0.02^{+0.71}_{-0.02}$	0
$\geq 3e/\mu, \text{ on-}Z$					
Inclusive	52 ± 16	391 ± 70	40 ± 10	480 ± 7	446
100 GeV	13 ± 4	57 ± 12	2.7 ± 1.2	73 ± 13	53
200 GeV	1.7 ± 0.5	9.6 ± 2.6	$0.5^{+0.8}_{-0.5}$	11.8 ± 2.8	13
300 GeV	0.24 ± 0.09	2.3 ± 0.8	$0^{+0.69}_{-0}$	2.6 ± 1.1	1
$2e/\mu + \geq 1\tau, \text{ on-}Z$					
Inclusive	3.0 ± 0.9	26 ± 5	640 ± 180	670 ± 180	554
100 GeV	0.93 ± 0.30	5.3 ± 1.3	8.1 ± 2.5	14.3 ± 2.9	17
200 GeV	$0.13^{+0.14}_{-0.13}$	1.2 ± 0.4	$0.4^{+0.8}_{-0.4}$	1.7 ± 0.9	3
300 GeV	0.02 ± 0.01	0.35 ± 0.16	$0^{+0.7}_{-0}$	$0.4^{+0.7}_{-0.4}$	1

Table 16. Expected and observed event yields for the high- H_T^{jets} , E_T^{miss} signal regions.

E_T^{miss}	\geq	$t\bar{t} + V(V)$	$VV(V)$	Reducible	Total	Observed
$\geq 3e/\mu, \text{ off-}Z, \text{ no-OSSF}$						
Inclusive	1.9 ± 0.6	6.1 ± 1.2	10.4 ± 2.9	18.4 ± 3.3	18	
100 GeV	0.53 ± 0.22	0.66 ± 0.19	1.4 ± 0.8	2.6 ± 0.9	0	
200 GeV	0 ± 0.003	0.08 ± 0.03	0 ± 0.7	0.08 ± 0.08	0	
300 GeV	0 ± 0.003	0.01 ± 0.01	0 ± 0.7	0.01 ± 0.01	0	
$2e/\mu+ \geq 1\tau, \text{ off-}Z, \text{ no-OSSF}$						
Inclusive	0.63 ± 0.24	19.1 ± 2.5	105 ± 25	125 ± 25	125	
100 GeV	0.25 ± 0.12	0.85 ± 0.23	9.7 ± 3.0	10.8 ± 3.0	4	
200 GeV	0 ± 0.006	0.02 ± 0.01	0.06 ± 0.06	0.08 ± 0.08	0	
300 GeV	0 ± 0.003	0 ± 0.03	0 ± 0.71	0 ± 0.71	0	
$\geq 3e/\mu, \text{ off-}Z, \text{ OSSF}$						
Inclusive	3.1 ± 1.0	159 ± 18	21 ± 6	183 ± 19	168	
100 GeV	0.95 ± 0.34	7.2 ± 1.0	1.8 ± 1.0	9.9 ± 1.4	8	
200 GeV	0.06 ± 0.06	0.71 ± 0.16	0.09 ± 0.09	0.9 ± 0.7	1	
300 GeV	0.05 ± 0.07	0.11 ± 0.06	0 ± 0.6	0.16 ± 0.16	0	
$2e/\mu+ \geq 1\tau, \text{ off-}Z, \text{ OSSF}$						
Inclusive	0.41 ± 0.15	10.6 ± 1.2	530 ± 150	540 ± 150	539	
100 GeV	0.16 ± 0.08	0.84 ± 0.20	4.2 ± 1.5	5.2 ± 1.5	8	
200 GeV	0 ± 0.003	0.06 ± 0.05	0 ± 0.71	0.06 ± 0.06	0	
300 GeV	0 ± 0.003	0 ± 0.03	0 ± 0.71	0 ± 0.71	0	
$\geq 3e/\mu, \text{ on-}Z$						
Inclusive	8.4 ± 2.9	2450 ± 290	142 ± 35	2600 ± 290	2539	
100 GeV	1.2 ± 0.4	90 ± 9	3.0 ± 1.3	94 ± 9	70	
200 GeV	0.05 ± 0.02	6.2 ± 0.7	0.04 ± 0.04	6.3 ± 1.0	3	
300 GeV	0.01 ± 0.01	1.23 ± 0.26	0 ± 0.69	1.2 ± 0.7	0	
$2e/\mu+ \geq 1\tau, \text{ on-}Z$						
Inclusive	0.58 ± 0.23	112 ± 10	9600 ± 2600	9800 ± 2600	9149	
100 GeV	0.08 ± 0.04	6.8 ± 1.0	5.7 ± 2.0	12.6 ± 2.2	7	
200 GeV	0 ± 0.012	0.72 ± 0.18	0.4 ± 0.4	1.1 ± 0.8	0	
300 GeV	0 ± 0.003	0.20 ± 0.10	0 ± 0.7	0.20 ± 0.20	0	

Table 17. Expected and observed event yields for the low- H_T^{jets} , E_T^{miss} signal regions.

H_T^{leptons}	Expected	$\pm 1\sigma$	$\pm 2\sigma$	Observed	p_0	Significance
[GeV]	[fb]	[fb]	[fb]	[fb]		[σ]
$\geq 3e/\mu, \text{no-OSSF}$						
≥ 200	0.34	$+0.13$ -0.08	$+0.30$ -0.15	0.34	0.46	0.1
≥ 500	0.22	$+0.07$ -0.04	$+0.12$ -0.06	0.22	0.47	0.1
≥ 800	0.14	$+0.01$ -0.00	$+0.08$ -0.02	0.14	0.50	0.0
$2e/\mu + \geq 1\tau_{\text{had}}, \text{no-OSSF}$						
≥ 200	0.60	$+0.22$ -0.17	$+0.40$ -0.28	0.41	0.50	0.0
≥ 500	0.15	$+0.01$ -0.01	$+0.08$ -0.01	0.14	0.50	0.0
≥ 800	0.15	$+0.00$ -0.01	$+0.06$ -0.02	0.14	0.50	0.0
$\geq 3e/\mu, \text{OSSF}$						
≥ 200	1.2	$+0.5$ -0.3	$+1.0$ -0.5	0.70	0.50	0.0
≥ 500	0.26	$+0.03$ -0.06	$+0.10$ -0.10	0.18	0.50	0.0
≥ 800	0.16	$+0.05$ -0.01	$+0.13$ -0.02	0.15	0.50	0.0
$2e/\mu + \geq 1\tau_{\text{had}}, \text{OSSF}$						
≥ 200	1.8	$+0.6$ -0.4	$+1.2$ -0.7	1.68	0.50	0.0
≥ 500	0.16	$+0.06$ -0.02	$+0.14$ -0.03	0.14	0.50	0.0
≥ 800	0.16	$+0.00$ -0.02	$+0.05$ -0.03	0.14	0.50	0.0
$\geq 3e/\mu, \text{on-Z}$						
≥ 200	4.9	$+1.7$ -1.3	$+3.6$ -2.1	3.58	0.50	0.0
≥ 500	0.47	$+0.21$ -0.14	$+0.41$ -0.23	0.47	0.50	0.0
≥ 800	0.27	$+0.04$ -0.05	$+0.09$ -0.08	0.30	0.15	1.1
$2e/\mu + \geq 1\tau_{\text{had}}, \text{on-Z}$						
≥ 200	3.7	$+1.0$ -0.8	$+2.1$ -1.5	3.14	0.50	0.0
≥ 500	0.24	$+0.06$ -0.04	$+0.08$ -0.06	0.29	0.30	0.5
≥ 800	0.15	$+0.01$ -0.00	$+0.07$ -0.02	0.16	0.50	0.0

Table 18. Expected and observed limits, and corresponding p -values and significances (in standard deviations), for signal regions based on cuts on H_T^{leptons} .

Expected limits with confidence intervals of one and two standard deviations, observed limits, and one-sided p -values with corresponding significance in units of σ are provided in tables 18–25.

$p_T^{\ell,\min}$	Expected	$\pm 1\sigma$	$\pm 2\sigma$	Observed	p_0	Significance
[GeV]	[fb]	[fb]	[fb]	[fb]		[σ]
$\geq 3e/\mu$, no-OSSF						
≥ 50	0.25	$+0.04$ -0.04	$+0.09$ -0.07	0.29	0.10	1.3
≥ 100	0.13	$+0.02$ -0.00	$+0.09$ -0.00	0.15	0.50	0.0
≥ 150	0.14	$+0.01$ -0.01	$+0.07$ -0.03	0.14	0.50	0.0
$2e/\mu + \geq 1\tau_{had}$, no-OSSF						
≥ 50	0.34	$+0.13$ -0.08	$+0.31$ -0.13	0.31	0.50	0.0
≥ 100	0.15	$+0.00$ -0.00	$+0.07$ -0.02	0.14	0.50	0.0
≥ 150	0.15	$+0.00$ -0.01	$+0.07$ -0.02	0.14	0.50	0.0
$\geq 3e/\mu$, OSSF						
≥ 50	0.70	$+0.30$ -0.20	$+0.68$ -0.33	0.50	0.50	0.0
≥ 100	0.21	$+0.08$ -0.04	$+0.13$ -0.07	0.20	0.49	0.0
≥ 150	0.14	$+0.04$ -0.02	$+0.12$ -0.03	0.13	0.50	0.0
$2e/\mu + \geq 1\tau_{had}$, OSSF						
≥ 50	0.71	$+0.20$ -0.20	$+0.43$ -0.34	0.86	0.21	0.8
≥ 100	0.15	$+0.01$ -0.01	$+0.08$ -0.02	0.16	0.50	0.0
≥ 150	0.16	$+0.00$ -0.02	$+0.05$ -0.03	0.16	0.50	0.0
$\geq 3e/\mu$, on-Z						
≥ 50	2.3	$+0.8$ -0.6	$+1.8$ -1.0	1.77	0.50	0.0
≥ 100	0.44	$+0.20$ -0.13	$+0.42$ -0.22	0.69	0.09	1.4
≥ 150	0.31	$+0.06$ -0.01	$+0.28$ -0.03	0.30	0.48	0.1
$2e/\mu + \geq 1\tau_{had}$, on-Z						
≥ 50	1.3	$+0.4$ -0.3	$+1.0$ -0.6	1.05	0.50	0.0
≥ 100	0.16	$+0.07$ -0.01	$+0.13$ -0.02	0.16	0.50	0.0
≥ 150	0.15	$+0.00$ -0.01	$+0.08$ -0.02	0.15	0.50	0.0

Table 19. Expected and observed limits, and corresponding p -values and significances (in standard deviations), for signal regions based on cuts on $p_T^{\ell,\min}$.

b tags	Expected	$\pm 1\sigma$	$\pm 2\sigma$	Observed	p_0	Significance
	[fb]	[fb]	[fb]	[fb]		[σ]
$\geq 3e/\mu$, no-OSSF						
≥ 1	0.59	$+0.23$ -0.17	$+0.41$ -0.28	0.64	0.35	0.4
≥ 2	0.30	$+0.09$ -0.10	$+0.21$ -0.15	0.32	0.40	0.3
$2e/\mu + \geq 1\tau_{\text{had}}$, no-OSSF						
≥ 1	2.4	$+0.7$ -0.6	$+1.6$ -1.0	2.44	0.45	0.1
≥ 2	0.96	$+0.35$ -0.25	$+0.72$ -0.43	1.07	0.35	0.4
$\geq 3e/\mu$, OSSF						
≥ 1	0.92	$+0.35$ -0.25	$+0.79$ -0.41	0.86	0.50	0.0
≥ 2	0.45	$+0.18$ -0.10	$+0.28$ -0.16	0.47	0.45	0.1
$2e/\mu + \geq 1\tau_{\text{had}}$, OSSF						
≥ 1	1.8	$+0.6$ -0.4	$+1.2$ -0.7	1.57	0.50	0.0
≥ 2	0.55	$+0.22$ -0.16	$+0.39$ -0.26	0.43	0.50	0.0
$\geq 3e/\mu$, on-Z						
≥ 1	3.9	$+1.3$ -1.0	$+2.7$ -1.7	3.91	0.49	0.0
≥ 2	0.89	$+0.33$ -0.24	$+0.73$ -0.39	0.70	0.50	0.0
$2e/\mu + \geq 1\tau_{\text{had}}$, on-Z						
≥ 1	9.4	$+2.5$ -2.1	$+5.1$ -3.7	9.38	0.50	0.0
≥ 2	0.79	$+0.30$ -0.21	$+0.68$ -0.35	0.66	0.50	0.0

Table 20. Expected and observed limits, and corresponding p -values and significances (in standard deviations), for signal regions based on cuts on the number of b -tagged jets.

m_{eff}	Expected	$\pm 1\sigma$	$\pm 2\sigma$	Observed	p_0	Significance
[GeV]	[fb]	[fb]	[fb]	[fb]		[σ]
$\geq 3e/\mu, \text{no-OSSF}$						
≥ 600	0.27	$+0.04$ -0.06	$+0.09$ -0.10	0.25	0.50	0.0
≥ 1000	0.18	$+0.06$ -0.02	$+0.12$ -0.04	0.19	0.37	0.3
≥ 1500	0.15	$+0.01$ -0.01	$+0.07$ -0.01	0.15	0.50	0.0
$2e/\mu + \geq 1\tau_{\text{had}}, \text{no-OSSF}$						
≥ 600	0.68	$+0.20$ -0.19	$+0.41$ -0.32	0.77	0.34	0.4
≥ 1000	0.24	$+0.05$ -0.06	$+0.10$ -0.09	0.22	0.50	0.0
≥ 1500	0.18	$+0.06$ -0.01	$+0.11$ -0.02	0.20	0.26	0.6
$\geq 3e/\mu, \text{OSSF}$						
≥ 600	0.65	$+0.21$ -0.18	$+0.41$ -0.30	0.49	0.50	0.0
≥ 1000	0.25	$+0.11$ -0.05	$+0.25$ -0.09	0.16	0.50	0.0
≥ 1500	0.15	$+0.05$ -0.01	$+0.12$ -0.01	0.14	0.50	0.0
$2e/\mu + \geq 1\tau_{\text{had}}, \text{OSSF}$						
≥ 600	0.66	$+0.21$ -0.18	$+0.40$ -0.30	0.69	0.44	0.1
≥ 1000	0.23	$+0.06$ -0.04	$+0.11$ -0.06	0.22	0.50	0.0
≥ 1500	0.15	$+0.00$ -0.00	$+0.05$ -0.02	0.15	0.50	0.0
$\geq 3e/\mu, \text{on-}Z$						
≥ 600	3.2	$+1.0$ -0.8	$+2.1$ -1.3	2.93	0.50	0.0
≥ 1000	0.90	$+0.20$ -0.17	$+0.75$ -0.33	0.91	0.48	0.0
≥ 1500	0.26	$+0.04$ -0.07	$+0.09$ -0.10	0.22	0.50	0.0
$2e/\mu + \geq 1\tau_{\text{had}}, \text{on-}Z$						
≥ 600	1.7	$+0.6$ -0.4	$+1.2$ -0.7	1.49	0.50	0.0
≥ 1000	0.38	$+0.14$ -0.09	$+0.32$ -0.15	0.64	0.05	1.7
≥ 1500	0.18	$+0.06$ -0.01	$+0.12$ -0.02	0.20	0.29	0.5

Table 21. Expected and observed limits, and corresponding p -values and significances (in standard deviations), for signal regions based on cuts on m_{eff} .

m_{eff} [GeV]	Expected [fb]	$\pm 1\sigma$ [fb]	$\pm 2\sigma$ [fb]	Observed [fb]	p_0	Significance [σ]
$\geq 3e/\mu$, no-OSSF						
≥ 0	0.37	+0.14 -0.09	+0.34 -0.16	0.41	0.34	0.4
≥ 600	0.22	+0.07 -0.04	+0.13 -0.06	0.24	0.44	0.2
≥ 1200	0.15	+0.02 -0.01	+0.07 -0.02	0.15	0.50	0.0
$2e/\mu + \geq 1\tau_{\text{had}}$, no-OSSF						
≥ 0	0.87	+0.33 -0.23	+0.73 -0.39	0.77	0.50	0.0
≥ 600	0.43	+0.17 -0.12	+0.31 -0.17	0.42	0.50	0.0
≥ 1200	0.21	+0.07 -0.02	+0.12 -0.02	0.27	0.17	1.0
$\geq 3e/\mu$, OSSF						
≥ 0	0.57	+0.23 -0.17	+0.41 -0.27	0.48	0.50	0.0
≥ 600	0.39	+0.16 -0.10	+0.34 -0.15	0.35	0.50	0.0
≥ 1200	0.18	+0.06 -0.02	+0.12 -0.03	0.19	0.40	0.2
$2e/\mu + \geq 1\tau_{\text{had}}$, OSSF						
≥ 0	0.60	+0.22 -0.17	+0.40 -0.28	0.62	0.45	0.1
≥ 600	0.34	+0.12 -0.09	+0.30 -0.12	0.32	0.50	0.0
≥ 1200	0.25	+0.05 -0.04	+0.10 -0.04	0.28	0.16	1.0
$\geq 3e/\mu$, on-Z						
≥ 0	2.0	+0.7 -0.5	+1.6 -0.9	1.21	0.50	0.0
≥ 600	1.1	+0.4 -0.3	+0.9 -0.5	0.84	0.50	0.0
≥ 1200	0.29	+0.01 -0.06	+0.07 -0.11	0.27	0.50	0.0
$2e/\mu + \geq 1\tau_{\text{had}}$, on-Z						
≥ 0	0.69	+0.21 -0.20	+0.43 -0.32	0.60	0.50	0.0
≥ 600	0.39	+0.17 -0.11	+0.33 -0.16	0.42	0.42	0.2
≥ 1200	0.16	+0.06 -0.02	+0.13 -0.03	0.14	0.50	0.0

Table 22. Expected and observed limits, and corresponding p -values and significances (in standard deviations), for signal regions based on cuts on m_{eff} . All signal regions above have an additional requirement of $E_T^{\text{miss}} \geq 100$ GeV.

m_{eff} [GeV]	Expected [fb]	$\pm 1\sigma$ [fb]	$\pm 2\sigma$ [fb]	Observed [fb]	p_0	Significance [σ]
$\geq 3e/\mu$, on-Z						
≥ 0	2.5	+0.9 -0.7	+1.9 -1.1	1.83	0.50	0.0
≥ 600	0.84	+0.18 -0.20	+0.57 -0.36	0.86	0.46	0.1
≥ 1200	0.26	+0.04 -0.06	+0.09 -0.07	0.22	0.50	0.0
$2e/\mu + \geq 1\tau_{\text{had}}$, on-Z						
≥ 0	1.45	+0.45 -0.35	+0.99 -0.59	1.31	0.50	0.0
≥ 600	0.39	+0.14 -0.09	+0.33 -0.15	0.48	0.25	0.7
≥ 1200	0.15	+0.01 -0.00	+0.08 -0.02	0.15	0.50	0.0

Table 23. Expected and observed limits, and corresponding p -values and significances (in standard deviations), for signal regions based on cuts on m_{eff} . All signal regions above have an additional requirement of $m_T^W \geq 100$ GeV.

E_T^{miss} [GeV]	Expected [fb]	$\pm 1\sigma$ [fb]	$\pm 2\sigma$ [fb]	Observed [fb]	p_0	Significance [σ]
$\geq 3e/\mu, \text{no-OSSF}$						
≥ 0	0.50	+0.22 -0.15	+0.42 -0.24	0.77	0.09	1.3
≥ 100	0.28	+0.01 -0.04	+0.05 -0.07	0.29	0.08	1.4
≥ 200	0.15	+0.04 -0.01	+0.10 -0.02	0.15	0.50	0.0
≥ 300	0.15	+0.02 -0.01	+0.09 -0.01	0.14	0.50	0.0
$2e/\mu + \geq 1\tau_{\text{had}}, \text{no-OSSF}$						
≥ 0	2.0	+0.6 -0.5	+1.4 -0.8	2.00	0.40	0.3
≥ 100	0.73	+0.19 -0.20	+0.43 -0.34	0.81	0.36	0.4
≥ 200	0.22	+0.07 -0.05	+0.12 -0.06	0.23	0.48	0.0
≥ 300	0.15	+0.00 -0.01	+0.08 -0.02	0.14	0.50	0.0
$\geq 3e/\mu, \text{OSSF}$						
≥ 0	1.2	+0.4 -0.3	+1.0 -0.5	1.11	0.50	0.0
≥ 100	0.42	+0.16 -0.11	+0.30 -0.15	0.35	0.50	0.0
≥ 200	0.21	+0.08 -0.04	+0.13 -0.05	0.24	0.37	0.3
≥ 300	0.16	+0.04 -0.01	+0.12 -0.01	0.15	0.50	0.0
$2e/\mu + \geq 1\tau_{\text{had}}, \text{OSSF}$						
≥ 0	2.2	+0.7 -0.5	+1.4 -0.9	1.88	0.50	0.0
≥ 100	0.46	+0.16 -0.12	+0.28 -0.19	0.41	0.50	0.0
≥ 200	0.19	+0.05 -0.01	+0.11 -0.03	0.19	0.37	0.3
≥ 300	0.14	+0.01 -0.00	+0.06 -0.01	0.13	0.50	0.0
$\geq 3e/\mu, \text{on-Z}$						
≥ 0	7.2	+2.2 -1.8	+4.7 -3.0	6.38	0.50	0.0
≥ 100	1.3	+0.5 -0.4	+1.1 -0.6	0.96	0.50	0.0
≥ 200	0.51	+0.22 -0.15	+0.40 -0.24	0.55	0.41	0.2
≥ 300	0.23	+0.07 -0.06	+0.12 -0.10	0.18	0.50	0.0
$2e/\mu + \geq 1\tau_{\text{had}}, \text{on-Z}$						
≥ 0	12.4	+3.3 -2.8	+6.6 -4.9	10.66	0.50	0.0
≥ 100	0.53	+0.23 -0.16	+0.41 -0.26	0.64	0.30	0.5
≥ 200	0.24	+0.05 -0.05	+0.10 -0.07	0.29	0.25	0.7
≥ 300	0.22	+0.08 -0.04	+0.12 -0.06	0.23	0.48	0.0

Table 24. Expected and observed limits, and corresponding p -values and significances (in standard deviations), for signal regions based on cuts on E_T^{miss} . All signal regions above have an additional requirement of $H_T^{\text{jets}} \geq 150$ GeV.

E_T^{miss} [GeV]	Expected [fb]	$\pm 1\sigma$ [fb]	$\pm 2\sigma$ [fb]	Observed [fb]	p_0	Significance [σ]
$\geq 3e/\mu$, no-OSSF						
≥ 0	0.58	$+0.23$ -0.17	$+0.41$ -0.27	0.56	0.50	0.0
≥ 100	0.21	$+0.07$ -0.06	$+0.13$ -0.08	0.15	0.50	0.0
≥ 200	0.16	$+0.01$ -0.01	$+0.08$ -0.02	0.15	0.50	0.0
≥ 300	0.14	$+0.01$ -0.01	$+0.01$ -0.01	0.14	0.50	0.0
$2e/\mu + \geq 1\tau_{\text{had}}$, no-OSSF						
≥ 0	2.5	$+0.8$ -0.6	$+1.7$ -1.1	2.48	0.50	0.0
≥ 100	0.38	$+0.15$ -0.11	$+0.33$ -0.17	0.22	0.50	0.0
≥ 200	0.14	$+0.00$ -0.00	$+0.06$ -0.01	0.14	0.50	0.0
≥ 300	0.15	$+0.00$ -0.01	$+0.05$ -0.02	0.14	0.50	0.0
$\geq 3e/\mu$, OSSF						
≥ 0	2.2	$+0.8$ -0.6	$+1.8$ -1.0	1.80	0.50	0.0
≥ 100	0.39	$+0.16$ -0.09	$+0.34$ -0.17	0.34	0.50	0.0
≥ 200	0.18	$+0.06$ -0.02	$+0.12$ -0.04	0.19	0.45	0.1
≥ 300	0.14	$+0.01$ -0.00	$+0.08$ -0.01	0.15	0.50	0.0
$2e/\mu + \geq 1\tau_{\text{had}}$, OSSF						
≥ 0	12.4	$+3.3$ -2.8	$+6.6$ -4.9	12.32	0.50	0.0
≥ 100	0.36	$+0.15$ -0.08	$+0.32$ -0.13	0.43	0.18	0.9
≥ 200	0.15	$+0.01$ -0.01	$+0.08$ -0.02	0.14	0.50	0.0
≥ 300	0.13	$+0.01$ -0.01	$+0.05$ -0.03	0.13	0.50	0.0
$\geq 3e/\mu$, on-Z						
≥ 0	26	$+9$ -7	$+19$ -11	24.77	0.50	0.0
≥ 100	1.2	$+0.5$ -0.3	$+1.1$ -0.6	0.69	0.50	0.0
≥ 200	0.31	$+0.16$ -0.10	$+0.38$ -0.16	0.20	0.50	0.0
≥ 300	0.19	$+0.07$ -0.05	$+0.11$ -0.05	0.14	0.50	0.0
$2e/\mu + \geq 1\tau_{\text{had}}$, on-Z						
≥ 0	205	$+50$ -45	$+102$ -79	194.36	0.50	0.0
≥ 100	0.40	$+0.17$ -0.11	$+0.33$ -0.17	0.29	0.50	0.0
≥ 200	0.17	$+0.07$ -0.02	$+0.13$ -0.04	0.14	0.50	0.0
≥ 300	0.14	$+0.03$ -0.01	$+0.10$ -0.02	0.13	0.50	0.0

Table 25. Expected and observed limits, and corresponding p -values and significances (in standard deviations), for signal regions based on cuts on E_T^{miss} . All signal regions above have an additional requirement of $H_T^{\text{jets}} < 150$ GeV.

Open Access. This article is distributed under the terms of the Creative Commons Attribution License ([CC-BY 4.0](#)), which permits any use, distribution and reproduction in any medium, provided the original author(s) and source are credited.

References

- [1] ATLAS collaboration, *Measurement of WZ production in proton-proton collisions at $\sqrt{s} = 7 \text{ TeV}$ with the ATLAS detector*, *Eur. Phys. J. C* **72** (2012) 2173 [[arXiv:1208.1390](#)] [[INSPIRE](#)].
- [2] ATLAS collaboration, *Measurement of ZZ production in pp collisions at $\sqrt{s} = 7 \text{ TeV}$ and limits on anomalous ZZZ and $Z Z \gamma$ couplings with the ATLAS detector*, *JHEP* **03** (2013) 128 [[arXiv:1211.6096](#)] [[INSPIRE](#)].
- [3] CMS collaboration, *Measurement of the $pp \rightarrow ZZ$ production cross section and constraints on anomalous triple gauge couplings in four-lepton final states at $\sqrt{s} = 8 \text{ TeV}$* , *Phys. Lett. B* **740** (2015) 250 [[arXiv:1406.0113](#)] [[INSPIRE](#)].
- [4] ATLAS collaboration, *Fiducial and differential cross sections of Higgs boson production measured in the four-lepton decay channel in pp collisions at $\sqrt{s} = 8 \text{ TeV}$ with the ATLAS detector*, *Phys. Lett. B* **738** (2014) 234 [[arXiv:1408.3226](#)] [[INSPIRE](#)].
- [5] CMS collaboration, *Measurement of the properties of a Higgs boson in the four-lepton final state*, *Phys. Rev. D* **89** (2014) 092007 [[arXiv:1312.5353](#)] [[INSPIRE](#)].
- [6] S. Matsumoto, T. Nabeshima and K. Yoshioka, *Seesaw Neutrino Signals at the Large Hadron Collider*, *JHEP* **06** (2010) 058 [[arXiv:1004.3852](#)] [[INSPIRE](#)].
- [7] A. Belyaev, C. Leroy and R.R. Mehdiyev, *Production of excited neutrino at LHC*, *Eur. Phys. J. C* **41S2** (2005) 1 [[hep-ph/0401066](#)] [[INSPIRE](#)].
- [8] A. Zee, *Charged Scalar Field and Quantum Number Violations*, *Phys. Lett. B* **161** (1985) 141 [[INSPIRE](#)].
- [9] A. Zee, *Quantum Numbers of Majorana Neutrino Masses*, *Nucl. Phys. B* **264** (1986) 99 [[INSPIRE](#)].
- [10] K.S. Babu, *Model of 'Calculable' Majorana Neutrino Masses*, *Phys. Lett. B* **203** (1988) 132 [[INSPIRE](#)].
- [11] H. Miyazawa, *Baryon Number Changing Currents*, *Prog. Theor. Phys.* **36** (1966) 1266.
- [12] P. Ramond, *Dual Theory for Free Fermions*, *Phys. Rev. D* **3** (1971) 2415 [[INSPIRE](#)].
- [13] Yu. A. Golfand and E.P. Likhtman, *Extension of the Algebra of Poincaré Group Generators and Violation of p Invariance*, *JETP Lett.* **13** (1971) 323 [[INSPIRE](#)].
- [14] A. Neveu and J.H. Schwarz, *Factorizable dual model of pions*, *Nucl. Phys. B* **31** (1971) 86 [[INSPIRE](#)].
- [15] A. Neveu and J.H. Schwarz, *Quark Model of Dual Pions*, *Phys. Rev. D* **4** (1971) 1109 [[INSPIRE](#)].
- [16] J.-L. Gervais and B. Sakita, *Field Theory Interpretation of Supergauges in Dual Models*, *Nucl. Phys. B* **34** (1971) 632 [[INSPIRE](#)].
- [17] D.V. Volkov and V.P. Akulov, *Is the Neutrino a Goldstone Particle?*, *Phys. Lett. B* **46** (1973) 109 [[INSPIRE](#)].
- [18] J. Wess and B. Zumino, *A Lagrangian Model Invariant Under Supergauge Transformations*, *Phys. Lett. B* **49** (1974) 52 [[INSPIRE](#)].

- [19] J. Wess and B. Zumino, *Supergauge Transformations in Four-Dimensions*, *Nucl. Phys.* **B** **70** (1974) 39 [[INSPIRE](#)].
- [20] J.A. Aguilar-Saavedra, R. Benbrik, S. Heinemeyer and M. Pérez-Victoria, *Handbook of vectorlike quarks: Mixing and single production*, *Phys. Rev.* **D** **88** (2013) 094010 [[arXiv:1306.0572](#)] [[INSPIRE](#)].
- [21] T.G. Rizzo, *Doubly Charged Higgs Bosons and Lepton Number Violating Processes*, *Phys. Rev.* **D** **25** (1982) 1355 [[INSPIRE](#)].
- [22] H. Georgi and M. Machacek, *Doubly charged Higgs bosons*, *Nucl. Phys.* **B** **262** (1985) 463 [[INSPIRE](#)].
- [23] J.E. Cieza Montalvo, N.V. Cortez, J. Sa Borges and M.D. Tonasse, *Searching for doubly charged Higgs bosons at the LHC in a 3-3-1 model*, *Nucl. Phys.* **B** **756** (2006) 1 [Erratum *ibid.* **B** **796** (2008) 422] [[hep-ph/0606243](#)] [[INSPIRE](#)].
- [24] J.F. Gunion, R. Vega and J. Wudka, *Higgs triplets in the standard model*, *Phys. Rev.* **D** **42** (1990) 1673 [[INSPIRE](#)].
- [25] U. Baur, M. Spira and P.M. Zerwas, *Excited Quark and Lepton Production at Hadron Colliders*, *Phys. Rev.* **D** **42** (1990) 815 [[INSPIRE](#)].
- [26] CMS collaboration, *Search for anomalous production of multilepton events in pp collisions at $\sqrt{s} = 7 \text{ TeV}$* , *JHEP* **06** (2012) 169 [[arXiv:1204.5341](#)] [[INSPIRE](#)].
- [27] CMS collaboration, *Search for anomalous production of events with three or more leptons in pp collisions at $\sqrt{s} = 8 \text{ TeV}$* , *Phys. Rev.* **D** **90** (2014) 032006 [[arXiv:1404.5801](#)] [[INSPIRE](#)].
- [28] ATLAS collaboration, *Search for direct production of charginos and neutralinos in events with three leptons and missing transverse momentum in $\sqrt{s} = 8 \text{ TeV}$ pp collisions with the ATLAS detector*, *JHEP* **04** (2014) 169 [[arXiv:1402.7029](#)] [[INSPIRE](#)].
- [29] ATLAS collaboration, *Search for supersymmetry at $\sqrt{s} = 8 \text{ TeV}$ in final states with jets and two same-sign leptons or three leptons with the ATLAS detector*, *JHEP* **06** (2014) 035 [[arXiv:1404.2500](#)] [[INSPIRE](#)].
- [30] ATLAS collaboration, *Search for supersymmetry in events with four or more leptons in $\sqrt{s} = 8 \text{ TeV}$ pp collisions with the ATLAS detector*, *Phys. Rev.* **D** **90** (2014) 052001 [[arXiv:1405.5086](#)] [[INSPIRE](#)].
- [31] CDF collaboration, T. Aaltonen et al., *Search for Supersymmetry in $p\bar{p}$ Collisions at $\sqrt{s} = 1.96 \text{ TeV}$ Using the Trilepton Signature of Chargino-Neutralino Production*, *Phys. Rev. Lett.* **101** (2008) 251801 [[arXiv:0808.2446](#)] [[INSPIRE](#)].
- [32] D0 collaboration, V.M. Abazov et al., *Search for associated production of charginos and neutralinos in the trilepton final state using 2.3 fb^{-1} of data*, *Phys. Lett.* **B** **680** (2009) 34 [[arXiv:0901.0646](#)] [[INSPIRE](#)].
- [33] ATLAS collaboration, *Search for new phenomena in events with three charged leptons at $/sqrts = 7 \text{ TeV}$ with the ATLAS detector*, *Phys. Rev.* **D** **87** (2013) 052002 [[arXiv:1211.6312](#)] [[INSPIRE](#)].
- [34] ATLAS collaboration, *The ATLAS Experiment at the CERN Large Hadron Collider*, **2008 JINST** **3** S08003 [[INSPIRE](#)].
- [35] ATLAS collaboration, *Performance of the ATLAS Trigger System in 2010*, *Eur. Phys. J.* **C** **72** (2012) 1849 [[arXiv:1110.1530](#)] [[INSPIRE](#)].
- [36] ATLAS collaboration, *Electron performance measurements with the ATLAS detector using the 2010 LHC proton-proton collision data*, *Eur. Phys. J.* **C** **72** (2012) 1909 [[arXiv:1110.3174](#)] [[INSPIRE](#)].

- [37] ATLAS collaboration, *Measurement of the muon reconstruction performance of the ATLAS detector using 2011 and 2012 LHC proton-proton collision data*, *Eur. Phys. J. C* **74** (2014) 3130 [[arXiv:1407.3935](#)] [[INSPIRE](#)].
- [38] M. Cacciari, G.P. Salam and G. Soyez, *The anti- k_t jet clustering algorithm*, *JHEP* **04** (2008) 063 [[arXiv:0802.1189](#)] [[INSPIRE](#)].
- [39] ATLAS collaboration, *Jet energy measurement with the ATLAS detector in proton-proton collisions at $\sqrt{s} = 7$ TeV*, *Eur. Phys. J. C* **73** (2013) 2304 [[arXiv:1112.6426](#)] [[INSPIRE](#)].
- [40] ATLAS collaboration, *Jet energy resolution in proton-proton collisions at $\sqrt{s} = 7$ TeV recorded in 2010 with the ATLAS detector*, *Eur. Phys. J. C* **73** (2013) 2306 [[arXiv:1210.6210](#)] [[INSPIRE](#)].
- [41] ATLAS collaboration, *Calibration of the performance of b-tagging for c and light-flavour jets in the 2012 ATLAS data*, [ATLAS-CONF-2014-046](#) (2014).
- [42] ATLAS collaboration, *Identification of Hadronic Decays of Tau Leptons in 2012 Data with the ATLAS Detector*, [ATLAS-CONF-2013-064](#).
- [43] ATLAS collaboration, *Performance of Missing Transverse Momentum Reconstruction in Proton-Proton Collisions at 7 TeV with ATLAS*, *Eur. Phys. J. C* **72** (2012) 1844 [[arXiv:1108.5602](#)] [[INSPIRE](#)].
- [44] ATLAS collaboration, *The ATLAS Simulation Infrastructure*, *Eur. Phys. J. C* **70** (2010) 823 [[arXiv:1005.4568](#)] [[INSPIRE](#)].
- [45] GEANT4 collaboration, S. Agostinelli et al., *GEANT4: A Simulation toolkit*, *Nucl. Instrum. Meth. A* **506** (2003) 250 [[INSPIRE](#)].
- [46] ATLAS collaboration, *Electron reconstruction and identification efficiency measurements with the ATLAS detector using the 2011 LHC proton-proton collision data*, *Eur. Phys. J. C* **74** (2014) 2941 [[arXiv:1404.2240](#)] [[INSPIRE](#)].
- [47] ATLAS collaboration, *Electron efficiency measurements with the ATLAS detector using the 2012 LHC proton-proton collision data*, [ATLAS-CONF-2014-032](#).
- [48] T. Sjöstrand et al., *High-energy physics event generation with PYTHIA 6.1*, *Comput. Phys. Commun.* **135** (2001) 238 [[hep-ph/0010017](#)] [[INSPIRE](#)].
- [49] T. Gleisberg et al., *Event generation with SHERPA 1.1*, *JHEP* **02** (2009) 007 [[arXiv:0811.4622](#)] [[INSPIRE](#)].
- [50] J. Alwall, M. Herquet, F. Maltoni, O. Mattelaer and T. Stelzer, *MadGraph 5: Going Beyond*, *JHEP* **06** (2011) 128 [[arXiv:1106.0522](#)] [[INSPIRE](#)].
- [51] ATLAS collaboration, *Photon Conversions at $\sqrt{s} = 900$ GeV measured with the ATLAS Detector*, [ATLAS-CONF-2010-007](#) (2010).
- [52] K. Arnold et al., *VBFNLO: A Parton level Monte Carlo for processes with electroweak bosons*, *Comput. Phys. Commun.* **180** (2009) 1661 [[arXiv:0811.4559](#)] [[INSPIRE](#)].
- [53] M.L. Mangano, M. Moretti, F. Piccinini, R. Pittau and A.D. Polosa, *ALPGEN, a generator for hard multiparton processes in hadronic collisions*, *JHEP* **07** (2003) 001 [[hep-ph/0206293](#)] [[INSPIRE](#)].
- [54] G. Corcella et al., *HERWIG 6: An Event generator for hadron emission reactions with interfering gluons (including supersymmetric processes)*, *JHEP* **01** (2001) 010 [[hep-ph/0011363](#)] [[INSPIRE](#)].
- [55] J.M. Butterworth, J.R. Forshaw and M.H. Seymour, *Multiparton interactions in photoproduction at HERA*, *Z. Phys. C* **72** (1996) 637 [[hep-ph/9601371](#)] [[INSPIRE](#)].

- [56] J.M. Campbell and R.K. Ellis, $t\bar{t}W^{+-}$ production and decay at NLO, *JHEP* **07** (2012) 052 [[arXiv:1204.5678](#)] [[INSPIRE](#)].
- [57] M.V. Garzelli, A. Kardos, C.G. Papadopoulos and Z. Trócsányi, Z^0 -boson production in association with a top anti-top pair at NLO accuracy with parton shower effects, *Phys. Rev. D* **85** (2012) 074022 [[arXiv:1111.1444](#)] [[INSPIRE](#)].
- [58] T. Melia, P. Nason, R. Rontsch and G. Zanderighi, W^+W^- , WZ and ZZ production in the *POWHEG BOX*, *JHEP* **11** (2011) 078 [[arXiv:1107.5051](#)] [[INSPIRE](#)].
- [59] T. Sjöstrand, S. Mrenna and P.Z. Skands, *A Brief Introduction to PYTHIA 8.1*, *Comput. Phys. Commun.* **178** (2008) 852 [[arXiv:0710.3820](#)] [[INSPIRE](#)].
- [60] H.-L. Lai et al., New parton distributions for collider physics, *Phys. Rev. D* **82** (2010) 074024 [[arXiv:1007.2241](#)] [[INSPIRE](#)].
- [61] A. Sherstnev and R.S. Thorne, Parton Distributions for LO Generators, *Eur. Phys. J. C* **55** (2008) 553 [[arXiv:0711.2473](#)] [[INSPIRE](#)].
- [62] J. Pumplin et al., New generation of parton distributions with uncertainties from global QCD analysis, *JHEP* **07** (2002) 012 [[hep-ph/0201195](#)] [[INSPIRE](#)].
- [63] ATLAS collaboration, Summary of ATLAS Pythia 8 tunes, ATL-PHYS-PUB-2012-003 (2012).
- [64] ATLAS collaboration, Further ATLAS tunes of PYTHIA6 and Pythia 8, ATL-PHYS-PUB-2011-014 (2011).
- [65] P.Z. Skands, Tuning Monte Carlo Generators: The Perugia Tunes, *Phys. Rev. D* **82** (2010) 074018 [[arXiv:1005.3457](#)] [[INSPIRE](#)].
- [66] ATLAS collaboration, Luminosity Determination in pp Collisions at $\sqrt{s} = 7$ TeV Using the ATLAS Detector at the LHC, *Eur. Phys. J. C* **71** (2011) 1630 [[arXiv:1101.2185](#)] [[INSPIRE](#)].
- [67] M. Rubin, G.P. Salam and S. Sapeta, Giant QCD K -factors beyond NLO, *JHEP* **09** (2010) 084 [[arXiv:1006.2144](#)] [[INSPIRE](#)].
- [68] F. Campanario and S. Sapeta, WZ production beyond NLO for high- p_T observables, *Phys. Lett. B* **718** (2012) 100 [[arXiv:1209.4595](#)] [[INSPIRE](#)].
- [69] ATLAS collaboration, Measurement of the production cross section of jets in association with a Z boson in pp collisions at $\sqrt{s} = 7$ TeV with the ATLAS detector, *JHEP* **07** (2013) 032 [[arXiv:1304.7098](#)] [[INSPIRE](#)].
- [70] A.L. Read, Presentation of search results: the CL_s technique, *J. Phys. G* **28** (2002) 2693.
- [71] ATLAS Collaboration, Search for anomalous production of prompt same-sign lepton pairs and doubly charged Higgs bosons with $\sqrt{s} = 8$ TeV pp collisions using the ATLAS detector, to be submitted to JHEP (2014).
- [72] CMS collaboration, A search for a doubly-charged Higgs boson in pp collisions at $\sqrt{s} = 7$ TeV, *Eur. Phys. J. C* **72** (2012) 2189 [[arXiv:1207.2666](#)] [[INSPIRE](#)].
- [73] CMS collaboration, Search for excited leptons in pp collisions at $\sqrt{s} = 7$ TeV, *Phys. Lett. B* **720** (2013) 309 [[arXiv:1210.2422](#)] [[INSPIRE](#)].
- [74] ATLAS collaboration, Search for excited electrons and muons in $\sqrt{s} = 8$ TeV proton-proton collisions with the ATLAS detector, *New J. Phys.* **15** (2013) 093011 [[arXiv:1308.1364](#)] [[INSPIRE](#)].
- [75] L3 collaboration, P. Achard et al., Search for excited leptons at LEP, *Phys. Lett. B* **568** (2003) 23 [[hep-ex/0306016](#)] [[INSPIRE](#)].

The ATLAS collaboration

G. Aad⁸⁵, B. Abbott¹¹³, J. Abdallah¹⁵², S. Abdel Khalek¹¹⁷, O. Abdinov¹¹, R. Aben¹⁰⁷, B. Abi¹¹⁴, M. Abolins⁹⁰, O.S. AbouZeid¹⁵⁹, H. Abramowicz¹⁵⁴, H. Abreu¹⁵³, R. Abreu³⁰, Y. Abulaiti^{147a,147b}, B.S. Acharya^{165a,165b,a}, L. Adamczyk^{38a}, D.L. Adams²⁵, J. Adelman¹⁰⁸, S. Adomeit¹⁰⁰, T. Adye¹³¹, T. Agatonovic-Jovin^{13a}, J.A. Aguilar-Saavedra^{126a,126f}, M. Agustoni¹⁷, S.P. Ahlen²², F. Ahmadov^{65,b}, G. Aielli^{134a,134b}, H. Akerstedt^{147a,147b}, T.P.A. Åkesson⁸¹, G. Akimoto¹⁵⁶, A.V. Akimov⁹⁶, G.L. Alberghi^{20a,20b}, J. Albert¹⁷⁰, S. Albrand⁵⁵, M.J. Alconada Verzini⁷¹, M. Aleksa³⁰, I.N. Aleksandrov⁶⁵, C. Alexa^{26a}, G. Alexander¹⁵⁴, G. Alexandre⁴⁹, T. Alexopoulos¹⁰, M. Alhroob¹¹³, G. Alimonti^{91a}, L. Alio⁸⁵, J. Alison³¹, B.M.M. Allbrooke¹⁸, L.J. Allison⁷², P.P. Allport⁷⁴, A. Aloisio^{104a,104b}, A. Alonso³⁶, F. Alonso⁷¹, C. Alpigiani⁷⁶, A. Altheimer³⁵, B. Alvarez Gonzalez⁹⁰, M.G. Alviggi^{104a,104b}, K. Amako⁶⁶, Y. Amaral Coutinho^{24a}, C. Amelung²³, D. Amidei⁸⁹, S.P. Amor Dos Santos^{126a,126c}, A. Amorim^{126a,126b}, S. Amoroso⁴⁸, N. Amram¹⁵⁴, G. Amundsen²³, C. Anastopoulos¹⁴⁰, L.S. Ancu⁴⁹, N. Andari³⁰, T. Andeen³⁵, C.F. Anders^{58b}, G. Anders³⁰, K.J. Anderson³¹, A. Andreazza^{91a,91b}, V. Andrei^{58a}, X.S. Anduaga⁷¹, S. Angelidakis⁹, I. Angelozzi¹⁰⁷, P. Anger⁴⁴, A. Angerami³⁵, F. Anghinolfi³⁰, A.V. Anisenkov^{109,c}, N. Anjos¹², A. Annovi⁴⁷, M. Antonelli⁴⁷, A. Antonov⁹⁸, J. Antos^{145b}, F. Anulli^{133a}, M. Aoki⁶⁶, L. Aperio Bella¹⁸, G. Arabidze⁹⁰, Y. Arai⁶⁶, J.P. Araque^{126a}, A.T.H. Arce⁴⁵, F.A. Arduh⁷¹, J-F. Arguin⁹⁵, S. Argyropoulos⁴², M. Arik^{19a}, A.J. Armbruster³⁰, O. Arnaez³⁰, V. Arnal⁸², H. Arnold⁴⁸, M. Arratia²⁸, O. Arslan²¹, A. Artamonov⁹⁷, G. Artoni²³, S. Asai¹⁵⁶, N. Asbah⁴², A. Ashkenazi¹⁵⁴, B. Åsman^{147a,147b}, L. Asquith¹⁵⁰, K. Assamagan²⁵, R. Astalos^{145a}, M. Atkinson¹⁶⁶, N.B. Atlay¹⁴², B. Auerbach⁶, K. Augsten¹²⁸, M. Aurousseau^{146b}, G. Avolio³⁰, B. Axen¹⁵, G. Azuelos^{95,d}, Y. Azuma¹⁵⁶, M.A. Baak³⁰, A.E. Baas^{58a}, C. Bacci^{135a,135b}, H. Bachacou¹³⁷, K. Bachas¹⁵⁵, M. Backes³⁰, M. Backhaus³⁰, E. Badescu^{26a}, P. Bagiacchi^{133a,133b}, P. Bagnaia^{133a,133b}, Y. Bai^{33a}, T. Bain³⁵, J.T. Baines¹³¹, O.K. Baker¹⁷⁷, P. Balek¹²⁹, F. Balli⁸⁴, E. Banas³⁹, Sw. Banerjee¹⁷⁴, A.A.E. Bannoura¹⁷⁶, H.S. Bansil¹⁸, L. Barak¹⁷³, S.P. Baranov⁹⁶, E.L. Barberio⁸⁸, D. Barberis^{50a,50b}, M. Barbero⁸⁵, T. Barillari¹⁰¹, M. Barisonzi¹⁷⁶, T. Barklow¹⁴⁴, N. Barlow²⁸, S.L. Barnes⁸⁴, B.M. Barnett¹³¹, R.M. Barnett¹⁵, Z. Barnovska⁵, A. Baroncelli^{135a}, G. Barone⁴⁹, A.J. Barr¹²⁰, F. Barreiro⁸², J. Barreiro Guimarães da Costa⁵⁷, R. Bartoldus¹⁴⁴, A.E. Barton⁷², P. Bartos^{145a}, V. Bartsch¹⁵⁰, A. Bassalat¹¹⁷, A. Basye¹⁶⁶, R.L. Bates⁵³, S.J. Batista¹⁵⁹, J.R. Batley²⁸, M. Battaglia¹³⁸, M. Battistin³⁰, F. Bauer¹³⁷, H.S. Bawa^{144,e}, J.B. Beacham¹¹⁰, M.D. Beattie⁷², T. Beau⁸⁰, P.H. Beauchemin¹⁶², R. Beccherle^{124a,124b}, P. Bechtle²¹, H.P. Beck^{17,f}, K. Becker¹²⁰, S. Becker¹⁰⁰, M. Beckingham¹⁷¹, C. Becot¹¹⁷, A.J. Beddall^{19c}, A. Beddall^{19c}, S. Bedikian¹⁷⁷, V.A. Bednyakov⁶⁵, C.P. Bee¹⁴⁹, L.J. Beemster¹⁰⁷, T.A. Beermann¹⁷⁶, M. Begel²⁵, K. Behr¹²⁰, C. Belanger-Champagne⁸⁷, P.J. Bell⁴⁹, W.H. Bell⁴⁹, G. Bella¹⁵⁴, L. Bellagamba^{20a}, A. Bellerive²⁹, M. Bellomo⁸⁶, K. Belotskiy⁹⁸, O. Beltramello³⁰, O. Benary¹⁵⁴, D. Benchekroun^{136a}, K. Bendtz^{147a,147b}, N. Benekos¹⁶⁶, Y. Benhammou¹⁵⁴, E. Benhar Noccioli⁴⁹, J.A. Benitez Garcia^{160b}, D.P. Benjamin⁴⁵, J.R. Bensinger²³, S. Bentvelsen¹⁰⁷, D. Berge¹⁰⁷, E. Bergeaas Kuutmann¹⁶⁷, N. Berger⁵, F. Berghaus¹⁷⁰, J. Beringer¹⁵, C. Bernard²², N.R. Bernard⁸⁶, C. Bernius¹¹⁰, F.U. Bernlochner²¹, T. Berry⁷⁷, P. Berta¹²⁹, C. Bertella⁸³, G. Bertoli^{147a,147b}, F. Bertolucci^{124a,124b}, C. Bertsche¹¹³, D. Bertsche¹¹³, M.I. Besana^{91a}, G.J. Besjes¹⁰⁶, O. Bessidskaia Bylund^{147a,147b}, M. Bessner⁴², N. Besson¹³⁷, C. Betancourt⁴⁸, S. Bethke¹⁰¹, A.J. Bevan⁷⁶, W. Bhimji⁴⁶, R.M. Bianchi¹²⁵, L. Bianchini²³, M. Bianco³⁰, O. Biebel¹⁰⁰, S.P. Bieniek⁷⁸, K. Bierwagen⁵⁴, M. Biglietti^{135a}, J. Bilbao De Mendizabal⁴⁹, H. Bilonkon⁴⁷, M. Bindi⁵⁴, S. Binet¹¹⁷, A. Bingul^{19c}, C. Bini^{133a,133b}, C.W. Black¹⁵¹, J.E. Black¹⁴⁴, K.M. Black²², D. Blackburn¹³⁹, R.E. Blair⁶, J.-B. Blanchard¹³⁷, T. Blazek^{145a}, I. Bloch⁴², C. Blocker²³, W. Blum^{83,*}, U. Blumenschein⁵⁴, G.J. Bobbink¹⁰⁷, V.S. Bobrovnikov^{109,c}, S.S. Bocchetta⁸¹, A. Bocci⁴⁵, C. Bock¹⁰⁰, C.R. Boddy¹²⁰, M. Boehler⁴⁸, T.T. Boek¹⁷⁶, J.A. Bogaerts³⁰, A.G. Bogdanchikov¹⁰⁹, A. Bogouch^{92,*}, C. Bohm^{147a}, V. Boisvert⁷⁷, T. Bold^{38a}, V. Boldea^{26a}, A.S. Boldyrev⁹⁹, M. Bomben⁸⁰, M. Bona⁷⁶, M. Boonekamp¹³⁷, A. Borisov¹³⁰, G. Borissov⁷², S. Borromi⁴², J. Bortfeldt¹⁰⁰, V. Bortolotto^{60a}, K. Bos¹⁰⁷, D. Boscherini^{20a}, M. Bosman¹², H. Boterenbrood¹⁰⁷, J. Boudreau¹²⁵, J. Bouffard²,

- E.V. Bouhova-Thacker⁷², D. Boumediene³⁴, C. Bourdarios¹¹⁷, N. Bousson¹¹⁴, S. Boutouil^{136d}, A. Boveia³¹, J. Boyd³⁰, I.R. Boyko⁶⁵, I. Bozic^{13a}, J. Bracinik¹⁸, A. Brandt⁸, G. Brandt¹⁵, O. Brandt^{58a}, U. Bratzler¹⁵⁷, B. Brau⁸⁶, J.E. Brau¹¹⁶, H.M. Braun^{176,*}, S.F. Brazzale^{165a,165c}, B. Brelier¹⁵⁹, K. Brendlinger¹²², A.J. Brennan⁸⁸, R. Brenner¹⁶⁷, S. Bressler¹⁷³, K. Bristow^{146c}, T.M. Bristow⁴⁶, D. Britton⁵³, F.M. Brochu²⁸, I. Brock²¹, R. Brock⁹⁰, J. Bronner¹⁰¹, G. Brooijmans³⁵, T. Brooks⁷⁷, W.K. Brooks^{32b}, J. Brosamer¹⁵, E. Brost¹¹⁶, J. Brown⁵⁵, P.A. Bruckman de Renstrom³⁹, D. Bruncko^{145b}, R. Bruneliere⁴⁸, S. Brunet⁶¹, A. Bruni^{20a}, G. Bruni^{20a}, M. Bruschi^{20a}, L. Bryngemark⁸¹, T. Buanes¹⁴, Q. Buat¹⁴³, F. Bucci⁴⁹, P. Buchholz¹⁴², A.G. Buckley⁵³, S.I. Buda^{26a}, I.A. Budagov⁶⁵, F. Buehrer⁴⁸, L. Bugge¹¹⁹, M.K. Bugge¹¹⁹, O. Bulekov⁹⁸, A.C. Bundred⁷⁴, H. Burckhart³⁰, S. Burdin⁷⁴, B. Burghgrave¹⁰⁸, S. Burke¹³¹, I. Burmeister⁴³, E. Busato³⁴, D. Büscher⁴⁸, V. Büscher⁸³, P. Bussey⁵³, C.P. Buszello¹⁶⁷, B. Butler⁵⁷, J.M. Butler²², A.I. Butt³, C.M. Buttar⁵³, J.M. Butterworth⁷⁸, P. Butti¹⁰⁷, W. Buttinger²⁸, A. Buzatu⁵³, M. Byszewski¹⁰, S. Cabrera Urbán¹⁶⁸, D. Caforio^{20a,20b}, O. Cakir^{4a}, P. Calafuria¹⁵, A. Calandri¹³⁷, G. Calderini⁸⁰, P. Calfayan¹⁰⁰, L.P. Caloba^{24a}, D. Calvet³⁴, S. Calvet³⁴, R. Camacho Toro⁴⁹, S. Camarda⁴², D. Cameron¹¹⁹, L.M. Caminada¹⁵, R. Caminal Armadans¹², S. Campana³⁰, M. Campanelli⁷⁸, A. Campoverde¹⁴⁹, V. Canale^{104a,104b}, A. Canepa^{160a}, M. Cano Bret⁷⁶, J. Cantero⁸², R. Cantrill^{126a}, T. Cao⁴⁰, M.D.M. Capeans Garrido³⁰, I. Caprini^{26a}, M. Caprini^{26a}, M. Capua^{37a,37b}, R. Caputo⁸³, R. Cardarelli^{134a}, T. Carli³⁰, G. Carlino^{104a}, L. Carminati^{91a,91b}, S. Caron¹⁰⁶, E. Carquin^{32a}, G.D. Carrillo-Montoya^{146c}, J.R. Carter²⁸, J. Carvalho^{126a,126c}, D. Casadei⁷⁸, M.P. Casado¹², M. Casolino¹², E. Castaneda-Miranda^{146b}, A. Castelli¹⁰⁷, V. Castillo Gimenez¹⁶⁸, N.F. Castro^{126a}, P. Catastini⁵⁷, A. Catinaccio³⁰, J.R. Catmore¹¹⁹, A. Cattai³⁰, G. Cattani^{134a,134b}, J. Caudron⁸³, V. Cavaliere¹⁶⁶, D. Cavalli^{91a}, M. Cavalli-Sforza¹², V. Cavasinni^{124a,124b}, F. Ceradini^{135a,135b}, B.C. Cerio⁴⁵, K. Cerny¹²⁹, A.S. Cerqueira^{24b}, A. Cerri¹⁵⁰, L. Cerrito⁷⁶, F. Cerutti¹⁵, M. Cerv³⁰, A. Cervelli¹⁷, S.A. Cetin^{19b}, A. Chafaq^{136a}, D. Chakraborty¹⁰⁸, I. Chalupkova¹²⁹, P. Chang¹⁶⁶, B. Chapleau⁸⁷, J.D. Chapman²⁸, D. Charfeddine¹¹⁷, D.G. Charlton¹⁸, C.C. Chau¹⁵⁹, C.A. Chavez Barajas¹⁵⁰, S. Cheatham¹⁵³, A. Chegwidden⁹⁰, S. Chekanov⁶, S.V. Chekulaev^{160a}, G.A. Chelkov^{65,g}, M.A. Chelstowska⁸⁹, C. Chen⁶⁴, H. Chen²⁵, K. Chen¹⁴⁹, L. Chen^{33d,h}, S. Chen^{33c}, X. Chen^{33f}, Y. Chen⁶⁷, H.C. Cheng⁸⁹, Y. Cheng³¹, A. Cheplakov⁶⁵, E. Cheremushkina¹³⁰, R. Cherkaoui El Moursli^{136e}, V. Chernyatin^{25,*}, E. Cheu⁷, L. Chevalier¹³⁷, V. Chiarella⁴⁷, G. Chiefari^{104a,104b}, J.T. Childers⁶, A. Chilingarov⁷², G. Chiodini^{73a}, A.S. Chisholm¹⁸, R.T. Chislett⁷⁸, A. Chitan^{26a}, M.V. Chizhov⁶⁵, S. Chouridou⁹, B.K.B. Chow¹⁰⁰, D. Chromeck-Burckhart³⁰, M.L. Chu¹⁵², J. Chudoba¹²⁷, J.J. Chwastowski³⁹, L. Chytka¹¹⁵, G. Ciapetti^{133a,133b}, A.K. Ciftci^{4a}, R. Ciftci^{4a}, D. Cinca⁵³, V. Cindro⁷⁵, A. Ciocio¹⁵, Z.H. Citron¹⁷³, M. Citterio^{91a}, M. Ciubancan^{26a}, A. Clark⁴⁹, P.J. Clark⁴⁶, R.N. Clarke¹⁵, W. Cleland¹²⁵, J.C. Clemens⁸⁵, C. Clement^{147a,147b}, Y. Coadou⁸⁵, M. Cobal^{165a,165c}, A. Coccaro¹³⁹, J. Cochran⁶⁴, L. Coffey²³, J.G. Cogan¹⁴⁴, B. Cole³⁵, S. Cole¹⁰⁸, A.P. Colijn¹⁰⁷, J. Collot⁵⁵, T. Colombo^{58c}, G. Compostella¹⁰¹, P. Conde Muiño^{126a,126b}, E. Coniavitis⁴⁸, S.H. Connell^{146b}, I.A. Connolly⁷⁷, S.M. Consonni^{91a,91b}, V. Consorti⁴⁸, S. Constantinescu^{26a}, C. Conta^{121a,121b}, G. Conti⁵⁷, F. Conventi^{104a,i}, M. Cooke¹⁵, B.D. Cooper⁷⁸, A.M. Cooper-Sarkar¹²⁰, N.J. Cooper-Smith⁷⁷, K. Copic¹⁵, T. Cornelissen¹⁷⁶, M. Corradi^{20a}, F. Corriveau^{87,j}, A. Corso-Radu¹⁶⁴, A. Cortes-Gonzalez¹², G. Cortiana¹⁰¹, G. Costa^{91a}, M.J. Costa¹⁶⁸, D. Costanzo¹⁴⁰, D. Côté⁸, G. Cottin²⁸, G. Cowan⁷⁷, B.E. Cox⁸⁴, K. Cranmer¹¹⁰, G. Cree²⁹, S. Crépé-Renaudin⁵⁵, F. Crescioli⁸⁰, W.A. Cribbs^{147a,147b}, M. Crispin Ortuzar¹²⁰, M. Cristinziani²¹, V. Croft¹⁰⁶, G. Crosetti^{37a,37b}, T. Cuhadar Donszelmann¹⁴⁰, J. Cummings¹⁷⁷, M. Curatolo⁴⁷, C. Cuthbert¹⁵¹, H. Czirr¹⁴², P. Czodrowski³, S. D'Auria⁵³, M. D'Onofrio⁷⁴, M.J. Da Cunha Sargedas De Sousa^{126a,126b}, C. Da Via⁸⁴, W. Dabrowski^{38a}, A. Dafinca¹²⁰, T. Dai⁸⁹, O. Dale¹⁴, F. Dallaire⁹⁵, C. Dallapiccola⁸⁶, M. Dam³⁶, A.C. Daniells¹⁸, M. Danner¹⁶⁹, M. Dano Hoffmann¹³⁷, V. Dao⁴⁸, G. Darbo^{50a}, S. Darmora⁸, J. Dassoulas⁷⁴, A. Dattagupta⁶¹, W. Davey²¹, C. David¹⁷⁰, T. Davidek¹²⁹, E. Davies^{120,k}, M. Davies¹⁵⁴, O. Davignon⁸⁰, A.R. Davison⁷⁸, P. Davison⁷⁸, Y. Davygora^{58a}, E. Dawe¹⁴³, I. Dawson¹⁴⁰, R.K. Daya-Ishmukhametova⁸⁶, K. De⁸, R. de Asmundis^{104a}, S. De Castro^{20a,20b}, S. De Cecco⁸⁰,

- N. De Groot¹⁰⁶, P. de Jong¹⁰⁷, H. De la Torre⁸², F. De Lorenzi⁶⁴, L. De Nooij¹⁰⁷, D. De Pedis^{133a}, A. De Salvo^{133a}, U. De Sanctis¹⁵⁰, A. De Santo¹⁵⁰, J.B. De Vivie De Regie¹¹⁷, W.J. Dearnaley⁷², R. Debbe²⁵, C. Debenedetti¹³⁸, B. Dechenaux⁵⁵, D.V. Dedovich⁶⁵, I. Deigaard¹⁰⁷, J. Del Peso⁸², T. Del Prete^{124a,124b}, F. Deliot¹³⁷, C.M. Delitzsch⁴⁹, M. Deliyergiyev⁷⁵, A. Dell'Acqua³⁰, L. Dell'Asta²², M. Dell'Orso^{124a,124b}, M. Della Pietra^{104a,i}, D. della Volpe⁴⁹, M. Delmastro⁵, P.A. Delsart⁵⁵, C. Deluca¹⁰⁷, D.A. DeMarco¹⁵⁹, S. Demers¹⁷⁷, M. Demichev⁶⁵, A. Demilly⁸⁰, S.P. Denisov¹³⁰, D. Derendarz³⁹, J.E. Derkaoui^{136d}, F. Derue⁸⁰, P. Dervan⁷⁴, K. Desch²¹, C. Deterre⁴², P.O. Deviveiros³⁰, A. Dewhurst¹³¹, S. Dhaliwal¹⁰⁷, A. Di Ciaccio^{134a,134b}, L. Di Ciaccio⁵, A. Di Domenico^{133a,133b}, C. Di Donato^{104a,104b}, A. Di Girolamo³⁰, B. Di Girolamo³⁰, A. Di Mattia¹⁵³, B. Di Micco^{135a,135b}, R. Di Nardo⁴⁷, A. Di Simone⁴⁸, R. Di Sipio^{20a,20b}, D. Di Valentino²⁹, F.A. Dias⁴⁶, M.A. Diaz^{32a}, E.B. Diehl⁸⁹, J. Dietrich¹⁶, T.A. Dietzsch^{58a}, S. Diglio⁸⁵, A. Dimitrijevska^{13a}, J. Dingfelder²¹, P. Dita^{26a}, S. Dita^{26a}, F. Dittus³⁰, F. Djama⁸⁵, T. Djobava^{51b}, J.I. Djupsland^{58a}, M.A.B. do Vale^{24c}, D. Dobos³⁰, C. Doglioni⁴⁹, T. Doherty⁵³, T. Dohmae¹⁵⁶, J. Dolejsi¹²⁹, Z. Dolezal¹²⁹, B.A. Dolgoshein^{98,*}, M. Donadelli^{24d}, S. Donati^{124a,124b}, P. Dondero^{121a,121b}, J. Donini³⁴, J. Dopke¹³¹, A. Doria^{104a}, M.T. Dova⁷¹, A.T. Doyle⁵³, M. Dris¹⁰, J. Dubbert⁸⁹, S. Dube¹⁵, E. Dubreuil³⁴, E. Duchovni¹⁷³, G. Duckeck¹⁰⁰, O.A. Ducu^{26a}, D. Duda¹⁷⁶, A. Dudarev³⁰, F. Dudziak⁶⁴, L. Duflot¹¹⁷, L. Duguid⁷⁷, M. Dührssen³⁰, M. Dunford^{58a}, H. Duran Yildiz^{4a}, M. Düren⁵², A. Durglishvili^{51b}, D. Duschinger⁴⁴, M. Dwuznik^{38a}, M. Dyndal^{38a}, W. Edson², N.C. Edwards⁴⁶, W. Ehrenfeld²¹, T. Eifert³⁰, G. Eigen¹⁴, K. Einsweiler¹⁵, T. Ekelof¹⁶⁷, M. El Kacimi^{136c}, M. Ellert¹⁶⁷, S. Elles⁵, F. Ellinghaus⁸³, A.A. Elliot¹⁷⁰, N. Ellis³⁰, J. Elmsheuser¹⁰⁰, M. Elsing³⁰, D. Emeliyanov¹³¹, Y. Enari¹⁵⁶, O.C. Endner⁸³, M. Endo¹¹⁸, R. Engelmann¹⁴⁹, J. Erdmann⁴³, A. Ereditato¹⁷, D. Eriksson^{147a}, G. Ernis¹⁷⁶, J. Ernst², M. Ernst²⁵, J. Ernwein¹³⁷, S. Errede¹⁶⁶, E. Ertel⁸³, M. Escalier¹¹⁷, H. Esch⁴³, C. Escobar¹²⁵, B. Esposito⁴⁷, A.I. Etienne¹³⁷, E. Etzion¹⁵⁴, H. Evans⁶¹, A. Ezhilov¹²³, L. Fabbri^{20a,20b}, G. Facini³¹, R.M. Fakhruddinov¹³⁰, S. Falciano^{133a}, R.J. Falla⁷⁸, J. Faltova¹²⁹, Y. Fang^{33a}, M. Fanti^{91a,91b}, A. Farbin⁸, A. Farilla^{135a}, T. Farooque¹², S. Farrell¹⁵, S.M. Farrington¹⁷¹, P. Farthouat³⁰, F. Fassi^{136e}, P. Fassnacht³⁰, D. Fassouliotis⁹, A. Favareto^{50a,50b}, L. Fayard¹¹⁷, P. Federic^{145a}, O.L. Fedin^{123,l}, W. Fedorko¹⁶⁹, S. Feigl³⁰, L. Feligioni⁸⁵, C. Feng^{33d}, E.J. Feng⁶, H. Feng⁸⁹, A.B. Fenyuk¹³⁰, P. Fernandez Martinez¹⁶⁸, S. Fernandez Perez³⁰, S. Ferrag⁵³, J. Ferrando⁵³, A. Ferrari¹⁶⁷, P. Ferrari¹⁰⁷, R. Ferrari^{121a}, D.E. Ferreira de Lima⁵³, A. Ferrer¹⁶⁸, D. Ferrere⁴⁹, C. Ferretti⁸⁹, A. Ferretto Parodi^{50a,50b}, M. Fiascaris³¹, F. Fiedler⁸³, A. Filipčič⁷⁵, M. Filipuzzi⁴², F. Filthaut¹⁰⁶, M. Fincke-Keeler¹⁷⁰, K.D. Finelli¹⁵¹, M.C.N. Fiolhais^{126a,126c}, L. Fiorini¹⁶⁸, A. Firan⁴⁰, A. Fischer², J. Fischer¹⁷⁶, W.C. Fisher⁹⁰, E.A. Fitzgerald²³, M. Flechl⁴⁸, I. Fleck¹⁴², P. Fleischmann⁸⁹, S. Fleischmann¹⁷⁶, G.T. Fletcher¹⁴⁰, G. Fletcher⁷⁶, T. Flick¹⁷⁶, A. Floderus⁸¹, L.R. Flores Castillo^{60a}, M.J. Flowerdew¹⁰¹, A. Formica¹³⁷, A. Forti⁸⁴, D. Fournier¹¹⁷, H. Fox⁷², S. Fracchia¹², P. Francavilla⁸⁰, M. Franchini^{20a,20b}, S. Franchino³⁰, D. Francis³⁰, L. Franconi¹¹⁹, M. Franklin⁵⁷, M. Fraternali^{121a,121b}, S.T. French²⁸, C. Friedrich⁴², F. Friedrich⁴⁴, D. Froidevaux³⁰, J.A. Frost¹²⁰, C. Fukunaga¹⁵⁷, E. Fullana Torregrosa⁸³, B.G. Fulsom¹⁴⁴, J. Fuster¹⁶⁸, C. Gabaldon⁵⁵, O. Gabizon¹⁷⁶, A. Gabrielli^{20a,20b}, A. Gabrielli^{133a,133b}, S. Gadatsch¹⁰⁷, S. Gadomski⁴⁹, G. Gagliardi^{50a,50b}, P. Gagnon⁶¹, C. Galea¹⁰⁶, B. Galhardo^{126a,126c}, E.J. Gallas¹²⁰, B.J. Gallop¹³¹, P. Gallus¹²⁸, G. Galster³⁶, K.K. Gan¹¹¹, J. Gao^{33b,h}, Y.S. Gao^{144,e}, F.M. Garay Walls⁴⁶, F. Garberson¹⁷⁷, C. García¹⁶⁸, J.E. García Navarro¹⁶⁸, M. Garcia-Sciveres¹⁵, R.W. Gardner³¹, N. Garelli¹⁴⁴, V. Garonne³⁰, C. Gatti⁴⁷, G. Gaudio^{121a}, B. Gaur¹⁴², L. Gauthier⁹⁵, P. Gauzzi^{133a,133b}, I.L. Gavrilenko⁹⁶, C. Gay¹⁶⁹, G. Gaycken²¹, E.N. Gazis¹⁰, P. Ge^{33d}, Z. Gecse¹⁶⁹, C.N.P. Gee¹³¹, D.A.A. Geerts¹⁰⁷, Ch. Geich-Gimbel²¹, K. Gellerstedt^{147a,147b}, C. Gemme^{50a}, A. Gemmell⁵³, M.H. Genest⁵⁵, S. Gentile^{133a,133b}, M. George⁵⁴, S. George⁷⁷, D. Gerbaudo¹⁶⁴, A. Gershon¹⁵⁴, H. Ghazlane^{136b}, N. Ghodbane³⁴, B. Giacobbe^{20a}, S. Giagu^{133a,133b}, V. Giangiobbe¹², P. Giannetti^{124a,124b}, F. Gianotti³⁰, B. Gibbard²⁵, S.M. Gibson⁷⁷, M. Gilchriese¹⁵, T.P.S. Gillam²⁸, D. Gillberg³⁰, G. Gilles³⁴, D.M. Gingrich^{3,d}, N. Giokaris⁹, M.P. Giordani^{165a,165c}, R. Giordano^{104a,104b}, F.M. Giorgi^{20a}, F.M. Giorgi¹⁶, P.F. Giraud¹³⁷, D. Giugni^{91a}, C. Giuliani⁴⁸, M. Giulini^{58b}, B.K. Gjelsten¹¹⁹,

- S. Gkaitatzis¹⁵⁵, I. Gkialas¹⁵⁵, E.L. Gkougkousis¹¹⁷, L.K. Gladilin⁹⁹, C. Glasman⁸², J. Glatzer³⁰, P.C.F. Glaysher⁴⁶, A. Glazov⁴², G.L. Glonti⁶², M. Goblirsch-Kolb¹⁰¹, J.R. Goddard⁷⁶, J. Godlewski³⁰, S. Goldfarb⁸⁹, T. Golling⁴⁹, D. Golubkov¹³⁰, A. Gomes^{126a,126b,126d}, L.S. Gomez Fajardo⁴², R. Gonçalo^{126a}, J. Goncalves Pinto Firmino Da Costa¹³⁷, L. Gonella²¹, S. González de la Hoz¹⁶⁸, G. Gonzalez Parra¹², S. Gonzalez-Sevilla⁴⁹, L. Goossens³⁰, P.A. Gorbounov⁹⁷, H.A. Gordon²⁵, I. Gorelov¹⁰⁵, B. Gorini³⁰, E. Gorini^{73a,73b}, A. Gorišek⁷⁵, E. Gornicki³⁹, A.T. Goshaw⁴⁵, C. Gössling⁴³, M.I. Gostkin⁶⁵, M. Gouighri^{136a}, D. Goujdami^{136c}, M.P. Goulette⁴⁹, A.G. Goussiou¹³⁹, C. Goy⁵, H.M.X. Grabas¹³⁸, L. Graber⁵⁴, I. Grabowska-Bold^{38a}, P. Grafström^{20a,20b}, K-J. Grahn⁴², J. Gramling⁴⁹, E. Gramstad¹¹⁹, S. Grancagnolo¹⁶, V. Grassi¹⁴⁹, V. Gratchev¹²³, H.M. Gray³⁰, E. Graziani^{135a}, O.G. Grebenyuk¹²³, Z.D. Greenwood^{79,m}, K. Gregersen⁷⁸, I.M. Gregor⁴², P. Grenier¹⁴⁴, J. Griffiths⁸, A.A. Grillo¹³⁸, K. Grimm⁷², S. Grinstein^{12,n}, Ph. Gris³⁴, Y.V. Grishkevich⁹⁹, J.-F. Grivaz¹¹⁷, J.P. Grohs⁴⁴, A. Grohsjean⁴², E. Gross¹⁷³, J. Grosse-Knetter⁵⁴, G.C. Grossi^{134a,134b}, Z.J. Grout¹⁵⁰, L. Guan^{33b}, J. Guenther¹²⁸, F. Guescini⁴⁹, D. Guest¹⁷⁷, O. Gueta¹⁵⁴, C. Guicheney³⁴, E. Guido^{50a,50b}, T. Guillemin¹¹⁷, S. Guindon², U. Gul⁵³, C. Gumpert⁴⁴, J. Guo³⁵, S. Gupta¹²⁰, P. Gutierrez¹¹³, N.G. Gutierrez Ortiz⁵³, C. Gutschow⁷⁸, N. Guttman¹⁵⁴, C. Guyot¹³⁷, C. Gwenlan¹²⁰, C.B. Gwilliam⁷⁴, A. Haas¹¹⁰, C. Haber¹⁵, H.K. Hadavand⁸, N. Haddad^{136e}, P. Haefner²¹, S. Hageböck²¹, Z. Hajduk³⁹, H. Hakobyan¹⁷⁸, M. Haleem⁴², J. Haley¹¹⁴, D. Hall¹²⁰, G. Halladjian⁹⁰, G.D. Hallewell⁸⁵, K. Hamacher¹⁷⁶, P. Hamal¹¹⁵, K. Hamano¹⁷⁰, M. Hamer⁵⁴, A. Hamilton^{146a}, S. Hamilton¹⁶², G.N. Hamity^{146c}, P.G. Hamnett⁴², L. Han^{33b}, K. Hanagaki¹¹⁸, K. Hanawa¹⁵⁶, M. Hance¹⁵, P. Hanke^{58a}, R. Hanna¹³⁷, J.B. Hansen³⁶, J.D. Hansen³⁶, P.H. Hansen³⁶, K. Hara¹⁶¹, A.S. Hard¹⁷⁴, T. Harenberg¹⁷⁶, F. Hariri¹¹⁷, S. Harkusha⁹², R.D. Harrington⁴⁶, P.F. Harrison¹⁷¹, F. Hartjes¹⁰⁷, M. Hasegawa⁶⁷, S. Hasegawa¹⁰³, Y. Hasegawa¹⁴¹, A. Hasib¹¹³, S. Hassani¹³⁷, S. Haug¹⁷, M. Hauschild³⁰, R. Hauser⁹⁰, M. Havranek¹²⁷, C.M. Hawkes¹⁸, R.J. Hawkings³⁰, A.D. Hawkins⁸¹, T. Hayashi¹⁶¹, D. Hayden⁹⁰, C.P. Hays¹²⁰, J.M. Hays⁷⁶, H.S. Hayward⁷⁴, S.J. Haywood¹³¹, S.J. Head¹⁸, T. Heck⁸³, V. Hedberg⁸¹, L. Heelan⁸, S. Heim¹²², T. Heim¹⁷⁶, B. Heinemann¹⁵, L. Heinrich¹¹⁰, J. Hejbal¹²⁷, L. Helary²², M. Heller³⁰, S. Hellman^{147a,147b}, D. Hellmich²¹, C. Helsens³⁰, J. Henderson¹²⁰, R.C.W. Henderson⁷², Y. Heng¹⁷⁴, C. Henglert⁴², A. Henrichs¹⁷⁷, A.M. Henriques Correia³⁰, S. Henrot-Versille¹¹⁷, G.H. Herbert¹⁶, Y. Hernández Jiménez¹⁶⁸, R. Herrberg-Schubert¹⁶, G. Herten⁴⁸, R. Hertenberger¹⁰⁰, L. Hervas³⁰, G.G. Hesketh⁷⁸, N.P. Hessey¹⁰⁷, R. Hickling⁷⁶, E. Higón-Rodriguez¹⁶⁸, E. Hill¹⁷⁰, J.C. Hill²⁸, K.H. Hiller⁴², S.J. Hillier¹⁸, I. Hinchliffe¹⁵, E. Hines¹²², R.R. Hinman¹⁵, M. Hirose¹⁵⁸, D. Hirschbuehl¹⁷⁶, J. Hobbs¹⁴⁹, N. Hod¹⁰⁷, M.C. Hodgkinson¹⁴⁰, P. Hodgson¹⁴⁰, A. Hoecker³⁰, M.R. Hoeferkamp¹⁰⁵, F. Hoenig¹⁰⁰, D. Hoffmann⁸⁵, M. Hohlfeld⁸³, T.R. Holmes¹⁵, T.M. Hong¹²², L. Hooft van Huysduynen¹¹⁰, W.H. Hopkins¹¹⁶, Y. Horii¹⁰³, A.J. Horton¹⁴³, J-Y. Hostachy⁵⁵, S. Hou¹⁵², A. Hoummada^{136a}, J. Howard¹²⁰, J. Howarth⁴², M. Hrabovsky¹¹⁵, I. Hristova¹⁶, J. Hrivnac¹¹⁷, T. Hryna'ova⁵, A. Hrynevich⁹³, C. Hsu^{146c}, P.J. Hsu¹⁵², S.-C. Hsu¹³⁹, D. Hu³⁵, X. Hu⁸⁹, Y. Huang⁴², Z. Hubacek³⁰, F. Hubaut⁸⁵, F. Huegging²¹, T.B. Huffman¹²⁰, E.W. Hughes³⁵, G. Hughes⁷², M. Huhtinen³⁰, T.A. Hülsing⁸³, M. Hurwitz¹⁵, N. Huseynov^{65,b}, J. Huston⁹⁰, J. Huth⁵⁷, G. Iacobucci⁴⁹, G. Iakovovidis¹⁰, I. Ibragimov¹⁴², L. Iconomidou-Fayard¹¹⁷, E. Ideal¹⁷⁷, Z. Idrissi^{136e}, P. Iengo^{104a}, O. Igonkina¹⁰⁷, T. Iizawa¹⁷², Y. Ikegami⁶⁶, K. Ikematsu¹⁴², M. Ikeno⁶⁶, Y. Ilchenko^{31,o}, D. Iliadis¹⁵⁵, N. Ilic¹⁵⁹, Y. Inamaru⁶⁷, T. Ince¹⁰¹, P. Ioannou⁹, M. Iodice^{135a}, K. Iordanidou⁹, V. Ippolito⁵⁷, A. Irles Quiles¹⁶⁸, C. Isaksson¹⁶⁷, M. Ishino⁶⁸, M. Ishitsuka¹⁵⁸, R. Ishmukhametov¹¹¹, C. Issever¹²⁰, S. Istin^{19a}, J.M. Iturbe Ponce⁸⁴, R. Iuppa^{134a,134b}, J. Ivarsson⁸¹, W. Iwanski³⁹, H. Iwasaki⁶⁶, J.M. Izen⁴¹, V. Izzo^{104a}, B. Jackson¹²², M. Jackson⁷⁴, P. Jackson¹, M.R. Jaekel³⁰, V. Jain², K. Jakobs⁴⁸, S. Jakobsen³⁰, T. Jakoubek¹²⁷, J. Jakubek¹²⁸, D.O. Jamin¹⁵², D.K. Jana⁷⁹, E. Jansen⁷⁸, J. Janssen²¹, M. Janus¹⁷¹, G. Jarlskog⁸¹, N. Javadov^{65,b}, T. Javůrek⁴⁸, L. Jeanty¹⁵, J. Jejelava^{51a,p}, G.-Y. Jeng¹⁵¹, D. Jennens⁸⁸, P. Jenni^{48,q}, J. Jentzsch⁴³, C. Jeske¹⁷¹, S. Jézéquel⁵, H. Ji¹⁷⁴, J. Jia¹⁴⁹, Y. Jiang^{33b}, M. Jimenez Belenguer⁴², S. Jin^{33a}, A. Jinaru^{26a}, O. Jinnouchi¹⁵⁸, M.D. Joergensen³⁶, P. Johansson¹⁴⁰, K.A. Johns⁷, K. Jon-And^{147a,147b}, G. Jones¹⁷¹,

- R.W.L. Jones⁷², T.J. Jones⁷⁴, J. Jongmanns^{58a}, P.M. Jorge^{126a,126b}, K.D. Joshi⁸⁴, J. Jovicevic¹⁴⁸, X. Ju¹⁷⁴, C.A. Jung⁴³, P. Jussel⁶², A. Juste Rozas^{12,n}, M. Kaci¹⁶⁸, A. Kaczmarska³⁹, M. Kado¹¹⁷, H. Kagan¹¹¹, M. Kagan¹⁴⁴, E. Kajomovitz⁴⁵, C.W. Kalderon¹²⁰, S. Kama⁴⁰, A. Kamenshchikov¹³⁰, N. Kanaya¹⁵⁶, M. Kaneda³⁰, S. Kaneti²⁸, V.A. Kantserov⁹⁸, J. Kanzaki⁶⁶, B. Kaplan¹¹⁰, A. Kapliy³¹, D. Kar⁵³, K. Karakostas¹⁰, A. Karamaoun³, N. Karastathis¹⁰, M.J. Kareem⁵⁴, M. Karnevskiy⁸³, S.N. Karpov⁶⁵, Z.M. Karpova⁶⁵, K. Karthik¹¹⁰, V. Kartvelishvili⁷², A.N. Karyukhin¹³⁰, L. Kashif¹⁷⁴, G. Kasieczka^{58b}, R.D. Kass¹¹¹, A. Kastanas¹⁴, Y. Kataoka¹⁵⁶, A. Katre⁴⁹, J. Katzy⁴², V. Kaushik⁷, K. Kawagoe⁷⁰, T. Kawamoto¹⁵⁶, G. Kawamura⁵⁴, S. Kazama¹⁵⁶, V.F. Kazanin¹⁰⁹, M.Y. Kazarinov⁶⁵, R. Keeler¹⁷⁰, R. Kehoe⁴⁰, M. Keil⁵⁴, J.S. Keller⁴², J.J. Kempster⁷⁷, H. Keoshkerian⁵, O. Kepka¹²⁷, B.P. Kersevan⁷⁵, S. Kersten¹⁷⁶, K. Kessoku¹⁵⁶, J. Keung¹⁵⁹, R.A. Keyes⁸⁷, F. Khalil-zada¹¹, H. Khandanyan^{147a,147b}, A. Khanov¹¹⁴, A. Kharlamov¹⁰⁹, A. Khodinov⁹⁸, A. Khomich^{58a}, T.J. Khoo²⁸, G. Khoriauli²¹, V. Khovanskiy⁹⁷, E. Khramov⁶⁵, J. Khubua^{51b}, H.Y. Kim⁸, H. Kim^{147a,147b}, S.H. Kim¹⁶¹, N. Kimura¹⁵⁵, O. Kind¹⁶, B.T. King⁷⁴, M. King¹⁶⁸, R.S.B. King¹²⁰, S.B. King¹⁶⁹, J. Kirk¹³¹, A.E. Kiryunin¹⁰¹, T. Kishimoto⁶⁷, D. Kisielewska^{38a}, F. Kiss⁴⁸, K. Kiuchi¹⁶¹, E. Kladiva^{145b}, M. Klein⁷⁴, U. Klein⁷⁴, K. Kleinknecht⁸³, P. Klimek^{147a,147b}, A. Klimentov²⁵, R. Klingenberg⁴³, J.A. Klinger⁸⁴, T. Klioutchnikova³⁰, P.F. Klok¹⁰⁶, E.-E. Kluge^{58a}, P. Kluit¹⁰⁷, S. Kluth¹⁰¹, E. Knerner⁶², E.B.F.G. Knoops⁸⁵, A. Knue⁵³, D. Kobayashi¹⁵⁸, T. Kobayashi¹⁵⁶, M. Kobel⁴⁴, M. Kocian¹⁴⁴, P. Kodys¹²⁹, T. Koffman²⁹, E. Koffeman¹⁰⁷, L.A. Kogan¹²⁰, S. Kohlmann¹⁷⁶, Z. Kohout¹²⁸, T. Kohriki⁶⁶, T. Koi¹⁴⁴, H. Kolanoski¹⁶, I. Koletsou⁵, J. Koll⁹⁰, A.A. Komar^{96,*}, Y. Komori¹⁵⁶, T. Kondo⁶⁶, N. Kondrashova⁴², K. Köneke⁴⁸, A.C. König¹⁰⁶, S. König⁸³, T. Kono^{66,r}, R. Konoplich^{110,s}, N. Konstantinidis⁷⁸, R. Kopeliansky¹⁵³, S. Koperny^{38a}, L. Köpke⁸³, A.K. Kopp⁴⁸, K. Korcyl³⁹, K. Kordas¹⁵⁵, A. Korn⁷⁸, A.A. Korol^{109,c}, I. Korolkov¹², E.V. Korolkova¹⁴⁰, V.A. Korotkov¹³⁰, O. Kortner¹⁰¹, S. Kortner¹⁰¹, V.V. Kostyukhin²¹, V.M. Kotov⁶⁵, A. Kotwal⁴⁵, A. Kourkoumeli-Charalampidi¹⁵⁵, C. Kourkoumelis⁹, V. Kouskoura²⁵, A. Koutsman^{160a}, R. Kowalewski¹⁷⁰, T.Z. Kowalski^{38a}, W. Kozanecki¹³⁷, A.S. Kozhin¹³⁰, V.A. Kramarenko⁹⁹, G. Kramberger⁷⁵, D. Krasnopevtsev⁹⁸, M.W. Krasny⁸⁰, A. Krasznahorkay³⁰, J.K. Kraus²¹, A. Kravchenko²⁵, S. Kreiss¹¹⁰, M. Kretz^{58c}, J. Kretzschmar⁷⁴, K. Kreutzfeldt⁵², P. Krieger¹⁵⁹, K. Krizka³¹, K. Kroeninger⁴³, H. Kroha¹⁰¹, J. Kroll¹²², J. Kroseberg²¹, J. Krstic^{13a}, U. Kruchonak⁶⁵, H. Krüger²¹, N. Krumnack⁶⁴, Z.V. Krumshteyn⁶⁵, A. Kruse¹⁷⁴, M.C. Kruse⁴⁵, M. Kruskal²², T. Kubota⁸⁸, H. Kucuk⁷⁸, S. Kuday^{4c}, S. Kuehn⁴⁸, A. Kugel^{58c}, F. Kuger¹⁷⁵, A. Kuhl¹³⁸, T. Kuhl⁴², V. Kukhtin⁶⁵, Y. Kulchitsky⁹², S. Kuleshov^{32b}, M. Kuna^{133a,133b}, T. Kunigo⁶⁸, A. Kupco¹²⁷, H. Kurashige⁶⁷, Y.A. Kurochkin⁹², R. Kurumida⁶⁷, V. Kus¹²⁷, E.S. Kuwertz¹⁴⁸, M. Kuze¹⁵⁸, J. Kvita¹¹⁵, D. Kyriazopoulos¹⁴⁰, A. La Rosa⁴⁹, L. La Rotonda^{37a,37b}, C. Lacasta¹⁶⁸, F. Lacava^{133a,133b}, J. Lacey²⁹, H. Lacker¹⁶, D. Lacour⁸⁰, V.R. Lacuesta¹⁶⁸, E. Ladygin⁶⁵, R. Lafaye⁵, B. Laforge⁸⁰, T. Lagouri¹⁷⁷, S. Lai⁴⁸, H. Laier^{58a}, L. Lambourne⁷⁸, S. Lammers⁶¹, C.L. Lampen⁷, W. Lampl⁷, E. Lançon¹³⁷, U. Landgraf⁴⁸, M.P.J. Landon⁷⁶, V.S. Lang^{58a}, A.J. Lankford¹⁶⁴, F. Lanni²⁵, K. Lantzsch³⁰, S. Laplace⁸⁰, C. Lapoire²¹, J.F. Laporte¹³⁷, T. Lari^{91a}, F. Lasagni Manghi^{20a,20b}, M. Lassnig³⁰, P. Laurelli⁴⁷, W. Lavrijssen¹⁵, A.T. Law¹³⁸, P. Laycock⁷⁴, O. Le Dortz⁸⁰, E. Le Guiriec⁸⁵, E. Le Menedeu¹², T. LeCompte⁶, F. Ledroit-Guillon⁵⁵, C.A. Lee^{146b}, H. Lee¹⁰⁷, S.C. Lee¹⁵², L. Lee¹, G. Lefebvre⁸⁰, M. Lefebvre¹⁷⁰, F. Legger¹⁰⁰, C. Leggett¹⁵, A. Lehan⁷⁴, G. Lehmann Miotto³⁰, X. Lei⁷, W.A. Leight²⁹, A. Leisos¹⁵⁵, A.G. Leister¹⁷⁷, M.A.L. Leite^{24d}, R. Leitner¹²⁹, D. Lellouch¹⁷³, B. Lemmer⁵⁴, K.J.C. Leney⁷⁸, T. Lenz²¹, G. Lenzen¹⁷⁶, B. Lenzi³⁰, R. Leone⁷, S. Leone^{124a,124b}, C. Leonidopoulos⁴⁶, S. Leontsinis¹⁰, C. Leroy⁹⁵, C.G. Lester²⁸, C.M. Lester¹²², M. Levchenko¹²³, J. Levêque⁵, D. Levin⁸⁹, L.J. Levinson¹⁷³, M. Levy¹⁸, A. Lewis¹²⁰, A.M. Leyko²¹, M. Leyton⁴¹, B. Li^{33b,t}, B. Li⁸⁵, H. Li¹⁴⁹, H.L. Li³¹, L. Li⁴⁵, L. Li^{33e}, S. Li⁴⁵, Y. Li^{33c,u}, Z. Liang¹³⁸, H. Liao³⁴, B. Libert^{134a}, P. Lichard³⁰, K. Lie¹⁶⁶, J. Liebal²¹, W. Liebig¹⁴, C. Limbach²¹, A. Limosani¹⁵¹, S.C. Lin^{152,v}, T.H. Lin⁸³, F. Linde¹⁰⁷, B.E. Lindquist¹⁴⁹, J.T. Linnemann⁹⁰, E. Lipeles¹²², A. Lipniacka¹⁴, M. Lisovyi⁴², T.M. Liss¹⁶⁶, D. Lissauer²⁵, A. Lister¹⁶⁹, A.M. Litke¹³⁸, B. Liu¹⁵², D. Liu¹⁵², J. Liu⁸⁵, J.B. Liu^{33b}, K. Liu^{33b,w}, L. Liu⁸⁹, M. Liu⁴⁵, M. Liu^{33b}, Y. Liu^{33b},

- M. Livan^{121a,121b}, A. Lleres⁵⁵, J. Llorente Merino⁸², S.L. Lloyd⁷⁶, F. Lo Sterzo¹⁵², E. Lobodzinska⁴², P. Loch⁷, W.S. Lockman¹³⁸, F.K. Loebinger⁸⁴, A.E. Loevschall-Jensen³⁶, A. Loginov¹⁷⁷, T. Lohse¹⁶, K. Lohwasser⁴², M. Lokajicek¹²⁷, B.A. Long²², J.D. Long⁸⁹, R.E. Long⁷², K.A.Looper¹¹¹, L. Lopes^{126a}, D. Lopez Mateos⁵⁷, B. Lopez Paredes¹⁴⁰, I. Lopez Paz¹², J. Lorenz¹⁰⁰, N. Lorenzo Martinez⁶¹, M. Losada¹⁶³, P. Loscutoff¹⁵, X. Lou^{33a}, A. Lounis¹¹⁷, J. Love⁶, P.A. Love⁷², A.J. Lowe^{144,e}, F. Lu^{33a}, N. Lu⁸⁹, H.J. Lubatti¹³⁹, C. Luci^{133a,133b}, A. Lucotte⁵⁵, F. Luehring⁶¹, W. Lukas⁶², L. Luminari^{133a}, O. Lundberg^{147a,147b}, B. Lund-Jensen¹⁴⁸, M. Lungwitz⁸³, D. Lynn²⁵, R. Lysak¹²⁷, E. Lytken⁸¹, H. Ma²⁵, L.L. Ma^{33d}, G. Maccarrone⁴⁷, A. Macchiolo¹⁰¹, J. Machado Miguens^{126a,126b}, D. Macina³⁰, D. Madaffari⁸⁵, R. Madar⁴⁸, H.J. Maddocks⁷², W.F. Mader⁴⁴, A. Madsen¹⁶⁷, M. Maeno⁸, T. Maeno²⁵, A. Maevskiy⁹⁹, E. Magradze⁵⁴, K. Mahboubi⁴⁸, J. Mahlstedt¹⁰⁷, S. Mahmoud⁷⁴, C. Maiani¹³⁷, C. Maidantchik^{24a}, A.A. Maier¹⁰¹, A. Maio^{126a,126b,126d}, S. Majewski¹¹⁶, Y. Makida⁶⁶, N. Makovec¹¹⁷, P. Mal^{137,x}, B. Malaescu⁸⁰, Pa. Malecki³⁹, V.P. Maleev¹²³, F. Malek⁵⁵, U. Mallik⁶³, D. Malon⁶, C. Malone¹⁴⁴, S. Maltezos¹⁰, V.M. Malyshev¹⁰⁹, S. Malyukov³⁰, J. Mamuzic^{13b}, B. Mandelli³⁰, L. Mandelli^{91a}, I. Mandić⁷⁵, R. Mandrysch⁶³, J. Maneira^{126a,126b}, A. Manfredini¹⁰¹, L. Manhaes de Andrade Filho^{24b}, J.A. Manjarres Ramos^{160b}, A. Mann¹⁰⁰, P.M. Manning¹³⁸, A. Manousakis-Katsikakis⁹, B. Mansoulie¹³⁷, R. Mantifel⁸⁷, M. Mantoani⁵⁴, L. Mapelli³⁰, L. March^{146c}, J.F. Marchand²⁹, G. Marchiori⁸⁰, M. Marcisovsky¹²⁷, C.P. Marino¹⁷⁰, M. Marjanovic^{13a}, F. Marroquin^{24a}, S.P. Marsden⁸⁴, Z. Marshall¹⁵, L.F. Marti¹⁷, S. Marti-Garcia¹⁶⁸, B. Martin³⁰, B. Martin⁹⁰, T.A. Martin¹⁷¹, V.J. Martin⁴⁶, B. Martin dit Latour¹⁴, H. Martinez¹³⁷, M. Martinez^{12,n}, S. Martin-Haugh¹³¹, A.C. Martyniuk⁷⁸, M. Marx¹³⁹, F. Marzano^{133a}, A. Marzin³⁰, L. Masetti⁸³, T. Mashimo¹⁵⁶, R. Mashinistov⁹⁶, J. Masik⁸⁴, A.L. Maslennikov^{109,c}, I. Massa^{20a,20b}, L. Massa^{20a,20b}, N. Massol⁵, P. Mastrandrea¹⁴⁹, A. Mastroberardino^{37a,37b}, T. Masubuchi¹⁵⁶, P. Mättig¹⁷⁶, J. Mattmann⁸³, J. Maurer^{26a}, S.J. Maxfield⁷⁴, D.A. Maximov^{109,c}, R. Mazini¹⁵², S.M. Mazza^{91a,91b}, L. Mazzaferro^{134a,134b}, G. Mc Goldrick¹⁵⁹, S.P. Mc Kee⁸⁹, A. McCarn⁸⁹, R.L. McCarthy¹⁴⁹, T.G. McCarthy²⁹, N.A. McCubbin¹³¹, K.W. McFarlane^{56,*}, J.A. McFayden⁷⁸, G. Mchedlidze⁵⁴, S.J. McMahon¹³¹, R.A. McPherson^{170,j}, J. Mechnick¹⁰⁷, M. Medinnis⁴², S. Meehan³¹, S. Mehlhase¹⁰⁰, A. Mehta⁷⁴, K. Meier^{58a}, C. Meineck¹⁰⁰, B. Meirose⁴¹, C. Melachrinos³¹, B.R. Mellado Garcia^{146c}, F. Meloni¹⁷, A. Mengarelli^{20a,20b}, S. Menke¹⁰¹, E. Meoni¹⁶², K.M. Mercurio⁵⁷, S. Mergelmeyer²¹, N. Meric¹³⁷, P. Mermod⁴⁹, L. Merola^{104a,104b}, C. Meroni^{91a}, F.S. Merritt³¹, H. Merritt¹¹¹, A. Messina^{30,y}, J. Metcalfe²⁵, A.S. Mete¹⁶⁴, C. Meyer⁸³, C. Meyer¹²², J-P. Meyer¹³⁷, J. Meyer³⁰, R.P. Middleton¹³¹, S. Migas⁷⁴, S. Miglioranza^{165a,165c}, L. Mijović²¹, G. Mikenberg¹⁷³, M. Mikestikova¹²⁷, M. Mikuž⁷⁵, A. Milic³⁰, D.W. Miller³¹, C. Mills⁴⁶, A. Milov¹⁷³, D.A. Milstead^{147a,147b}, A.A. Minaenko¹³⁰, Y. Minami¹⁵⁶, I.A. Minashvili⁶⁵, A.I. Mincer¹¹⁰, B. Mindur^{38a}, M. Mineev⁶⁵, Y. Ming¹⁷⁴, L.M. Mir¹², G. Mirabelli^{133a}, T. Mitami¹⁷², J. Mitrevski¹⁰⁰, V.A. Mitsou¹⁶⁸, A. Miucci⁴⁹, P.S. Miyagawa¹⁴⁰, J.U. Mjörnmark⁸¹, T. Moa^{147a,147b}, K. Mochizuki⁸⁵, S. Mohapatra³⁵, W. Mohr⁴⁸, S. Molander^{147a,147b}, R. Moles-Valls¹⁶⁸, K. Mönig⁴², C. Monini⁵⁵, J. Monk³⁶, E. Monnier⁸⁵, J. Montejo Berlingen¹², F. Monticelli⁷¹, S. Monzani^{133a,133b}, R.W. Moore³, N. Morange⁶³, D. Moreno¹⁶³, M. Moreno Llácer⁵⁴, P. Morettini^{50a}, M. Morgenstern⁴⁴, M. Morii⁵⁷, V. Morisbak¹¹⁹, S. Moritz⁸³, A.K. Morley¹⁴⁸, G. Mornacchi³⁰, J.D. Morris⁷⁶, A. Morton⁴², L. Morvaj¹⁰³, H.G. Moser¹⁰¹, M. Mosidze^{51b}, J. Moss¹¹¹, K. Motohashi¹⁵⁸, R. Mount¹⁴⁴, E. Mountricha²⁵, S.V. Mouraviev^{96,*}, E.J.W. Moyse⁸⁶, S. Muanza⁸⁵, R.D. Mudd¹⁸, F. Mueller^{58a}, J. Mueller¹²⁵, K. Mueller²¹, T. Mueller²⁸, D. Muenstermann⁴⁹, P. Mullen⁵³, Y. Munwes¹⁵⁴, J.A. Murillo Quijada¹⁸, W.J. Murray^{171,131}, H. Musheghyan⁵⁴, E. Musto¹⁵³, A.G. Myagkov^{130,z}, M. Myska¹²⁸, O. Nackenhorst⁵⁴, J. Nadal⁵⁴, K. Nagai¹²⁰, R. Nagai¹⁵⁸, Y. Nagai⁸⁵, K. Nagano⁶⁶, A. Nagarkar¹¹¹, Y. Nagasaka⁵⁹, K. Nagata¹⁶¹, M. Nagel¹⁰¹, A.M. Nairz³⁰, Y. Nakahama³⁰, K. Nakamura⁶⁶, T. Nakamura¹⁵⁶, I. Nakano¹¹², H. Namasisivayam⁴¹, G. Nanava²¹, R.F. Naranjo Garcia⁴², R. Narayan^{58b}, T. Nattermann²¹, T. Naumann⁴², G. Navarro¹⁶³, R. Nayyar⁷, H.A. Neal⁸⁹, P.Yu. Nechaeva⁹⁶, T.J. Neep⁸⁴, P.D. Nef¹⁴⁴, A. Negri^{121a,121b}, G. Negri³⁰, M. Negrini^{20a}, S. Nektarijevic⁴⁹, C. Nellist¹¹⁷, A. Nelson¹⁶⁴, T.K. Nelson¹⁴⁴,

- S. Nemecek¹²⁷, P. Nemethy¹¹⁰, A.A. Nepomuceno^{24a}, M. Nessi^{30,aa}, M.S. Neubauer¹⁶⁶, M. Neumann¹⁷⁶, R.M. Neves¹¹⁰, P. Nevski²⁵, P.R. Newman¹⁸, D.H. Nguyen⁶, R.B. Nickerson¹²⁰, R. Nicolaidou¹³⁷, B. Nicquevert³⁰, J. Nielsen¹³⁸, N. Nikiforou³⁵, A. Nikiforov¹⁶, V. Nikolaenko^{130,z}, I. Nikolic-Audit⁸⁰, K. Nikolics⁴⁹, K. Nikolopoulos¹⁸, P. Nilsson²⁵, Y. Ninomiya¹⁵⁶, A. Nisati^{133a}, R. Nisius¹⁰¹, T. Nobe¹⁵⁸, M. Nomachi¹¹⁸, I. Nomidis²⁹, S. Norberg¹¹³, M. Nordberg³⁰, O. Novgorodova⁴⁴, S. Nowak¹⁰¹, M. Nozaki⁶⁶, L. Nozka¹¹⁵, K. Ntekas¹⁰, G. Nunes Hanninger⁸⁸, T. Nunnemann¹⁰⁰, E. Nurse⁷⁸, F. Nutti⁸⁸, B.J. O'Brien⁴⁶, F. O'grady⁷, D.C. O'Neil¹⁴³, V. O'Shea⁵³, F.G. Oakham^{29,d}, H. Oberlack¹⁰¹, T. Obermann²¹, J. Ocariz⁸⁰, A. Ochi⁶⁷, I. Ochoa⁷⁸, S. Oda⁷⁰, S. Odaka⁶⁶, H. Ogren⁶¹, A. Oh⁸⁴, S.H. Oh⁴⁵, C.C. Ohm¹⁵, H. Ohman¹⁶⁷, H. Oide³⁰, W. Okamura¹¹⁸, H. Okawa¹⁶¹, Y. Okumura³¹, T. Okuyama¹⁵⁶, A. Olariu^{26a}, A.G. Olchevski⁶⁵, S.A. Olivares Pino⁴⁶, D. Oliveira Damazio²⁵, E. Oliver Garcia¹⁶⁸, A. Olszewski³⁹, J. Olszowska³⁹, A. Onofre^{126a,126e}, P.U.E. Onyisi^{31,o}, C.J. Oram^{160a}, M.J. Oreglia³¹, Y. Oren¹⁵⁴, D. Orestano^{135a,135b}, N. Orlando^{73a,73b}, C. Oropeza Barrera⁵³, R.S. Orr¹⁵⁹, B. Osculati^{50a,50b}, R. Ospanov¹²², G. Otero y Garzon²⁷, H. Otono⁷⁰, M. Ouchrif^{136d}, E.A. Ouellette¹⁷⁰, F. Ould-Saada¹¹⁹, A. Ouraou¹³⁷, K.P. Oussoren¹⁰⁷, Q. Ouyang^{33a}, A. Ovcharova¹⁵, M. Owen⁸⁴, V.E. Ozcan^{19a}, N. Ozturk⁸, K. Pachal¹²⁰, A. Pacheco Pages¹², C. Padilla Aranda¹², M. Pagáčová⁴⁸, S. Pagan Griso¹⁵, E. Paganis¹⁴⁰, C. Pahl¹⁰¹, F. Paige²⁵, P. Pais⁸⁶, K. Pajchel¹¹⁹, G. Palacino^{160b}, S. Palestini³⁰, M. Palka^{38b}, D. Pallin³⁴, A. Palma^{126a,126b}, J.D. Palmer¹⁸, Y.B. Pan¹⁷⁴, E. Panagiotopoulou¹⁰, J.G. Panduro Vazquez⁷⁷, P. Pani¹⁰⁷, N. Panikashvili⁸⁹, S. Panitkin²⁵, D. Pantea^{26a}, L. Paolozzi^{134a,134b}, Th.D. Papadopoulos¹⁰, K. Papageorgiou¹⁵⁵, A. Paramonov⁶, D. Paredes Hernandez¹⁵⁵, M.A. Parker²⁸, F. Parodi^{50a,50b}, J.A. Parsons³⁵, U. Parzefall⁴⁸, E. Pasqualucci^{133a}, S. Passaggio^{50a}, A. Passeri^{135a}, F. Pastore^{135a,135b,*}, Fr. Pastore⁷⁷, G. Pásztor²⁹, S. Pataraia¹⁷⁶, N.D. Patel¹⁵¹, J.R. Pater⁸⁴, S. Patricelli^{104a,104b}, T. Pauly³⁰, J. Pearce¹⁷⁰, L.E. Pedersen³⁶, M. Pedersen¹¹⁹, S. Pedraza Lopez¹⁶⁸, R. Pedro^{126a,126b}, S.V. Peleganchuk¹⁰⁹, D. Pelikan¹⁶⁷, H. Peng^{33b}, B. Penning³¹, J. Penwell⁶¹, D.V. Perepelitsa²⁵, E. Perez Codina^{160a}, M.T. Pérez García-Estañ¹⁶⁸, L. Perini^{91a,91b}, H. Pernegger³⁰, S. Perrella^{104a,104b}, R. Peschke⁴², V.D. Peshekhanov⁶⁵, K. Peters³⁰, R.F.Y. Peters⁸⁴, B.A. Petersen³⁰, T.C. Petersen³⁶, E. Petit⁴², A. Petridis^{147a,147b}, C. Petridou¹⁵⁵, E. Petrolo^{133a}, F. Petrucci^{135a,135b}, N.E. Pettersson¹⁵⁸, R. Pezoa^{32b}, P.W. Phillips¹³¹, G. Piacquadio¹⁴⁴, E. Pianori¹⁷¹, A. Picazio⁴⁹, E. Piccaro⁷⁶, M. Piccinini^{20a,20b}, M.A. Pickering¹²⁰, R. Piegaia²⁷, D.T. Pignotti¹¹¹, J.E. Pilcher³¹, A.D. Pilkington⁷⁸, J. Pina^{126a,126b,126d}, M. Pinamonti^{165a,165c,ab}, A. Pinder¹²⁰, J.L. Pinfold³, A. Pingel³⁶, B. Pinto^{126a}, S. Pires⁸⁰, M. Pitt¹⁷³, C. Pizio^{91a,91b}, L. Plazak^{145a}, M.-A. Pleier²⁵, V. Pleskot¹²⁹, E. Plotnikova⁶⁵, P. Plucinski^{147a,147b}, D. Pluth⁶⁴, S. Poddar^{58a}, F. Podlaski³⁴, R. Poettgen⁸³, L. Poggioli¹¹⁷, D. Pohl²¹, M. Pohl⁴⁹, G. Polesello^{121a}, A. Pollicchio^{37a,37b}, R. Polifka¹⁵⁹, A. Polini^{20a}, C.S. Pollard⁵³, V. Polychronakos²⁵, K. Pommès³⁰, L. Pontecorvo^{133a}, B.G. Pope⁹⁰, G.A. Popeneiciu^{26b}, D.S. Popovic^{13a}, A. Poppleton³⁰, S. Pospisil¹²⁸, K. Potamianos¹⁵, I.N. Potrap⁶⁵, C.J. Potter¹⁵⁰, C.T. Potter¹¹⁶, G. Poulard³⁰, J. Poveda³⁰, V. Pozdnyakov⁶⁵, P. Pralavorio⁸⁵, A. Pranko¹⁵, S. Prasad³⁰, S. Prell⁶⁴, D. Price⁸⁴, J. Price⁷⁴, L.E. Price⁶, D. Prieur¹²⁵, M. Primavera^{73a}, S. Prince⁸⁷, M. Proissl⁴⁶, K. Prokofiev^{60c}, F. Prokoshin^{32b}, E. Protopapadaki¹³⁷, S. Protopopescu²⁵, J. Proudfoot⁶, M. Przybycien^{38a}, H. Przysiezniak⁵, E. Ptacek¹¹⁶, D. Puddu^{135a,135b}, E. Pueschel⁸⁶, D. Puldon¹⁴⁹, M. Purohit^{25,ac}, P. Puzo¹¹⁷, J. Qian⁸⁹, G. Qin⁵³, Y. Qin⁸⁴, A. Quadt⁵⁴, D.R. Quarrie¹⁵, W.B. Quayle^{165a,165b}, M. Queitsch-Maitland⁸⁴, D. Quilty⁵³, A. Qureshi^{160b}, V. Radeka²⁵, V. Radescu⁴², S.K. Radhakrishnan¹⁴⁹, P. Radloff¹¹⁶, P. Rados⁸⁸, F. Ragusa^{91a,91b}, G. Rahal¹⁷⁹, S. Rajagopalan²⁵, M. Rammensee³⁰, C. Rangel-Smith¹⁶⁷, K. Rao¹⁶⁴, F. Rauscher¹⁰⁰, S. Rave⁸³, T.C. Rave⁴⁸, T. Ravenscroft⁵³, M. Raymond³⁰, A.L. Read¹¹⁹, N.P. Readoff⁷⁴, D.M. Rebuzzi^{121a,121b}, A. Redelbach¹⁷⁵, G. Redlinger²⁵, R. Reece¹³⁸, K. Reeves⁴¹, L. Rehnisch¹⁶, H. Reisin²⁷, M. Relich¹⁶⁴, C. Rembser³⁰, H. Ren^{33a}, Z.L. Ren¹⁵², A. Renaud¹¹⁷, M. Rescigno^{133a}, S. Resconi^{91a}, O.L. Rezanova^{109,c}, P. Reznicek¹²⁹, R. Rezvani⁹⁵, R. Richter¹⁰¹, M. Ridel⁸⁰, P. Rieck¹⁶, J. Rieger⁵⁴, M. Rijssenbeek¹⁴⁹, A. Rimoldi^{121a,121b}, L. Rinaldi^{20a}, E. Ritsch⁶², I. Riu¹², F. Rizatdinova¹¹⁴, E. Rizvi⁷⁶, S.H. Robertson^{87,j}, A. Robichaud-Veronneau⁸⁷,

- D. Robinson²⁸, J.E.M. Robinson⁸⁴, A. Robson⁵³, C. Roda^{124a,124b}, L. Rodrigues³⁰, S. Roe³⁰, O. Røhne¹¹⁹, S. Rolli¹⁶², A. Romaniouk⁹⁸, M. Romano^{20a,20b}, E. Romero Adam¹⁶⁸, N. Rompotis¹³⁹, M. Ronzani⁴⁸, L. Roos⁸⁰, E. Ros¹⁶⁸, S. Rosati^{133a}, K. Rosbach⁴⁹, M. Rose⁷⁷, P. Rose¹³⁸, P.L. Rosendahl¹⁴, O. Rosenthal¹⁴², V. Rossetti^{147a,147b}, E. Rossi^{104a,104b}, L.P. Rossi^{50a}, R. Rosten¹³⁹, M. Rotaru^{26a}, I. Roth¹⁷³, J. Rothberg¹³⁹, D. Rousseau¹¹⁷, C.R. Royon¹³⁷, A. Rozanov⁸⁵, Y. Rozen¹⁵³, X. Ruan^{146c}, F. Rubbo¹², I. Rubinskiy⁴², V.I. Rud⁹⁹, C. Rudolph⁴⁴, M.S. Rudolph¹⁵⁹, F. Rihr⁴⁸, A. Ruiz-Martinez³⁰, Z. Rurikova⁴⁸, N.A. Rusakovich⁶⁵, A. Ruschke¹⁰⁰, H.L. Russell¹³⁹, J.P. Rutherford⁷, N. Ruthmann⁴⁸, Y.F. Ryabov¹²³, M. Rybar¹²⁹, G. Rybkin¹¹⁷, N.C. Ryder¹²⁰, A.F. Saavedra¹⁵¹, G. Sabato¹⁰⁷, S. Sacerdoti²⁷, A. Saddique³, H.F-W. Sadrozinski¹³⁸, R. Sadykov⁶⁵, F. Safai Tehrani^{133a}, H. Sakamoto¹⁵⁶, Y. Sakurai¹⁷², G. Salamanna^{135a,135b}, A. Salamon^{134a}, M. Saleem¹¹³, D. Salek¹⁰⁷, P.H. Sales De Bruin¹³⁹, D. Salihagic¹⁰¹, A. Salnikov¹⁴⁴, J. Salt¹⁶⁸, D. Salvatore^{37a,37b}, F. Salvatore¹⁵⁰, A. Salvucci¹⁰⁶, A. Salzburger³⁰, D. Sampsonidis¹⁵⁵, A. Sanchez^{104a,104b}, J. Sánchez¹⁶⁸, V. Sanchez Martinez¹⁶⁸, H. Sandaker¹⁴, R.L. Sandbach⁷⁶, H.G. Sander⁸³, M.P. Sanders¹⁰⁰, M. Sandhoff¹⁷⁶, T. Sandoval²⁸, C. Sandoval¹⁶³, R. Sandstroem¹⁰¹, D.P.C. Sankey¹³¹, A. Sansoni⁴⁷, C. Santoni³⁴, R. Santonic^{134a,134b}, H. Santos^{126a}, I. Santoyo Castillo¹⁵⁰, K. Sapp¹²⁵, A. Sapronov⁶⁵, J.G. Saraiva^{126a,126d}, B. Sarrazin²¹, G. Sartisohn¹⁷⁶, O. Sasaki⁶⁶, Y. Sasaki¹⁵⁶, K. Sato¹⁶¹, G. Sauvage^{5,*}, E. Sauvan⁵, G. Savage⁷⁷, P. Savard^{159,d}, C. Sawyer¹²⁰, L. Sawyer^{79,m}, D.H. Saxon⁵³, J. Saxon³¹, C. Sbarra^{20a}, A. Sbrizzi^{20a,20b}, T. Scanlon⁷⁸, D.A. Scannicchio¹⁶⁴, M. Scarcella¹⁵¹, V. Scarfone^{37a,37b}, J. Schaarschmidt¹⁷³, P. Schacht¹⁰¹, D. Schaefer³⁰, R. Schaefer⁴², S. Schaepe²¹, S. Schaetzl^{58b}, U. Schäfer⁸³, A.C. Schaffer¹¹⁷, D. Schaire¹⁰⁰, R.D. Schamberger¹⁴⁹, V. Scharf^{58a}, V.A. Schegelsky¹²³, D. Scheirich¹²⁹, M. Schernau¹⁶⁴, C. Schiavi^{50a,50b}, J. Schieck¹⁰⁰, C. Schillo⁴⁸, M. Schioppa^{37a,37b}, S. Schlenker³⁰, E. Schmidt⁴⁸, K. Schmieden³⁰, C. Schmitt⁸³, S. Schmitt^{58b}, B. Schneider¹⁷, Y.J. Schnellbach⁷⁴, U. Schnoor⁴⁴, L. Schoeffel¹³⁷, A. Schoening^{58b}, B.D. Schoenrock⁹⁰, A.L.S. Schorlemmer⁵⁴, M. Schott⁸³, D. Schouten^{160a}, J. Schovancova²⁵, S. Schramm¹⁵⁹, M. Schreyer¹⁷⁵, C. Schroeder⁸³, N. Schuh⁸³, M.J. Schultens²¹, H.-C. Schultz-Coulon^{58a}, H. Schulz¹⁶, M. Schumacher⁴⁸, B.A. Schumm¹³⁸, Ph. Schune¹³⁷, C. Schwanenberger⁸⁴, A. Schwartzman¹⁴⁴, T.A. Schwarz⁸⁹, Ph. Schwegler¹⁰¹, Ph. Schwemling¹³⁷, R. Schwienhorst⁹⁰, J. Schwindling¹³⁷, T. Schwindt²¹, M. Schwoerer⁵, F.G. Sciacca¹⁷, E. Scifo¹¹⁷, G. Sciolla²³, F. Scuri^{124a,124b}, F. Scutti²¹, J. Searcy⁸⁹, G. Sedov⁴², E. Sedykh¹²³, P. Seema²¹, S.C. Seidel¹⁰⁵, A. Seiden¹³⁸, F. Seifert¹²⁸, J.M. Seixas^{24a}, G. Sekhniaidze^{104a}, S.J. Sekula⁴⁰, K.E. Selbach⁴⁶, D.M. Seliverstov^{123,*}, G. Sellers⁷⁴, N. Semprini-Cesari^{20a,20b}, C. Serfon³⁰, L. Serin¹¹⁷, L. Serkin⁵⁴, T. Serre⁸⁵, R. Seuster^{160a}, H. Severini¹¹³, T. Sfiligoj⁷⁵, F. Sforza¹⁰¹, A. Sfyrla³⁰, E. Shabalina⁵⁴, M. Shamim¹¹⁶, L.Y. Shan^{33a}, R. Shang¹⁶⁶, J.T. Shank²², M. Shapiro¹⁵, P.B. Shatalov⁹⁷, K. Shaw^{165a,165b}, A. Shcherbakova^{147a,147b}, C.Y. Shehu¹⁵⁰, P. Sherwood⁷⁸, L. Shi^{152,ad}, S. Shimizu⁶⁷, C.O. Shimmin¹⁶⁴, M. Shimojima¹⁰², M. Shiyakova⁶⁵, A. Shmeleva⁹⁶, D. Shoaleh Saadi⁹⁵, M.J. Shochet³¹, S. Shojaii^{91a,91b}, D. Short¹²⁰, S. Shrestha¹¹¹, E. Shulga⁹⁸, M.A. Shupe⁷, S. Shushkevich⁴², P. Sicho¹²⁷, O. Sidiropoulou¹⁵⁵, D. Sidorov¹¹⁴, A. Sidoti^{133a}, F. Siegert⁴⁴, Dj. Sijacki^{13a}, J. Silva^{126a,126d}, Y. Silver¹⁵⁴, D. Silverstein¹⁴⁴, S.B. Silverstein^{147a}, V. Simak¹²⁸, O. Simard⁵, Lj. Simic^{13a}, S. Simion¹¹⁷, E. Simioni⁸³, B. Simmons⁷⁸, D. Simon³⁴, R. Simoniello^{91a,91b}, P. Sinervo¹⁵⁹, N.B. Sinev¹¹⁶, G. Siragusa¹⁷⁵, A. Sircar⁷⁹, A.N. Sisakyan^{65,*}, S.Yu. Sivoklokov⁹⁹, J. Sjölin^{147a,147b}, T.B. Sjursen¹⁴, H.P. Skottowe⁵⁷, P. Skubic¹¹³, M. Slater¹⁸, T. Slavicek¹²⁸, M. Slawinska¹⁰⁷, K. Sliwa¹⁶², V. Smakhtin¹⁷³, B.H. Smart⁴⁶, L. Smestad¹⁴, S.Yu. Smirnov⁹⁸, Y. Smirnov⁹⁸, L.N. Smirnova^{99,ae}, O. Smirnova⁸¹, K.M. Smith⁵³, M. Smith³⁵, M. Smizanska⁷², K. Smolek¹²⁸, A.A. Snesarev⁹⁶, G. Snidero⁷⁶, S. Snyder²⁵, R. Sobie^{170,j}, F. Socher⁴⁴, A. Soffer¹⁵⁴, D.A. Soh^{152,ad}, C.A. Solans³⁰, M. Solar¹²⁸, J. Solc¹²⁸, E.Yu. Soldatov⁹⁸, U. Soldevila¹⁶⁸, A.A. Solodkov¹³⁰, A. Soloshenko⁶⁵, O.V. Solovyanov¹³⁰, V. Solovyev¹²³, P. Sommer⁴⁸, H.Y. Song^{33b}, N. Soni¹, A. Sood¹⁵, A. Sopczak¹²⁸, B. Sopko¹²⁸, V. Sopko¹²⁸, V. Sorin¹², M. Sosebee⁸, R. Soualah^{165a,165c}, P. Soueid⁹⁵, A.M. Soukharev^{109,c}, D. South⁴², S. Spagnolo^{73a,73b}, F. Spanò⁷⁷, W.R. Spearman⁵⁷, F. Spettel¹⁰¹, R. Spighi^{20a}, G. Spigo³⁰, L.A. Spiller⁸⁸, M. Spousta¹²⁹, T. Spreitzer¹⁵⁹,

- R.D. St. Denis^{53,*}, S. Staerz⁴⁴, J. Stahlman¹²², R. Stamen^{58a}, S. Stamm¹⁶, E. Stanecka³⁹, C. Stanescu^{135a}, M. Stanescu-Bellu⁴², M.M. Stanitzki⁴², S. Stapnes¹¹⁹, E.A. Starchenko¹³⁰, J. Stark⁵⁵, P. Staroba¹²⁷, P. Starovoitov⁴², R. Staszewski³⁹, P. Stavina^{145a,*}, P. Steinberg²⁵, B. Stelzer¹⁴³, H.J. Stelzer³⁰, O. Stelzer-Chilton^{160a}, H. Stenzel⁵², S. Stern¹⁰¹, G.A. Stewart⁵³, J.A. Stillings²¹, M.C. Stockton⁸⁷, M. Stoebe⁸⁷, G. Stoica^{26a}, P. Stolte⁵⁴, S. Stonjek¹⁰¹, A.R. Stradling⁸, A. Straessner⁴⁴, M.E. Stramaglia¹⁷, J. Strandberg¹⁴⁸, S. Strandberg^{147a,147b}, A. Strandlie¹¹⁹, E. Strauss¹⁴⁴, M. Strauss¹¹³, P. Strizenec^{145b}, R. Ströhmer¹⁷⁵, D.M. Strom¹¹⁶, R. Stroynowski⁴⁰, A. Strubig¹⁰⁶, S.A. Stucci¹⁷, B. Stugu¹⁴, N.A. Styles⁴², D. Su¹⁴⁴, J. Su¹²⁵, R. Subramaniam⁷⁹, A. Succurro¹², Y. Sugaya¹¹⁸, C. Suhr¹⁰⁸, M. Suk¹²⁸, V.V. Sulin⁹⁶, S. Sultansoy^{4d}, T. Sumida⁶⁸, S. Sun⁵⁷, X. Sun^{33a}, J.E. Sundermann⁴⁸, K. Suruliz¹⁵⁰, G. Susinno^{37a,37b}, M.R. Sutton¹⁵⁰, Y. Suzuki⁶⁶, M. Svatos¹²⁷, S. Swedish¹⁶⁹, M. Swiatlowski¹⁴⁴, I. Sykora^{145a}, T. Sykora¹²⁹, D. Ta⁹⁰, C. Taccini^{135a,135b}, K. Tackmann⁴², J. Taenzer¹⁵⁹, A. Taffard¹⁶⁴, R. Tafirout^{160a}, N. Taiblum¹⁵⁴, H. Takai²⁵, R. Takashima⁶⁹, H. Takeda⁶⁷, T. Takeshita¹⁴¹, Y. Takubo⁶⁶, M. Talby⁸⁵, A.A. Talyshев^{109,c}, J.Y.C. Tam¹⁷⁵, K.G. Tan⁸⁸, J. Tanaka¹⁵⁶, R. Tanaka¹¹⁷, S. Tanaka¹³², S. Tanaka⁶⁶, A.J. Tanasijczuk¹⁴³, B.B. Tannenwald¹¹¹, N. Tannoury²¹, S. Tapprogge⁸³, S. Tarem¹⁵³, F. Tarrade²⁹, G.F. Tartarelli^{91a}, P. Tas¹²⁹, M. Tasevsky¹²⁷, T. Tashiro⁶⁸, E. Tassi^{37a,37b}, A. Tavares Delgado^{126a,126b}, Y. Tayalati^{136d}, F.E. Taylor⁹⁴, G.N. Taylor⁸⁸, W. Taylor^{160b}, F.A. Teischinger³⁰, M. Teixeira Dias Castanheira⁷⁶, P. Teixeira-Dias⁷⁷, K.K. Temming⁴⁸, H. Ten Kate³⁰, P.K. Teng¹⁵², J.J. Teoh¹¹⁸, F. Tepel¹⁷⁶, S. Terada⁶⁶, K. Terashi¹⁵⁶, J. Terron⁸², S. Terzo¹⁰¹, M. Testa⁴⁷, R.J. Teuscher^{159,j}, J. Therhaag²¹, T. Theveneaux-Pelzer³⁴, J.P. Thomas¹⁸, J. Thomas-Wilsker⁷⁷, E.N. Thompson³⁵, P.D. Thompson¹⁸, R.J. Thompson⁸⁴, A.S. Thompson⁵³, L.A. Thomsen³⁶, E. Thomson¹²², M. Thomson²⁸, W.M. Thong⁸⁸, R.P. Thun^{89,*}, F. Tian³⁵, M.J. Tibbetts¹⁵, V.O. Tikhomirov^{96,af}, Yu.A. Tikhonov^{109,c}, S. Timoshenko⁹⁸, E. Tiouchichine⁸⁵, P. Tipton¹⁷⁷, S. Tisserant⁸⁵, T. Todorov⁵, S. Todorova-Nova¹²⁹, J. Tojo⁷⁰, S. Tokár^{145a}, K. Tokushuku⁶⁶, K. Tollefson⁹⁰, E. Tolley⁵⁷, L. Tomlinson⁸⁴, M. Tomoto¹⁰³, L. Tompkins³¹, K. Toms¹⁰⁵, N.D. Topilin⁶⁵, E. Torrence¹¹⁶, H. Torres¹⁴³, E. Torró Pastor¹⁶⁸, J. Toth^{85,ag}, F. Touchard⁸⁵, D.R. Tovey¹⁴⁰, H.L. Tran¹¹⁷, T. Trefzger¹⁷⁵, L. Tremblet³⁰, A. Tricoli³⁰, I.M. Trigger^{160a}, S. Trincaz-Duvold⁸⁰, M.F. Tripiana¹², W. Trischuk¹⁵⁹, B. Trocmé⁵⁵, C. Troncon^{91a}, M. Trottier-McDonald¹⁵, M. Trovatelli^{135a,135b}, P. True⁹⁰, M. Trzebinski³⁹, A. Trzupek³⁹, C. Tsarouchas³⁰, J.C-L. Tseng¹²⁰, P.V. Tsiareshka⁹², D. Tsionou¹³⁷, G. Tsipolitis¹⁰, N. Tsirintanis⁹, S. Tsiskaridze¹², V. Tsiskaridze⁴⁸, E.G. Tskhadadze^{51a}, I.I. Tsukerman⁹⁷, V. Tsulaia¹⁵, S. Tsuno⁶⁶, D. Tsybychev¹⁴⁹, A. Tudorache^{26a}, V. Tudorache^{26a}, A.N. Tuna¹²², S.A. Tupputi^{20a,20b}, S. Turchikhin^{99,ae}, D. Turecek¹²⁸, I. Turk Cakir^{4c}, R. Turra^{91a,91b}, A.J. Turvey⁴⁰, P.M. Tuts³⁵, A. Tykhonov⁴⁹, M. Tylmad^{147a,147b}, M. Tyndel¹³¹, I. Ueda¹⁵⁶, R. Ueno²⁹, M. Ughetto⁸⁵, M. Ugland¹⁴, M. Uhlenbrock²¹, F. Ukegawa¹⁶¹, G. Unal³⁰, A. Undrus²⁵, G. Unel¹⁶⁴, F.C. Ungaro⁴⁸, Y. Unno⁶⁶, C. Unverdorben¹⁰⁰, J. Urban^{145b}, D. Urbaniec³⁵, P. Urquijo⁸⁸, G. Usai⁸, A. Usanova⁶², L. Vacavant⁸⁵, V. Vacek¹²⁸, B. Vachon⁸⁷, N. Valencic¹⁰⁷, S. Valentinetto^{20a,20b}, A. Valero¹⁶⁸, L. Valery³⁴, S. Valkar¹²⁹, E. Valladolid Gallego¹⁶⁸, S. Vallecorsa⁴⁹, J.A. Valls Ferrer¹⁶⁸, W. Van Den Wollenberg¹⁰⁷, P.C. Van Der Deijl¹⁰⁷, R. van der Geer¹⁰⁷, H. van der Graaf¹⁰⁷, R. Van Der Leeuw¹⁰⁷, D. van der Ster³⁰, N. van Eldik³⁰, P. van Gemmeren⁶, J. Van Nieuwkoop¹⁴³, I. van Vulpen¹⁰⁷, M.C. van Woerden³⁰, M. Vanadia^{133a,133b}, W. Vandelli³⁰, R. Vanguri¹²², A. Vaniachine⁶, P. Vankov⁴², F. Vannucci⁸⁰, G. Vardanyan¹⁷⁸, R. Vari^{133a}, E.W. Varnes⁷, T. Varol⁸⁶, D. Varouchas⁸⁰, A. Vartapetian⁸, K.E. Varvell¹⁵¹, F. Vazeille³⁴, T. Vazquez Schroeder⁵⁴, J. Veatch⁷, F. Veloso^{126a,126c}, T. Velz²¹, S. Veneziano^{133a}, A. Ventura^{73a,73b}, D. Ventura⁸⁶, M. Venturi¹⁷⁰, N. Venturi¹⁵⁹, A. Venturini²³, V. Vercesi^{121a}, M. Verducci^{133a,133b}, W. Verkerke¹⁰⁷, J.C. Vermeulen¹⁰⁷, A. Vest⁴⁴, M.C. Vetterli^{143,d}, O. Viazlo⁸¹, I. Vichou¹⁶⁶, T. Vickey^{146c,ah}, O.E. Vickey Boeriu^{146c}, G.H.A. Viehhauser¹²⁰, S. Vie¹⁶⁹, R. Vigne³⁰, M. Villa^{20a,20b}, M. Villaplana Perez^{91a,91b}, E. Vilucchi⁴⁷, M.G. Vincter²⁹, V.B. Vinogradov⁶⁵, J. Virzi¹⁵, I. Vivarelli¹⁵⁰, F. Vives Vaque³, S. Vlachos¹⁰, D. Vladoiu¹⁰⁰, M. Vlasak¹²⁸, A. Vogel²¹, M. Vogel^{32a}, P. Vokac¹²⁸, G. Volpi^{124a,124b}, M. Volpi⁸⁸, H. von der Schmitt¹⁰¹, H. von Radziewski⁴⁸, E. von Toerne²¹, V. Vorobel¹²⁹,

K. Vorobev⁹⁸, M. Vos¹⁶⁸, R. Voss³⁰, J.H. Vossebeld⁷⁴, N. Vranjes¹³⁷, M. Vranjes Milosavljevic^{13a}, V. Vrba¹²⁷, M. Vreeswijk¹⁰⁷, T. Vu Anh⁴⁸, R. Vuillermet³⁰, I. Vukotic³¹, Z. Vykydal¹²⁸, P. Wagner²¹, W. Wagner¹⁷⁶, H. Wahlberg⁷¹, S. Wahrmund⁴⁴, J. Wakabayashi¹⁰³, J. Walder⁷², R. Walker¹⁰⁰, W. Walkowiak¹⁴², R. Wall¹⁷⁷, P. Waller⁷⁴, B. Walsh¹⁷⁷, C. Wang^{33c}, C. Wang⁴⁵, F. Wang¹⁷⁴, H. Wang¹⁵, H. Wang⁴⁰, J. Wang⁴², J. Wang^{33a}, K. Wang⁸⁷, R. Wang¹⁰⁵, S.M. Wang¹⁵², T. Wang²¹, X. Wang¹⁷⁷, C. Wanotayaroj¹¹⁶, A. Warburton⁸⁷, C.P. Ward²⁸, D.R. Wardrope⁷⁸, M. Warsinsky⁴⁸, A. Washbrook⁴⁶, C. Wasicki⁴², P.M. Watkins¹⁸, A.T. Watson¹⁸, I.J. Watson¹⁵¹, M.F. Watson¹⁸, G. Watts¹³⁹, S. Watts⁸⁴, B.M. Waugh⁷⁸, S. Webb⁸⁴, M.S. Weber¹⁷, S.W. Weber¹⁷⁵, J.S. Webster³¹, A.R. Weidberg¹²⁰, B. Weinert⁶¹, J. Weingarten⁵⁴, C. Weiser⁴⁸, H. Weits¹⁰⁷, P.S. Wells³⁰, T. Wenaus²⁵, D. Wendland¹⁶, Z. Weng^{152,ad}, T. Wengler³⁰, S. Wenig³⁰, N. Wermes²¹, M. Werner⁴⁸, P. Werner³⁰, M. Wessels^{58a}, J. Wetter¹⁶², K. Whalen²⁹, A. White⁸, M.J. White¹, R. White^{32b}, S. White^{124a,124b}, D. Whiteson¹⁶⁴, D. Wicke¹⁷⁶, F.J. Wickens¹³¹, W. Wiedenmann¹⁷⁴, M. Wielers¹³¹, P. Wienemann²¹, C. Wiglesworth³⁶, L.A.M. Wiik-Fuchs²¹, P.A. Wijeratne⁷⁸, A. Wildauer¹⁰¹, M.A. Wildt^{42,ai}, H.G. Wilkens³⁰, H.H. Williams¹²², S. Williams²⁸, C. Willis⁹⁰, S. Willocq⁸⁶, A. Wilson⁸⁹, J.A. Wilson¹⁸, I. Wingerter-Seez⁵, F. Winklmeier¹¹⁶, B.T. Winter²¹, M. Wittgen¹⁴⁴, J. Wittkowski¹⁰⁰, S.J. Wollstadt⁸³, M.W. Wolter³⁹, H. Wolters^{126a,126c}, B.K. Wosiek³⁹, J. Wotschack³⁰, M.J. Woudstra⁸⁴, K.W. Wozniak³⁹, M. Wright⁵³, M. Wu⁵⁵, S.L. Wu¹⁷⁴, X. Wu⁴⁹, Y. Wu⁸⁹, T.R. Wyatt⁸⁴, B.M. Wynne⁴⁶, S. Xella³⁶, M. Xiao¹³⁷, D. Xu^{33a}, L. Xu^{33b,aj}, B. Yabsley¹⁵¹, S. Yacoob^{146b,ak}, R. Yakabe⁶⁷, M. Yamada⁶⁶, H. Yamaguchi¹⁵⁶, Y. Yamaguchi¹¹⁸, A. Yamamoto⁶⁶, S. Yamamoto¹⁵⁶, T. Yamamura¹⁵⁶, T. Yamanaka¹⁵⁶, K. Yamauchi¹⁰³, Y. Yamazaki⁶⁷, Z. Yan²², H. Yang^{33e}, H. Yang¹⁷⁴, Y. Yang¹¹¹, S. Yanush⁹³, L. Yao^{33a}, W-M. Yao¹⁵, Y. Yasu⁶⁶, E. Yatsenko⁴², K.H. Yau Wong²¹, J. Ye⁴⁰, S. Ye²⁵, I. Yeletskikh⁶⁵, A.L. Yen⁵⁷, E. Yildirim⁴², M. Yilmaz^{4b}, K. Yorita¹⁷², R. Yoshida⁶, K. Yoshihara¹⁵⁶, C. Young¹⁴⁴, C.J.S. Young³⁰, S. Youssef²², D.R. Yu¹⁵, J. Yu⁸, J.M. Yu⁸⁹, J. Yu¹¹⁴, L. Yuan⁶⁷, A. Yurkewicz¹⁰⁸, I. Yusuff^{28,al}, B. Zabinski³⁹, R. Zaidan⁶³, A.M. Zaitsev^{130,z}, A. Zaman¹⁴⁹, S. Zambito²³, L. Zanello^{133a,133b}, D. Zanzi⁸⁸, C. Zeitnitz¹⁷⁶, M. Zeman¹²⁸, A. Zemla^{38a}, K. Zengel²³, O. Zenin¹³⁰, T. Ženiš^{145a}, D. Zerwas¹¹⁷, G. Zevi della Porta⁵⁷, D. Zhang⁸⁹, F. Zhang¹⁷⁴, H. Zhang⁹⁰, J. Zhang⁶, L. Zhang¹⁵², R. Zhang^{33b}, X. Zhang^{33d}, Z. Zhang¹¹⁷, X. Zhao⁴⁰, Y. Zhao^{33d}, Z. Zhao^{33b}, A. Zhemchugov⁶⁵, J. Zhong¹²⁰, B. Zhou⁸⁹, C. Zhou⁴⁵, L. Zhou³⁵, L. Zhou⁴⁰, N. Zhou¹⁶⁴, C.G. Zhu^{33d}, H. Zhu^{33a}, J. Zhu⁸⁹, Y. Zhu^{33b}, X. Zhuang^{33a}, K. Zhukov⁹⁶, A. Zibell¹⁷⁵, D. Ziemińska⁶¹, N.I. Zimine⁶⁵, C. Zimmermann⁸³, R. Zimmermann²¹, S. Zimmermann²¹, S. Zimmermann⁴⁸, Z. Zinonos⁵⁴, M. Ziolkowski¹⁴², G. Zobernig¹⁷⁴, A. Zoccoli^{20a,20b}, M. zur Nedden¹⁶, G. Zurzolo^{104a,104b}, L. Zwalski³⁰.

¹ Department of Physics, University of Adelaide, Adelaide, Australia

² Physics Department, SUNY Albany, Albany NY, U.S.A.

³ Department of Physics, University of Alberta, Edmonton AB, Canada

⁴ ^(a) Department of Physics, Ankara University, Ankara; ^(b) Department of Physics, Gazi University, Ankara; ^(c) Istanbul Aydin University, Istanbul; ^(d) Division of Physics, TOBB University of Economics and Technology, Ankara, Turkey

⁵ LAPP, CNRS/IN2P3 and Université de Savoie, Annecy-le-Vieux, France

⁶ High Energy Physics Division, Argonne National Laboratory, Argonne IL, United States of America

⁷ Department of Physics, University of Arizona, Tucson AZ, U.S.A.

⁸ Department of Physics, The University of Texas at Arlington, Arlington TX, U.S.A.

⁹ Physics Department, University of Athens, Athens, Greece

¹⁰ Physics Department, National Technical University of Athens, Zografou, Greece

¹¹ Institute of Physics, Azerbaijan Academy of Sciences, Baku, Azerbaijan

¹² Institut de Física d'Altes Energies and Departament de Física de la Universitat Autònoma de Barcelona, Barcelona, Spain

¹³ ^(a) Institute of Physics, University of Belgrade, Belgrade; ^(b) Vinca Institute of Nuclear Sciences, University of Belgrade, Belgrade, Serbia

- ¹⁴ Department for Physics and Technology, University of Bergen, Bergen, Norway
- ¹⁵ Physics Division, Lawrence Berkeley National Laboratory and University of California, Berkeley CA, U.S.A.
- ¹⁶ Department of Physics, Humboldt University, Berlin, Germany
- ¹⁷ Albert Einstein Center for Fundamental Physics and Laboratory for High Energy Physics, University of Bern, Bern, Switzerland
- ¹⁸ School of Physics and Astronomy, University of Birmingham, Birmingham, United Kingdom
- ¹⁹ ^(a) Department of Physics, Bogazici University, Istanbul; ^(b) Department of Physics, Dogus University, Istanbul; ^(c) Department of Physics Engineering, Gaziantep University, Gaziantep, Turkey
- ²⁰ ^(a) INFN Sezione di Bologna; ^(b) Dipartimento di Fisica e Astronomia, Università di Bologna, Bologna, Italy
- ²¹ Physikalisches Institut, University of Bonn, Bonn, Germany
- ²² Department of Physics, Boston University, Boston MA, U.S.A.
- ²³ Department of Physics, Brandeis University, Waltham MA, U.S.A.
- ²⁴ ^(a) Universidade Federal do Rio De Janeiro COPPE/EE/IF, Rio de Janeiro; ^(b) Electrical Circuits Department, Federal University of Juiz de Fora (UFJF), Juiz de Fora; ^(c) Federal University of Sao Joao del Rei (UFSJ), Sao Joao del Rei; ^(d) Instituto de Fisica, Universidade de Sao Paulo, Sao Paulo, Brazil
- ²⁵ Physics Department, Brookhaven National Laboratory, Upton NY, U.S.A.
- ²⁶ ^(a) National Institute of Physics and Nuclear Engineering, Bucharest; ^(b) National Institute for Research and Development of Isotopic and Molecular Technologies, Physics Department, Cluj Napoca; ^(c) University Politehnica Bucharest, Bucharest; ^(d) West University in Timisoara, Timisoara, Romania
- ²⁷ Departamento de Física, Universidad de Buenos Aires, Buenos Aires, Argentina
- ²⁸ Cavendish Laboratory, University of Cambridge, Cambridge, United Kingdom
- ²⁹ Department of Physics, Carleton University, Ottawa ON, Canada
- ³⁰ CERN, Geneva, Switzerland
- ³¹ Enrico Fermi Institute, University of Chicago, Chicago IL, U.S.A.
- ³² ^(a) Departamento de Física, Pontificia Universidad Católica de Chile, Santiago; ^(b) Departamento de Física, Universidad Técnica Federico Santa María, Valparaíso, Chile
- ³³ ^(a) Institute of High Energy Physics, Chinese Academy of Sciences, Beijing; ^(b) Department of Modern Physics, University of Science and Technology of China, Anhui; ^(c) Department of Physics, Nanjing University, Jiangsu; ^(d) School of Physics, Shandong University, Shandong; ^(e) Physics Department, Shanghai Jiao Tong University, Shanghai; ^(f) Physics Department, Tsinghua University, Beijing 100084, China
- ³⁴ Laboratoire de Physique Corpusculaire, Clermont Université and Université Blaise Pascal and CNRS/IN2P3, Clermont-Ferrand, France
- ³⁵ Nevis Laboratory, Columbia University, Irvington NY, U.S.A.
- ³⁶ Niels Bohr Institute, University of Copenhagen, Kobenhavn, Denmark
- ³⁷ ^(a) INFN Gruppo Collegato di Cosenza, Laboratori Nazionali di Frascati; ^(b) Dipartimento di Fisica, Università della Calabria, Rende, Italy
- ³⁸ ^(a) AGH University of Science and Technology, Faculty of Physics and Applied Computer Science, Krakow; ^(b) Marian Smoluchowski Institute of Physics, Jagiellonian University, Krakow, Poland
- ³⁹ The Henryk Niewodniczanski Institute of Nuclear Physics, Polish Academy of Sciences, Krakow, Poland
- ⁴⁰ Physics Department, Southern Methodist University, Dallas TX, U.S.A.
- ⁴¹ Physics Department, University of Texas at Dallas, Richardson TX, U.S.A.
- ⁴² DESY, Hamburg and Zeuthen, Germany
- ⁴³ Institut für Experimentelle Physik IV, Technische Universität Dortmund, Dortmund, Germany
- ⁴⁴ Institut für Kern- und Teilchenphysik, Technische Universität Dresden, Dresden, Germany
- ⁴⁵ Department of Physics, Duke University, Durham NC, U.S.A.

- ⁴⁶ SUPA - School of Physics and Astronomy, University of Edinburgh, Edinburgh, United Kingdom
⁴⁷ INFN Laboratori Nazionali di Frascati, Frascati, Italy
⁴⁸ Fakultät für Mathematik und Physik, Albert-Ludwigs-Universität, Freiburg, Germany
⁴⁹ Section de Physique, Université de Genève, Geneva, Switzerland
⁵⁰ ^(a) INFN Sezione di Genova; ^(b) Dipartimento di Fisica, Università di Genova, Genova, Italy
⁵¹ ^(a) E. Andronikashvili Institute of Physics, Iv. Javakhishvili Tbilisi State University, Tbilisi; ^(b) High Energy Physics Institute, Tbilisi State University, Tbilisi, Georgia
⁵² II Physikalisches Institut, Justus-Liebig-Universität Giessen, Giessen, Germany
⁵³ SUPA - School of Physics and Astronomy, University of Glasgow, Glasgow, United Kingdom
⁵⁴ II Physikalisches Institut, Georg-August-Universität, Göttingen, Germany
⁵⁵ Laboratoire de Physique Subatomique et de Cosmologie, Université Grenoble-Alpes, CNRS/IN2P3, Grenoble, France
⁵⁶ Department of Physics, Hampton University, Hampton VA, U.S.A.
⁵⁷ Laboratory for Particle Physics and Cosmology, Harvard University, Cambridge MA, U.S.A.
⁵⁸ ^(a) Kirchhoff-Institut für Physik, Ruprecht-Karls-Universität Heidelberg, Heidelberg; ^(b) Physikalisches Institut, Ruprecht-Karls-Universität Heidelberg, Heidelberg; ^(c) ZITI Institut für technische Informatik, Ruprecht-Karls-Universität Heidelberg, Mannheim, Germany
⁵⁹ Faculty of Applied Information Science, Hiroshima Institute of Technology, Hiroshima, Japan
⁶⁰ ^(a) Department of Physics, The Chinese University of Hong Kong, Shatin, N.T., Hong Kong; ^(b) Department of Physics, The University of Hong Kong, Hong Kong; ^(c) Department of Physics, The Hong Kong University of Science and Technology, Clear Water Bay, Kowloon, Hong Kong, China
⁶¹ Department of Physics, Indiana University, Bloomington IN, U.S.A.
⁶² Institut für Astro- und Teilchenphysik, Leopold-Franzens-Universität, Innsbruck, Austria
⁶³ University of Iowa, Iowa City IA, U.S.A.
⁶⁴ Department of Physics and Astronomy, Iowa State University, Ames IA, U.S.A.
⁶⁵ Joint Institute for Nuclear Research, JINR Dubna, Dubna, Russia
⁶⁶ KEK, High Energy Accelerator Research Organization, Tsukuba, Japan
⁶⁷ Graduate School of Science, Kobe University, Kobe, Japan
⁶⁸ Faculty of Science, Kyoto University, Kyoto, Japan
⁶⁹ Kyoto University of Education, Kyoto, Japan
⁷⁰ Department of Physics, Kyushu University, Fukuoka, Japan
⁷¹ Instituto de Física La Plata, Universidad Nacional de La Plata and CONICET, La Plata, Argentina
⁷² Physics Department, Lancaster University, Lancaster, United Kingdom
⁷³ ^(a) INFN Sezione di Lecce; ^(b) Dipartimento di Matematica e Fisica, Università del Salento, Lecce, Italy
⁷⁴ Oliver Lodge Laboratory, University of Liverpool, Liverpool, United Kingdom
⁷⁵ Department of Physics, Jožef Stefan Institute and University of Ljubljana, Ljubljana, Slovenia
⁷⁶ School of Physics and Astronomy, Queen Mary University of London, London, United Kingdom
⁷⁷ Department of Physics, Royal Holloway University of London, Surrey, United Kingdom
⁷⁸ Department of Physics and Astronomy, University College London, London, United Kingdom
⁷⁹ Louisiana Tech University, Ruston LA, U.S.A.
⁸⁰ Laboratoire de Physique Nucléaire et de Hautes Energies, UPMC and Université Paris-Diderot and CNRS/IN2P3, Paris, France
⁸¹ Fysiska institutionen, Lunds universitet, Lund, Sweden
⁸² Departamento de Fisica Teorica C-15, Universidad Autonoma de Madrid, Madrid, Spain
⁸³ Institut für Physik, Universität Mainz, Mainz, Germany
⁸⁴ School of Physics and Astronomy, University of Manchester, Manchester, United Kingdom
⁸⁵ CPPM, Aix-Marseille Université and CNRS/IN2P3, Marseille, France
⁸⁶ Department of Physics, University of Massachusetts, Amherst MA, U.S.A.
⁸⁷ Department of Physics, McGill University, Montreal QC, Canada
⁸⁸ School of Physics, University of Melbourne, Victoria, Australia
⁸⁹ Department of Physics, The University of Michigan, Ann Arbor MI, U.S.A.

- ⁹⁰ Department of Physics and Astronomy, Michigan State University, East Lansing MI, U.S.A.
- ⁹¹ ^(a) INFN Sezione di Milano; ^(b) Dipartimento di Fisica, Università di Milano, Milano, Italy
- ⁹² B.I. Stepanov Institute of Physics, National Academy of Sciences of Belarus, Minsk, Republic of Belarus
- ⁹³ National Scientific and Educational Centre for Particle and High Energy Physics, Minsk, Republic of Belarus
- ⁹⁴ Department of Physics, Massachusetts Institute of Technology, Cambridge MA, U.S.A.
- ⁹⁵ Group of Particle Physics, University of Montreal, Montreal QC, Canada
- ⁹⁶ P.N. Lebedev Institute of Physics, Academy of Sciences, Moscow, Russia
- ⁹⁷ Institute for Theoretical and Experimental Physics (ITEP), Moscow, Russia
- ⁹⁸ National Research Nuclear University MEPhI, Moscow, Russia
- ⁹⁹ D.V. Skobeltsyn Institute of Nuclear Physics, M.V. Lomonosov Moscow State University, Moscow, Russia
- ¹⁰⁰ Fakultät für Physik, Ludwig-Maximilians-Universität München, München, Germany
- ¹⁰¹ Max-Planck-Institut für Physik (Werner-Heisenberg-Institut), München, Germany
- ¹⁰² Nagasaki Institute of Applied Science, Nagasaki, Japan
- ¹⁰³ Graduate School of Science and Kobayashi-Maskawa Institute, Nagoya University, Nagoya, Japan
- ¹⁰⁴ ^(a) INFN Sezione di Napoli; ^(b) Dipartimento di Fisica, Università di Napoli, Napoli, Italy
- ¹⁰⁵ Department of Physics and Astronomy, University of New Mexico, Albuquerque NM, U.S.A.
- ¹⁰⁶ Institute for Mathematics, Astrophysics and Particle Physics, Radboud University Nijmegen/Nikhef, Nijmegen, Netherlands
- ¹⁰⁷ Nikhef National Institute for Subatomic Physics and University of Amsterdam, Amsterdam, Netherlands
- ¹⁰⁸ Department of Physics, Northern Illinois University, DeKalb IL, U.S.A.
- ¹⁰⁹ Budker Institute of Nuclear Physics, SB RAS, Novosibirsk, Russia
- ¹¹⁰ Department of Physics, New York University, New York NY, U.S.A.
- ¹¹¹ Ohio State University, Columbus OH, U.S.A.
- ¹¹² Faculty of Science, Okayama University, Okayama, Japan
- ¹¹³ Homer L. Dodge Department of Physics and Astronomy, University of Oklahoma, Norman OK, U.S.A.
- ¹¹⁴ Department of Physics, Oklahoma State University, Stillwater OK, U.S.A.
- ¹¹⁵ Palacký University, RCPTM, Olomouc, Czech Republic
- ¹¹⁶ Center for High Energy Physics, University of Oregon, Eugene OR, U.S.A.
- ¹¹⁷ LAL, Université Paris-Sud and CNRS/IN2P3, Orsay, France
- ¹¹⁸ Graduate School of Science, Osaka University, Osaka, Japan
- ¹¹⁹ Department of Physics, University of Oslo, Oslo, Norway
- ¹²⁰ Department of Physics, Oxford University, Oxford, United Kingdom
- ¹²¹ ^(a) INFN Sezione di Pavia; ^(b) Dipartimento di Fisica, Università di Pavia, Pavia, Italy
- ¹²² Department of Physics, University of Pennsylvania, Philadelphia PA, U.S.A.
- ¹²³ Petersburg Nuclear Physics Institute, Gatchina, Russia
- ¹²⁴ ^(a) INFN Sezione di Pisa; ^(b) Dipartimento di Fisica E. Fermi, Università di Pisa, Pisa, Italy
- ¹²⁵ Department of Physics and Astronomy, University of Pittsburgh, Pittsburgh PA, U.S.A.
- ¹²⁶ ^(a) Laboratorio de Instrumentacao e Física Experimental de Particulas - LIP, Lisboa; ^(b) Faculdade de Ciências, Universidade de Lisboa, Lisboa; ^(c) Department of Physics, University of Coimbra, Coimbra; ^(d) Centro de Física Nuclear da Universidade de Lisboa, Lisboa; ^(e) Departamento de Física, Universidade do Minho, Braga; ^(f) Departamento de Física Teorica y del Cosmos and CAFPE, Universidad de Granada, Granada (Spain); ^(g) Dep Física and CEFITEC of Faculdade de Ciencias e Tecnologia, Universidade Nova de Lisboa, Caparica, Portugal
- ¹²⁷ Institute of Physics, Academy of Sciences of the Czech Republic, Praha, Czech Republic
- ¹²⁸ Czech Technical University in Prague, Praha, Czech Republic
- ¹²⁹ Faculty of Mathematics and Physics, Charles University in Prague, Praha, Czech Republic
- ¹³⁰ State Research Center Institute for High Energy Physics, Protvino, Russia

- ¹³¹ Particle Physics Department, Rutherford Appleton Laboratory, Didcot, United Kingdom
¹³² Ritsumeikan University, Kusatsu, Shiga, Japan
¹³³ (a) INFN Sezione di Roma; (b) Dipartimento di Fisica, Sapienza Università di Roma, Roma, Italy
¹³⁴ (a) INFN Sezione di Roma Tor Vergata; (b) Dipartimento di Fisica, Università di Roma Tor Vergata, Roma, Italy
¹³⁵ (a) INFN Sezione di Roma Tre; (b) Dipartimento di Matematica e Fisica, Università Roma Tre, Roma, Italy
¹³⁶ (a) Faculté des Sciences Ain Chock, Réseau Universitaire de Physique des Hautes Energies - Université Hassan II, Casablanca; (b) Centre National de l'Energie des Sciences Techniques Nucléaires, Rabat; (c) Faculté des Sciences Semlalia, Université Cadi Ayyad, LPHEA-Marrakech; (d) Faculté des Sciences, Université Mohammed Premier and LPTPM, Oujda; (e) Faculté des sciences, Université Mohammed V-Agdal, Rabat, Morocco
¹³⁷ DSM/IRFU (Institut de Recherches sur les Lois Fondamentales de l'Univers), CEA Saclay (Commissariat à l'Energie Atomique et aux Energies Alternatives), Gif-sur-Yvette, France
¹³⁸ Santa Cruz Institute for Particle Physics, University of California Santa Cruz, Santa Cruz CA, U.S.A.
¹³⁹ Department of Physics, University of Washington, Seattle WA, U.S.A.
¹⁴⁰ Department of Physics and Astronomy, University of Sheffield, Sheffield, United Kingdom
¹⁴¹ Department of Physics, Shinshu University, Nagano, Japan
¹⁴² Fachbereich Physik, Universität Siegen, Siegen, Germany
¹⁴³ Department of Physics, Simon Fraser University, Burnaby BC, Canada
¹⁴⁴ SLAC National Accelerator Laboratory, Stanfrod CA, U.S.A.
¹⁴⁵ (a) Faculty of Mathematics, Physics & Informatics, Comenius University, Bratislava; (b) Department of Subnuclear Physics, Institute of Experimental Physics of the Slovak Academy of Sciences, Kosice, Slovak Republic
¹⁴⁶ (a) Department of Physics, University of Cape Town, Cape Town; (b) Department of Physics, University of Johannesburg, Johannesburg; (c) School of Physics, University of the Witwatersrand, Johannesburg, South Africa
¹⁴⁷ (a) Department of Physics, Stockholm University; (b) The Oskar Klein Centre, Stockholm, Sweden
¹⁴⁸ Physics Department, Royal Institute of Technology, Stockholm, Sweden
¹⁴⁹ Departments of Physics & Astronomy and Chemistry, Stony Brook University, Stony Brook NY, U.S.A.
¹⁵⁰ Department of Physics and Astronomy, University of Sussex, Brighton, United Kingdom
¹⁵¹ School of Physics, University of Sydney, Sydney, Australia
¹⁵² Institute of Physics, Academia Sinica, Taipei, Taiwan
¹⁵³ Department of Physics, Technion: Israel Institute of Technology, Haifa, Israel
¹⁵⁴ Raymond and Beverly Sackler School of Physics and Astronomy, Tel Aviv University, Tel Aviv, Israel
¹⁵⁵ Department of Physics, Aristotle University of Thessaloniki, Thessaloniki, Greece
¹⁵⁶ International Center for Elementary Particle Physics and Department of Physics, The University of Tokyo, Tokyo, Japan
¹⁵⁷ Graduate School of Science and Technology, Tokyo Metropolitan University, Tokyo, Japan
¹⁵⁸ Department of Physics, Tokyo Institute of Technology, Tokyo, Japan
¹⁵⁹ Department of Physics, University of Toronto, Toronto ON, Canada
¹⁶⁰ (a) TRIUMF, Vancouver BC; (b) Department of Physics and Astronomy, York University, Toronto ON, Canada
¹⁶¹ Faculty of Pure and Applied Sciences, University of Tsukuba, Tsukuba, Japan
¹⁶² Department of Physics and Astronomy, Tufts University, Medford MA, U.S.A.
¹⁶³ Centro de Investigaciones, Universidad Antonio Narino, Bogota, Colombia
¹⁶⁴ Department of Physics and Astronomy, University of California Irvine, Irvine CA, U.S.A.
¹⁶⁵ (a) INFN Gruppo Collegato di Udine, Sezione di Trieste, Udine; (b) ICTP, Trieste; (c) Dipartimento di Chimica, Fisica e Ambiente, Università di Udine, Udine, Italy

- ¹⁶⁶ Department of Physics, University of Illinois, Urbana IL, U.S.A.
¹⁶⁷ Department of Physics and Astronomy, University of Uppsala, Uppsala, Sweden
¹⁶⁸ Instituto de Física Corpuscular (IFIC) and Departamento de Física Atómica, Molecular y Nuclear and Departamento de Ingeniería Electrónica and Instituto de Microelectrónica de Barcelona (IMB-CNM), University of Valencia and CSIC, Valencia, Spain
¹⁶⁹ Department of Physics, University of British Columbia, Vancouver BC, Canada
¹⁷⁰ Department of Physics and Astronomy, University of Victoria, Victoria BC, Canada
¹⁷¹ Department of Physics, University of Warwick, Coventry, United Kingdom
¹⁷² Waseda University, Tokyo, Japan
¹⁷³ Department of Particle Physics, The Weizmann Institute of Science, Rehovot, Israel
¹⁷⁴ Department of Physics, University of Wisconsin, Madison WI, U.S.A.
¹⁷⁵ Fakultät für Physik und Astronomie, Julius-Maximilians-Universität, Würzburg, Germany
¹⁷⁶ Fachbereich C Physik, Bergische Universität Wuppertal, Wuppertal, Germany
¹⁷⁷ Department of Physics, Yale University, New Haven CT, U.S.A.
¹⁷⁸ Yerevan Physics Institute, Yerevan, Armenia
¹⁷⁹ Centre de Calcul de l’Institut National de Physique Nucléaire et de Physique des Particules (IN2P3), Villeurbanne, France
- ^a Also at Department of Physics, King’s College London, London, United Kingdom
^b Also at Institute of Physics, Azerbaijan Academy of Sciences, Baku, Azerbaijan
^c Also at Novosibirsk State University, Novosibirsk, Russia
^d Also at TRIUMF, Vancouver BC, Canada
^e Also at Department of Physics, California State University, Fresno CA, U.S.A.
^f Also at Department of Physics, University of Fribourg, Fribourg, Switzerland
^g Also at Tomsk State University, Tomsk, Russia
^h Also at CPPM, Aix-Marseille Université and CNRS/IN2P3, Marseille, France
ⁱ Also at Università di Napoli Parthenope, Napoli, Italy
^j Also at Institute of Particle Physics (IPP), Canada
^k Also at Particle Physics Department, Rutherford Appleton Laboratory, Didcot, United Kingdom
^l Also at Department of Physics, St. Petersburg State Polytechnical University, St. Petersburg, Russia
^m Also at Louisiana Tech University, Ruston LA, U.S.A.
ⁿ Also at Institutio Catalana de Recerca i Estudis Avancats, ICREA, Barcelona, Spain
^o Also at Department of Physics, The University of Texas at Austin, Austin TX, U.S.A.
^p Also at Institute of Theoretical Physics, Ilia State University, Tbilisi, Georgia
^q Also at CERN, Geneva, Switzerland
^r Also at Ochadai Academic Production, Ochanomizu University, Tokyo, Japan
^s Also at Manhattan College, New York NY, U.S.A.
^t Also at Institute of Physics, Academia Sinica, Taipei, Taiwan
^u Also at LAL, Université Paris-Sud and CNRS/IN2P3, Orsay, France
^v Also at Academia Sinica Grid Computing, Institute of Physics, Academia Sinica, Taipei, Taiwan
^w Also at Laboratoire de Physique Nucléaire et de Hautes Energies, UPMC and Université Paris-Diderot and CNRS/IN2P3, Paris, France
^x Also at School of Physical Sciences, National Institute of Science Education and Research, Bhubaneswar, India
^y Also at Dipartimento di Fisica, Sapienza Università di Roma, Roma, Italy
^z Also at Moscow Institute of Physics and Technology State University, Dolgoprudny, Russia
^{aa} Also at Section de Physique, Université de Genève, Geneva, Switzerland
^{ab} Also at International School for Advanced Studies (SISSA), Trieste, Italy
^{ac} Also at Department of Physics and Astronomy, University of South Carolina, Columbia SC, U.S.A.
^{ad} Also at School of Physics and Engineering, Sun Yat-sen University, Guangzhou, China
^{ae} Also at Faculty of Physics, M.V.Lomonosov Moscow State University, Moscow, Russia

- ^{a_f} Also at National Research Nuclear University MEPhI, Moscow, Russia
^{a_g} Also at Institute for Particle and Nuclear Physics, Wigner Research Centre for Physics, Budapest, Hungary
^{a_h} Also at Department of Physics, Oxford University, Oxford, United Kingdom
^{a_i} Also at Institut für Experimentalphysik, Universität Hamburg, Hamburg, Germany
^{a_j} Also at Department of Physics, The University of Michigan, Ann Arbor MI, U.S.A.
^{a_k} Also at Discipline of Physics, University of KwaZulu-Natal, Durban, South Africa
^{a_l} Also at University of Malaya, Department of Physics, Kuala Lumpur, Malaysia
* Deceased